

Synthesis and Gene Silencing Activity of RNA Duplexes Containing
3'-Deoxy-3'-Thiothymidine

Siara Ruth Isaac

Department of Chemistry
McGill University
Montreal, Canada

July 2008

A thesis submitted to McGill University
in partial fulfillment of the requirement for the degree of
Master of Science

© Siara Isaac, 2008

Abstract

This thesis reports the first synthesis and biophysical characterization of oligoribonucleotides (RNA) containing 3'-deoxy-3'-thiothymidine (3'-S-dT) units. Optimized conditions for incorporating 3'-S-dT into 21-nt RNA strands is also reported. The impact of 3'-S-dT substitutions on the structure and stability of RNA:RNA duplexes was investigated by circular dichroism (CD) and UV/thermal (T_m) studies. Generally, replacement of the 3'-oxygen by a sulphur atom resulted in a significant decrease in the thermal stability of the duplex and strong positional effects were observed. No significant disruption of the A-form helical structure of the duplexes was detected by CD, although in some cases 3'-S-dT inserts led to a reduction in base-base stacking and/or local distortion of the duplex. Assays revealed that short interfering RNA (siRNA) duplexes containing 3'-S-dT on the guide strand were not efficient at down-regulating gene products, but those containing 3'-S-dT on the passenger strand OR on both strands exhibited activities that often surpassed those of unmodified siRNA duplexes. Substitutions at the scissile phosphate position of the passenger strand suggest that the non-bridging 3'-oxygen is not involved in the coordination of a metal ion during the rate determining step in RISC-induced RNA cleavage.

Résumé

Cette thèse présente la première synthèse et caractérisation biophysique d'oligoribonucleotides (ARN) contenant des unités de 3'-deoxy-3'-thiothymidine (3'-S-dT). Des conditions optimisées pour l'intégration de 3'-S-dT en 21-nt ARN sont aussi présentées. L'impact de la substitution de 3'-S-dT sur la structure et la stabilité des duplex ARN:ARN fut recherché systématiquement par l'entremise de dichroïsme circulaire (CD) et d'études UV/thermale (T_m). Généralement, le remplacement du 3'-oxygène par un atome de soufre résulta en une baisse significative de la stabilité thermique du duplex, et des effets de positionnement important furent observés. Aucune disruption significative de la structure hélicoïdale A-form du duplex ne fut détectée par le CD, quoi que parfois des inserts de 3'-S-dT entraînent une réduction des interactions base-base et/ou une distorsion locale du duplex. Des essais révélèrent que des duplex interférents d'ARN court (siRNA) contenant du 3'-S-dT sur le brin guide n'ont pas baissé la production de gènes, mais que celles contenant du 3'-S-dT sur le brin complémentaire OU sur les deux brins présentèrent des activités qui fréquemment surpassaient celles de duplex non-modifiés de siRNA. Les substitutions à la position phosphate de rupture du brin complémentaire suggèrent que l'étape déterminante du clivage par RISC n'implique pas le 3'-oxygène pour la coordination d'un ion de métal.

Acknowledgments

It has been a privilege to work in Dr. Masad J. Damha's lab. He is a great chemist and teacher, who clearly cares about his students as individuals. He always encouraged me to continue with my chemistry but he also supported me when my interests took me out of the lab. He allowed me to take on teaching responsibilities, to take classes in education and to explore science pedagogy. And through this, I have found my career. I am deeply grateful for his extended patience and support.

I would also like to thank my colleagues in the Damha research group, particularly Jonathan Watts and Robert Donga, who kept me company through long hours in the lab and provided invaluable mentorship and discussions (some chemical, some political). Thanks are also due to my team of editors: Jonathan Watts, Robert Donga, Alison Palmer, Jeremy Lackey, and Dr. Anne Noronha.

I have benefited from significant financial support from the McGill University Department of Chemistry, in the form of stipends and teaching assistantships. These last were also an excellent opportunity to gain experience in university-level teaching.

I acknowledge and appreciate the RNAi experiments performed by Dr. Francis Robert (Dr. Jerry Pelletier lab's, Department of Biochemistry, McGill) and the MS spectra obtained by Dr. Alain Tessier, Department of Chemistry and Biochemistry (Concordia) of the oligoribonucleotides. I would like to thank Dr. Karine Auclair for the use of the CD instrument, Dr. Nadim Saade for training and trouble shooting on the MS machine I used for the nucleoside synthesis and Dr. Paul Xia for maintenance and training on the NMR machines.

And finally, thank you to my friends and family for their support and patience. Thanks particularly to my husband Jean-Philippe Roy, Emily Cranston and the Third Floor Tea Club.

Table of Contents

	page
Abstract (Résumé)	2
Acknowledgements	3
Table of Contents	4
List of Figures	6
List of Tables	7
Abbreviations	8
Chapter 1. Introduction	
1.0 The Historical Context of Nucleic Acid Research	11
1.1 A Modern Understanding of Nucleic Acids	12
1.2 The Flow of Genetic Information	14
1.3 Furanose Conformation	14
1.4 Oligonucleotide-based Therapeutics	15
1.5 Antisense Gene Silencing	15
1.6 RNA interference	16
1.7 Chemical Modifications of Oligonucleotide for Therapeutics	18
1.8 Oligonucleotide Modifications in RNAi	18
1.9 Backbone Modifications	18
1.10 Sugar Modifications	19
1.11 Flexibility and Enzymatic Recognition	21
1.12 Thesis Objectives	22
1.13 References	22
Chapter 2. Experimental Materials and Methods	
2.1 General Methods	
2.1.1 General Reagents	28
2.1.2 Chromatography For Nucleosides And Intermediates	28
2.1.3 Instruments	28
2.2 Synthesis of 3'-Deoxy-3'-Thiothymidine Nucleoside and its 3'-S-Phosphorothioamidite Derivative	
2.2.1 5'-O-P-Monomethoxytritylthymidine (3.2)	29
2.2.2 3'-O-Methanesulphonyl-5'-(monomethoxytrityl)thymidine (3.3)	29
2.2.3 2,3'-dideoxy-5'-(monomethoxytrityl)anhydrothymidine (3.4)	30
2.2.4 3'-Acetylthio-3'-deoxy-5'-(monomethoxytrityl)thymidine (3.5)	30
2.2.5 3'-deoxy-3'-thio-5'-(monomethoxytrityl)thymidine (3.6)	30
2.2.6 3'-deoxy-5'-Monomethoxytritylthymidine-3'-S-phosphorothioamidite (3.8)	31
2.3 Oligonucleotide Synthesis	
2.3.1 General Reagents	31
2.3.2 Derivatization of Solid Support	32
2.3.3 General Automated Solid-Phase Synthesis of Oligonucleotides	32
2.4 Deprotection and Purification of Oligonucleotides	
2.4.1 General Reagents	33
2.4.2 Cleavage from CPG and Deprotection of Oligomers	34
2.4.3 Analysis and Purification by Polyacrylamide Gel Electrophoresis	34
2.4.4 Reversed-Phase HPLC Analysis and Purification of	35

	Oligonucleotides	
	2.4.5 Anion-Exchange HPLC Analysis of Oligonucleotides	35
	2.4.6 Desalting of Oligonucleotides	36
2.5	Characterization of Oligonucleotides	
	2.5.1 Characterization of Oligonucleotides by Mass Spectrometry	36
	2.5.2 UV-Thermal Denaturation of Oligonucleotides	36
	2.5.3 Circular Dichroism Spectroscopy (CD)	37
2.6	Biological Studies	
	2.6.1 RNAi Transfection	37
	2.6.2 Luciferase Activity Assay	38
	2.6.3 Luciferase mRNA Quantitation	38
2.7	References	38

Chapter 3: Synthesis of 3'-Deoxy-3'-thiothymidine and Its Incorporation into Oligonucleotides

3.1	Relevance of 3',5'-Linked 3'-S-Phosphorothiolate Linkages	39
3.2	Synthesis of 3'-Deoxy-3'-thiothymidine	39
3.3	Synthesis of Oligonucleotides Containing 3'-Deoxy-3'-thiothymidine Inserts	42
3.4	Activators for 3'-Thio Coupling	43
3.5	Oxidants for the Preparation of dT ₁₂ Containing a Single 3'-S-dT Unit	44
3.6	Alternative Phosphitylation Conditions	47
3.7	Phosphorothioamidite Stability	48
3.8	Optimised Synthesis Conditions for Oligonucleotides Containing 3'-Deoxy-3'-thiothymidine	49
3.9	References	49

Chapter 4: Physical and Biological Characterisation of Oligonucleotides Containing 3'-S-Phosphorothiolate Linkages

4.1	Introduction	52
4.2	3'-Phosphorothiolate Linkages and Conformation	52
4.3	A Library of Modified RNA Duplexes Containing 3'-Thio Linkages	53
4.4	Conformation and Thermal Stability of Duplexes	57
4.5	Analysis of Oligonucleotide Conformation by Circular Dichroism (CD)	61
4.6	Evaluation of the Gene Silencing Activity of 3'-thio modified siRNA	63
4.7	Conclusion	67
4.8	References	68

	Contribution to Knowledge	70
	Appendix 1: NMR Spectra	71
	Appendix 2: T_m & Thermodynamic Data	73
	Appendix 3: CD Data	76

List of Figures

	page
Chapter 1. Introduction	
Figure 1.1: Structure of DNA and RNA Oligonucleotides	12
Figure 1.2: Helical Structure of Duplex DNA	12
Figure 1.3: Watson-Crick Base Pairing Specificity in DNA Nucleobases	13
Figure 1.4: Furanose Conformation Preferences in DNA and RNA	14
Figure 1.5: RNAi Pathway	16
Figure 1.6: Schematic of siRNA Sequences	17
Figure 1.7: Four Common <i>Ribo</i> Modifications	20
Figure 1.8: Four Common 2'-Deoxy Modifications	21
Figure 1.9: Butanediol and 2',3'-Secouridine	22
Chapter 2: Experimental Materials and Methods	
Figure 2.1: Schematic of DNA Synthesiser Solid-Phase Synthesis of Oligonucleotides	33
Chapter 3: Synthesis of 3'-Deoxy-3'-thiothymidine and Its Incorporation into Oligonucleotides	
Figure 3.1: Cosstick's Synthetic Scheme for 3'-Deoxy-3'-thiothymidine and its Incorporation into a Dinucleotide	40
Figure 3.2: 3'-Deoxy-3'-(thioacetyl)thymidine Synthetic Scheme	40
Figure 3.3: Free Thiol and Disulfide Species Synthetic Scheme	41
Figure 3.4: 3'-S-Phosphorothioamidite Synthetic Scheme	42
Figure 3.5: Comparison of Oxidants for 3'-Thio Oligonucleotide Synthesis	44
Figure 3.6: Comparison of Oxidants Systems in the Preparation of dT ₁₂ Containing a Single 3'-S-Phosphorothiolate Linkage	45
Figure 3.7: HPLC trace of Crude Oligoribonucleotides	46
Figure 3.8: Schematic Illustration of Three Phosphitylation Methods	47
Figure 3.9: ³¹ P NMR of Phosphorothioamidite	48
Chapter 4: Physical and Biological Characterisation of Oligonucleotides Containing 3'-S-Phosphorothiolate Linkages	
Figure 4.1: Melting Temperature (<i>T_m</i>) Signatures of 5 Representative RNA:RNA Duplexes	59
Figure 4.2: CD Spectra of Native and Modified RNA:RNA Duplexes	62
Figure 4.3: CD Spectra of Guide and Passenger Strand Modified RNA:RNA Duplexes	63
Figure 4.4: RNAi Activity of Duplexes Modified Only on the Guide Strand	64
Figure 4.5: RNAi Activity of 3'-Thio Modified Passenger Strand with Native or Modified Guide Strands	65
Figure 4.6: RNAi Activity of Modified Passenger Strand with Native or Modified Guide Strands	67

List of Tables

	page
Chapter 1. Introduction	
Table 1.1: Characteristic Parameters Oligonucleotide Helices	13
Chapter 2: Experimental Materials and Methods	
Table 2.1: Reagents for Solid-Phase Synthesis of Oligonucleotides	33
Chapter 3: Synthesis of 3'-Deoxy-3'-thiothymidine and Its Incorporation into Oligonucleotides	
Table 3.1: Prevention of Disulfide Formation with DTT	41
Table 3.2: A Comparison of the pK_a and Structure of Relevant Activators	43
Table 3.3: Oxidants for the Preparation of Thymidylic Acid (12 mer) Containing a Single 3'-S-dT Residue	45
Table 3.4: Comparison of Overall Coupling Efficacy for Mixed Sequence 21mers with 2 Oxidants	46
Table 3.5: Comparison of Coupling Efficacy for Alternative Phosphitylation Methods with dT-12mers	48
Table 3.6: Optimised Conditions for 3'-S-Phosphorothioamidite Coupling	49
Chapter 4: Physical and Biological Characterisation of Oligonucleotides Containing 3'-S-Phosphorothiolate Linkages	
Table 4.1: Mass Spectral Characterization of Selected Oligonucleotide Strands Used to Create the siRNA Duplex Library	54
Table 4.2: An Inventory of Duplexes with a Native RNA Passenger Strand and a Modified RNA Guide Strand	55
Table 4.3: An Inventory of Duplexes with a Native RNA Guide Strand and a Modified RNA Passenger Strand	56
Table 4.4: An Inventory of Duplexes with a 3'-Thio Modified RNA Guide Strand and a Modified RNA Passenger Strand	57
Table 4.5: Melting Temperatures (T_m) of dT and 3'-S-dT Modified Duplexes	60
Table 4.6: Melting Temperatures (T_m) of 3'-Thio and 2'-OMe Modified Duplexes	60
Table 4.7: Melting Temperatures (T_m) of Guide Strand Mismatches	61

Abbreviations

A	adenine
Å	angstrom
LNA	α -D-Locked Nucleic Acid
ANA	arabinonucleic acid
AON(s)	antisense oligonucleotide(s)
APS	ammonium persulfate
BPB	bromophenol blue
BTT	5-benzylthio-1-H-tetrazole
BzCl	benzoyl chloride
C	cytosine
©	copyright
CaH ₂	calcium hydride
CD	Circular Dichroism
CE	β -cyanoethyl
CH ₂ Cl ₂	methylene chloride
CH ₃ CN	acetonitrile
CPG	controlled pore glass
d	d doublet (NMR)
dd	doublet of doublet (NMR)
<i>d</i> ₆	six deuterium atoms
DCI	4,5-dicyanoimidazole
ddH ₂ O	double distilled water
Δ H	enthalpy variation
Δ S	entropy variation
DEPC	diethyl pyrocarbonate
DIPEA	N,N-diisopropylethylamine
DMAP	4-dimethylaminopyridine
DMSO	dimethyl sulfoxide
DMT	4,4' - dimethoxytrityl
DNA	deoxyribonucleic acid
ds	double stranded
<i>E. coli</i>	<i>Escherichia coli</i>
e.g.	for example
ϵ_{260}	molar extinction coefficients at 260
EDTA	ethylene-diamine tetraacetate dihydrate
eq	equivalent(s)
EtOH	ethanol
2'-FANA	2'-deoxy-2'-fluoro- β -D-arabinonucleic acid
g	gram
mg	milligram
μ g	microgram
G	guanine
h	hour(s)
HBTU	O-(benzotriazol-1-yl)-1,1,3,3-tetramethyluronium hexafluorophosphate
HOAc	acetic acid
HPLC	anion exchange liquid phase chromatography
<i>i.e</i>	that is

J	coupling constant
KCl	potassium chloride
l	path length of a UV cell
mL	milliliter
μL	microliter
λ	wavelength
LCAA	succinyl-derivatized long chain alkyl amine
M	molar
mM	millimolar
μM	micromolar
m	multiplet (NMR)
MeOH	methanol
MgCl ₂	magnesium chloride
min	minute(s)
MHz	mega hertz
mmol	millimole
μmol	micromole
MMT	monomethoxytrityl group
MMTCl	p-anisylchlorodiphenylmethane
mol	mole
<i>m/z</i>	mass to charge ratio
NaClO ₄	sodium perchlorate
Na ₂ HPO ₄	disodium hydrogen phosphate
NaHCO ₃	sodium bicarbonate
Na ₂ SO ₄	anhydrous sodium sulphate
NH ₄ OH	ammonium hydroxide
nm	nanometer
NMI	N-methylimidazole
NMR	nuclear magnetic resonance
OD	optical density
2'-O-MOE	2'-O-methoxyethyl
³² P	phosphorus 32
PAGE	polyacrylamide gel electrophoresis
ppm	parts per million
®	registered trademark
R _f	retention factor
RISC	RNAi induced silencing complex
RNA	ribonucleic acid
pre-mRNA	precursor messenger RNA
mRNA	RNA messenger
RNAi	RNA interference
siRNA	short interfering RNA
RNase H	ribonuclease H
s	s singulet (NMR)
t	t triplet (NMR)
T	thymine
TBAF	<i>tert</i> -butylammoniumfluoride
TBDMS	<i>tert</i> -butyldimethylsilane
TCA	trichloroacetic acid
TEA	triethylamine
TEMED	N,N,N',N'-tetramethylethylenediamine

THF	tetrahydrofuran
TLC	thin layer chromatography
T_m	melting temperature
TREAT-HF	triethylamine trihydrofluoride
Tris	2-Amino-2-(hydroxymethyl)-1,3-propanediol
™	trademark
U	uracil
UV	ultraviolet
UV-Vis	ultraviolet visible
V	volt(s)
v/v	volume per volume

Chapter 1: Introduction

1.0 The Historical Context of Nucleic Acid Research

The last half-century of explosive advances in genetics and biology were initiated by 2 contemporaries, Gregor Johann Mendel and Charles Darwin. The latter was greatly interested in mechanism of natural selection, first published in the *On the Origin of Species* in 1859,¹ but he did not attempt to explain how inheritance occurs. In contrast, Mendel studied the inheritance of traits in pea plants, presenting his observations as a special case in 1865.² These two great scientists were peripherally aware of each other's work, but the molecular and biological connections between their observations did not become apparent for some time.

As early as 1874, the necessity of a molecule to carry genetic information from one generation to another had been identified,³ but proved difficult to characterise. Although 2'-deoxyribonucleic acid (DNA) was known, having been discovered and characterized along with ribonucleic acid (RNA) by Friedrich Miescher in 1869,^{4,5} it was thought to be too simple to carry such complex information and the multitudinous variety of proteins was long thought to contain the key substance.

The discovery of DNA's true role started when Fred Griffith, who was engaged in the classification of streptococcal types, published his observations on the transformation of rough, attenuated *pneumococcus* to the smooth, virulent form through exposure to heat-killed *S. pneumococci* in 1928. This stimulated Oswald Avery and colleagues to examine the mechanism of transformation and thus identify DNA as the carrier of genetic information in 1944.⁶

The four component nucleotide bases, adenine, cytosine, guanine and thymine, (A, C, G and T) were readily identified but the structure of DNA was long obscured by the fact that most higher organisms have essentially equal amounts each type of base. This coincidence was circumvented in the late 1940s when Chargaff and his colleagues⁷ analysed the DNA from yeast and tubercle bacilli and found the G + C content to range from 36 % to 70%, highlighting the constant, near-unity ratios of A/T and G/C. The other essential piece that set the stage for elucidation of the structure of DNA was the excellent crystallographic work of Rosalind Franklin and co-workers in 1953.⁸

Shortly thereafter, James Watson and Francis Crick published their structure of DNA⁹ and (cleverly) hypothesized how it might explain the chemical mechanism by which cells could dependably pass on their characters to their daughter cells.^{9, 10} M. R. Pollock, in his 1970 address to the General Meeting of the Society for General Microbiology, identified Watson and Crick's finding as the "*culminating point in one of the most fundamental and important discoveries in*

biology of all time. This [is] because it not only shows how living systems replicate themselves (and not something different) but has led directly to an understanding of how their functional characters are expressed."¹¹ A greater understanding of this mechanism forms the basis of modern genetics and has enabled the work contained in this thesis.

1.1 A Modern Understanding of Nucleic Acids

DNA is a linear polymer of nucleotides, each consisting of a 2-deoxyribose pentafuranose ring with a pendant heterocyclic base, linked by negatively charged 3',5'-phosphodiester units. The 4 planar heterocyclic bases attach in a β orientation to the 1' position of the sugar; adenine (A) and guanine (G) are purines, consisting of two fused rings, thymine (T, found only in DNA), uracil (U, equivalent of T for RNA) and cytosine (C) are the monocyclic pyrimidines, as shown in **Figure 1.1**. The presence of a nitrogen atom in the ring confers the basic character of the nucleobases which are unprotonated at physiological pH.

The structure of RNA is analogous, with ribose in the pentafuranose form. As such, RNA is more sensitive towards chemical or enzymatic hydrolysis through participation of the 2'-hydroxyl group.

Figure 1.1: Structure of DNA and RNA Oligonucleotides

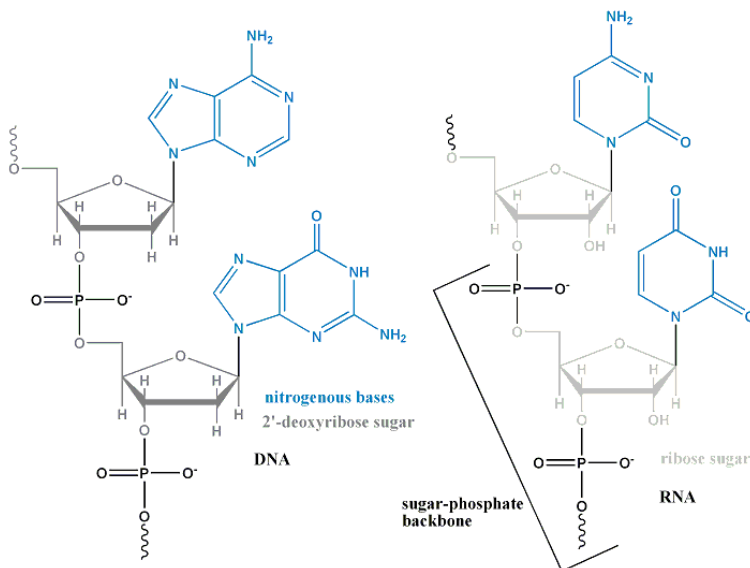
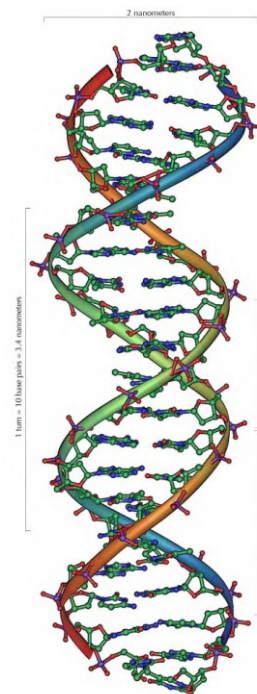
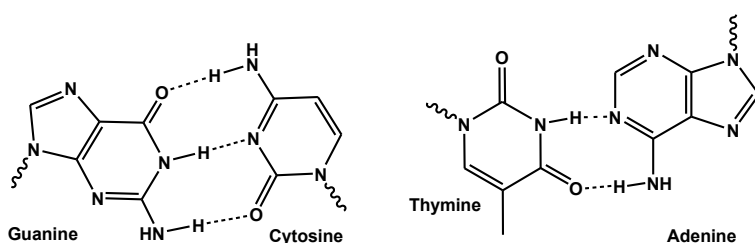


Figure 1.2: Helical Structure of Duplex DNA¹²



DNA exists principally in a double-stranded form (ds), where 2 complementary oligonucleotides hybridise in an anti-parallel fashion to form gently twisting ladder, as shown in **Figure 1.2**. This association is non-covalent and achieved through hydrogen bonds between complementary nitrogenous bases, called Watson-Crick base pairing, shown in **Figure 1.3**, as well as the π -stacking of neighbouring bases. The redundancy of structure confers fidelity to the storage of genetic information, as damage in one strand can be repaired by ‘reading’ the code of the complementary strand.

Figure 1.3: Watson-Crick Base Pairing Specificity in DNA Nucleobases



RNA has a much shorter cellular lifetime than DNA, and as it is not the depository of information between generations, it exists predominantly in the single stranded form (ss). When RNA does form a duplex with itself, the 2'-hydroxyl group cause changes in the parameters of the helical structure, as outlined in **Table 1.1**. A hybrid duplex between RNA and DNA, or duplexes containing modified bases generally have intermediate parameters.

Table 1.1: Characteristic Parameters Oligonucleotide Helices

	A form helices ¹³	B form helices ¹³
Classic Presentation	RNA:RNA	DNA:DNA
Helical sense	Right	Right
Residues per turn of the helix	11	10.4
Rise per base pair (bp)	2.56 Å	3.3 – 3.4 Å
Helix diameter	25.5 Å	23.7 Å
Major groove dimensions	Narrow and deep	Wide and deep
Minor groove dimensions	Broad and shallow	Narrow and deep
Sugar conformation	C3'-endo (<i>North</i>)	C2'-endo (<i>South</i>)
Base tilt	20°	-6°

1.2 The Flow of Genetic Information

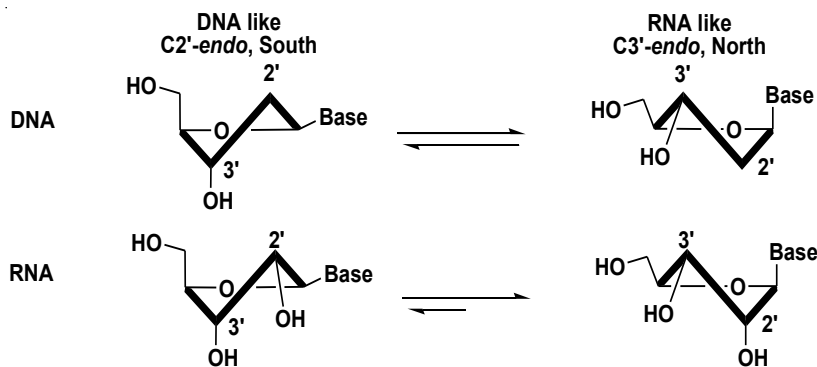
The process by which the information stored in DNA is expressed as functional proteins is an elegant and elaborate system. The role of RNA in protein synthesis had been suspected since 1939, based on experiments carried out by Torbjörn Caspersson, Jean Brachet and Jack Schultz, but was not confirmed until Hubert Chantrenne experiments on the messenger role played by RNA in the synthesis of proteins in ribosome in 1965.¹⁴ In the initial step, *transcription*, a short section of the DNA duplex is unwound and the sequence of a section of exposed single-stranded DNA is *transcribed* into precursor messenger RNA (pre-mRNA). The pre-mRNA is then spliced to remove non-coding sections (introns) and the remaining coding sequences (exons) are ligated to form a single strand of mature mRNA. The mRNA then migrates out of the nucleus to the cytoplasm, where the start codon (AUG, 5'-end of mRNA) is recognised by the ribosomal machinery and the sequence of bases is *translated* into a nascent protein by the successive addition of amino acids coordinated by transfer RNA (tRNA).

1.3 Furanose Conformation

The sugar moiety in nucleic acids is known to exist in rapidly inter-converting equilibrium between two extreme conformers, called *north* and *south*. The position of this equilibrium is influenced by an anomeric effect between the sugar ring oxygen and the nucleobase that favours a *north* conformation, and by several *gauche* effects, in particular between the 2' or 3' substituent and the ring oxygen, that favour a *north* conformation in RNA and *south* conformation in DNA. The anomeric effect predominates in mainly *north* RNA, with the additional *gauche* effects due to the 2' oxygen reinforcing this conformation, as shown in **Figure 1.4**.

The conformation of the monomers, *south* or *north*, dictate the global conformation of the helix formed by double-stranded nucleic acids and this has been shown to be very important for recognition by enzymes.

Figure 1.4: Furanose Conformation Preferences in DNA and RNA¹³



1.4 Oligonucleotide-based Therapeutics

Greater understanding of the central role of nucleic acids in cellular functions has led, naturally, to the desire to attack disease by the regulating gene expression of components in the disease pathway. The specificity and universality of Watson-Crick base pairing has identified chemically modified oligonucleotides as innovative therapies to achieve gene regulation or gene silencing, through exploitation of the RNA interference (microRNA, siRNA) and antisense pathways. A brief review of these latter two biological pathways is presented in the following sections. The idea of oligonucleotide-based antisense therapy dates back to the 1960s when Nirenberg *et al.* first demonstrated that hybridization of polyribouridylic acid with a complementary oligoadenylate prevented the translation of the ribouridylic acid into polyphenylalanine and established that oligonucleotide single-strandedness is required for protein biosynthesis.¹⁵

Using modified oligonucleotides as drugs to target and degrade specific mRNA sequences involved in disease pathways is attractive for several reasons: first it offers high specificity due to Watson-Crick base pairing; second, less drug is necessary as degrading a single mRNA will prevent the translation of multiple protein molecules; third, oligonucleotides can silence disease-causing genes that encode so called “non-druggable targets”, which are not amenable to conventional therapeutics such as small molecules, proteins or monoclonal antibodies; and finally, the base sequences of the oligonucleotide drug can readily be adapted to respond to mutations in the mRNA sequence.

1.5 Antisense Gene Silencing

The antisense approach to the down regulation of genes involves the activation of ubiquitous enzyme ribonuclease H (RNase H), which has been identified in viruses, bacteria, and eukaryotes,¹⁶ through the introduction of a DNA-like oligonucleotide. This strand is called an *antisense* strand because it is *anti*-parallel to the *sense* mRNA target. When these 2 strands hybridise to form a DNA/RNA hybrid duplex, the resulting complex can inhibit or prevent RNA transport, splicing or translation and, crucially, may trigger degradation by RNase H.^{17, 18} RNase H selectively cleaves the mRNA strand of DNA:RNA duplex,¹⁹ releasing the antisense strand to find another complementary mRNA and amplify its effect in a catalytic manner.

As native DNA is highly susceptible to nucleases, and therefore can only exert an antisense effect for a brief time,^{20, 21} several modifications have been investigated. These modifications must attempt to overcome several hurdles, including specificity/selectivity of mRNA recognition, biochemical stability (particularly against nucleases²²), affinity for target

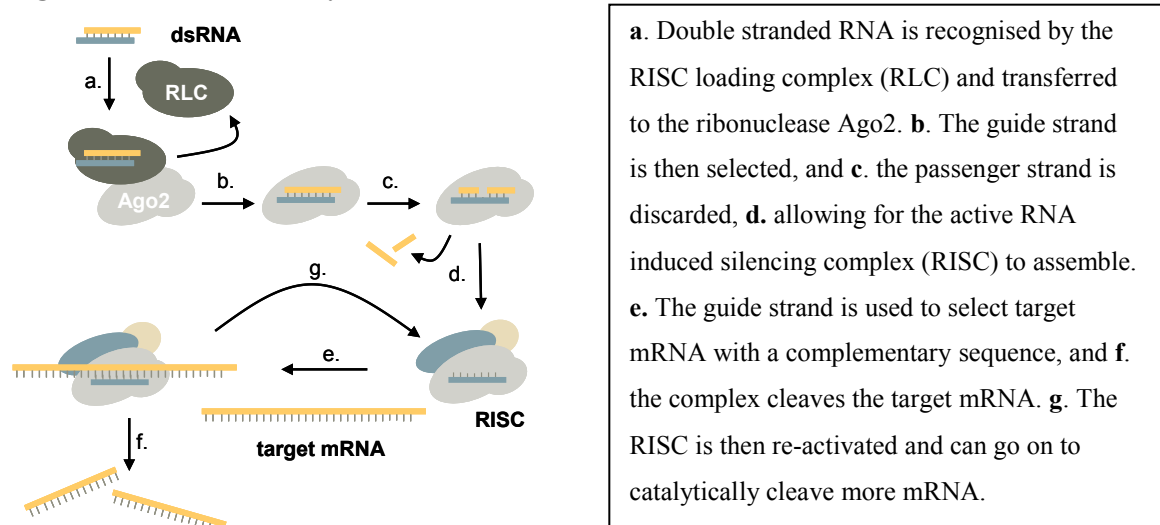
mRNA,²² cell uptake,²³ and finally, the ability to retain or improve RNase H activation.¹⁹ This last requirement is highly exigent and has resulted in disqualifying many likely candidates.

1.6 RNA interference

The RNA interference (RNAi) pathway is a relative newcomer to the field of oligonucleotide therapeutics, having been first reported by Andrew Fire and Craig Mello in 1998,²⁴ but its huge impact and wide use were promptly recognised by the awarding of the 2006 Nobel Prize in physiology or medicine. This pathway likely evolved as a defence mechanism against viral or bacterial invasions and has been identified in worm,²⁴ plant²⁵ and mammalian cells.²⁶ RNAi researchers have been able to take advantage of much of what was learned from the antisense strategy, allowing for the rapid development of methods that exploit RNAi. Several new reviews discuss recent advances, noting that although siRNA is still primarily used for gene function analysis, RNAi-based technologies are rapidly advancing to the clinic.^{27,28}

The mechanism of RNAi, shown in **Figure 1.5**, involves the selection of a guide strand from a short section of double stranded RNA and its use, through the RNA-induced silencing complex (RISC), to recognise and degrade target RNA.

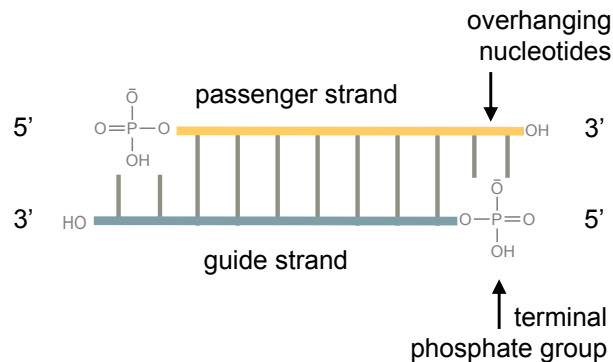
Figure 1.5: RNAi Pathway



The RNAi pathway is triggered by long double-stranded RNA (dsRNA)²⁴ which is cleaved into 21-25 nucleotides segments^{26, 29, 30} by an endogenous dsRNA specific RNase III enzyme called Dicer.³¹ These 21-25 nucleotide lengths of dsRNA are referred to as small interfering RNA (siRNA) and this is the length generally used for synthetic oligonucleotides therapeutics.²⁶ Using these shorter lengths avoids triggering the antiviral/interferon responses

caused by oligonucleotides longer than 30 base pairs, which can result in a global shut-off in protein synthesis as well as non-specific mRNA degradation.³² The most effective siRNA sequences have been found to possess two nucleotides overhangs at the 3'-end of each strand, as well as 5'-monophosphate and 3'-hydroxyl groups,^{29, 33} as shown in **Figure 1.6**.

Figure 1.6: Schematic of siRNA Sequences



The siRNA is taken up by a protein complex, called an RNA-induced silencing complex (RISC). RISC contains members of the highly diverse family of Argonaute proteins, characterized by the presence of the Piwi-Argonaute-Zwille (PAZ) and PIWI domains.³⁴ Ago2 is involved in the selection of the guide strand, through the asymmetric, ATP-dependant, unwinding of duplex.³⁵⁻³⁷ The guide strand is then used to recognize and bind RNA containing its complementary sequence, resulting in the cleavage of the target RNA by an endonuclease present in the complex.^{35, 37, 38} The endonuclease appears to be similar in structure to other known RNase H enzymes.³⁹ Synthetic ONs have been shown to achieve greater gene silencing through the siRNA pathway than the antisense pathway.^{26, 40-42}

Although only experimental testing can determine the most effective siRNA for a given target,²⁷ several design considerations for optimizing siRNA efficacy have been identified; a 30%–52% guanine-cytosine (GC) content, lack of secondary structure and homology with unintended targets in both the guide and target strands, lack of immuno-stimulatory sequences, and the presence or absence of certain bases at certain positions.²⁷ Other considerations include keeping the length under the 30-nt threshold for preventing triggering of an interferon response,²⁶ and introducing terminal phosphorothioate linkages or inverted abasic residues to provide some protection against exonuclease digestion.^{43, 44} It has been shown that the strand most easily unwound from its 5'-end is preferentially incorporated into RISC.^{45, 46} Thus, a design which ensure lower thermodynamic stability at the 5'-terminus of the desired guide strand is essential,²⁷ as either strand could potentially be selected.⁴⁵⁻⁴⁷

Although direct comparisons of different gene silencing methods are scarce, RNAi has generally been found to be more effective than antisense or ribozymes. One study found RNAi, which also produced more sustained silencing, to be 100-1000 fold more efficient than an phosphorothioate modified antisense optimized for the same target mRNA.⁴⁸

1.7 Chemical Modifications of Oligonucleotide for Therapeutics

Six key criteria have been identified for a successful oligonucleotide-based therapeutic: (i) it can be synthesized easily and in bulk; (ii) is stable *in vivo*; (iii) is able to enter the target cell; (iv) is retained by the target cell; (v) is able to interact with the cellular target; and (vi) it should not interact in a non-sequence-specific manner with other macromolecules.¹⁸

This thesis work considers factors related to the final 2 points in RNAi; particularly that the oligonucleotide forms stable and highly specific bonds with target mRNA, and are recognised and cleaved by the requisite enzymes in the RNAi pathway. Unfortunately the requirements of these 2 criteria are often in opposition, as constraining the sugar conformation favours the first but increased rigidity, due to sterics or electronics, interferes with the second. This theme will be further developed in the following sections.

1.8 Oligonucleotide Modifications in RNAi

Modifications to nucleotides can be classified under 3 categories; those involving the heterocyclic base, the sugar and the phosphodiester backbone. Many chemical modifications have been explored within the more mature field of antisense,⁴⁹⁻⁵¹ with particular focus on modifications at the C2' position of the sugar moiety.⁵² Many of the lessons learned with antisense can be transferred to RNAi as long as the differences in their mechanism of actions (cellular pathways) are considered. For both RNAi and antisense, an adequate melting temperature (T_m) with a complementary mRNA strand is a primary requirement.⁵⁰ Several comprehensive reviews of chemical modification in RNAi are available^{49, 53, 54} and the following sections present a selection of some relevant sugar and backbone modifications.

1.9 Backbone Modifications

The phosphorothioate backbone (PS), in which a sulphur atom replaces a non-bridging oxygen atom in the natural phosphodiester (PO) backbone, appears to extend the biological lifetime of synthetic oligonucleotides,⁵⁵ however this beneficial effect is partly due to association with serum and cell proteins which may contribute to its relatively high toxicity^{56, 57} and issues regarding non-sequence specific interactions.^{57, 58} It is recognised as a substrate for RNase H⁵⁹

which is essential to the antisense pathway and has been tested in human clinical trials.^{60, 61} The PS-DNA drug VitraveneTM, developed for the treatment of human cytomegalovirus (CMV) induced retinitis, is the first and only antisense drug available in the clinic.⁶² Additionally, the diastereomeric nature of the phosphorothioate (PS) linkage has proved useful as a probe for studying the stereochemical course of enzymatic reactions,⁶³ to locate protein-nucleic acid interactions,⁶⁴⁻⁶⁶ probe for metal ion-phosphate interactions,⁶⁵ investigate the structure of the substrate metal-ATP complex,⁶⁵ elucidate DNA structure, and for studying the involvement of cAMP in biological systems.⁶⁷ Unfortunately PS-DNA does not form strong duplexes with RNA⁶⁸ and is therefore less commonly used for RNAi strategies.

Another common modification is DNA or RNA strands containing 2',5'-linked phosphodiester linkages; 2',5'-RNA is found in some biological processes such as RNA splicing^{69, 70} and has also been investigated for the down-regulation of gene expression.⁷¹ For instance, DNA/2'5'-RNA chimeras and 2'5'-DNA show less non-specific binding to plasma and cellular proteins minimizing toxicity in the antisense application.⁷¹ A comparison of thermal melting temperatures (T_m) reveals the low duplex stability⁷² of 2',5'-RNA for mRNA and therefore lack of relevance to RNAi: RNA:RNA > DNA:DNA \approx DNA:RNA > RNA:2',5'-RNA > 2',5'-RNA: 2',5'-RNA > DNA: 2',5'-RNA (undetected).⁷³

1.10 Sugar Modifications

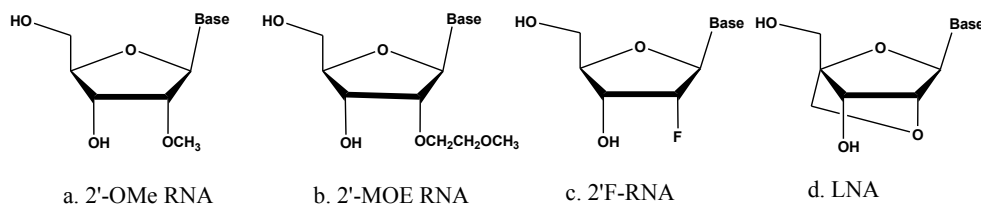
The formation of oligonucleotide duplexes is enthalpically favoured due to the hydrogen bonding interactions and stacking of the heterobases, although the increased order of the duplex structure is entropically unfavoured. Pre-organisation of the nucleotide is believed to reduce the entropy loss during duplex formation⁷³ while favoring base stacking and base-base hydrogen bonding (enthalpic gain).

It then follows that RNA-like nucleotides that favour *north* sugar conformations found in the highly stable RNA:RNA duplexes bind strongly to mRNA.⁵² Many analogs with this conformation have been constructed through modification at the 2'-carbohydrate position. Ribonucleotides with 2'-O-methyl (2'-O-Me), 2'-O-methoxyethyl (2'-O-MOE), and 2'-O-fluoro (2'-F-RNA) groups preferentially adopt *north* sugar conformations, shown in **Figure 1.7**, as this maintains the gauche effect between the electronegative atom at the 2' position and the ring oxygen. These modifications have been shown to increase the melting temperature (T_m) of RNA/RNA duplexes by 1.7, 2, and 3°C per modification, respectively.⁷⁴

“Locked” nucleic acid (β -D-LNA), **Figure 1.7**, contains a 2'-O, 4'-C-methylene bridge that forces the sugar to adopt a *north* conformation. This popular modification was developed

independently by Jesper Wengel's⁷⁵ and Takeshi Imanishi's research groups⁷⁶ with the goal of inducing high mRNA binding affinity via structural pre-organization of the sugar-phosphate backbone.⁷⁷ While this rigidity results in a stabilization of duplexes by at least 3°C per modification,⁷⁸ it may have a negative impact on nucleic acid:protein interactions. This aspect will be discussed in the following sections.

Figure 1.7: Four Common *Ribo* Modifications



Modified 2'-deoxynucleotides can also be induced to prefer a *north* conformation. For instance, 2'-deoxy-2'-fluoroarabinonucleic acids (2'F-ANA), **Figure 1.8**, favour a *south/east conformation* and have been shown to increase the melting temperature (T_m) of duplexes,⁷⁸ triplexes⁷⁹ and C-rich tetrads⁷⁹ by approximately 1°C per modification, although the nature of this stabilization is not well understood at present.

Substitution of the 3'-oxygen by nitrogen results in a relatively rigid N3'-P5' phosphoramidate backbone^{80, 81} and induces a *north* conformation in the pentafuranose ring.⁸⁰ Melting temperatures (T_m) of duplexes formed by an entirely modified poly(dA), poly(A) and a mixed-base 10mer were found to be higher relative to the corresponding unmodified sequences. The effect was the same whether the target strand was DNA or RNA.⁸²

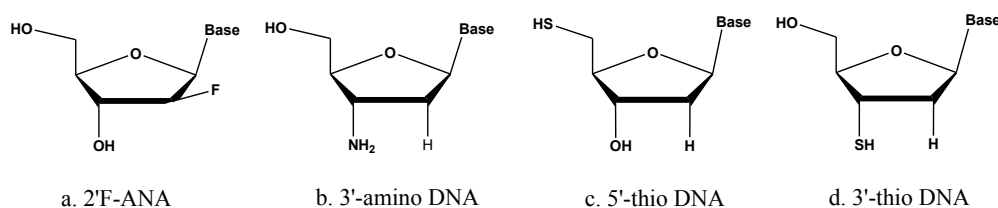
The isomeric sulphur linkage where one of the two bridging oxygen atoms in the phosphodiester linkage is replaced has received considerably less attention. This modification, **Figure 1.8**, was pioneered by Reist and co-workers, who in 1964 reported the synthesis of 5'-deoxy-5'-thiothymidine and 5'-deoxy-5'-thiouridine.⁸³ The first examples of oligo-5'-deoxy-5'-thionucleotides were reported by Chladek in 1972.⁸⁴ This modification displays resistance to hydrolysis by various exo and endonucleases,^{85, 86} and has been used in mechanistic studies of the hammerhead ribozyme.⁸⁷ More recently, our group has investigated the physicochemical and RNase H inducing properties of oligonucleotides containing 5'-deoxy-5'-thiothymidine units.⁸⁸ The conclusion stemming from these studies is that the 5'-S nucleotides maintain a typical deoxynucleotide *south* conformation.⁸⁹

The incorporation of 3'-thionucleosides in DNA oligonucleotides has been led by the research group of Prof. Richard Cosstick at the University of Liverpool. The benefits of this

modification, as enumerated by Cosstick, are that it is achiral, isopolar and isosteric with the natural congener. This thesis examines for the first time the physicochemical and biological properties of RNA strands incorporating 3'-deoxy-3'-thiothymidine units. As we will return to the characteristics of this modification in Chapter 3 in more detail, this brief introduction will suffice here.

A full slate of modified nucleosides have been introduced into siRNA duplexes. 2'-fluororibose substitutions have been found to be generally well tolerated,⁹⁰ although some reduction of silencing has been reported.⁴³ Incorporation of selected 2'-O-Me or 2'-deoxy residues^{91,92} or PS linkages⁴³ maintained silencing with some increase in resistance to nucleases,^{33,49} whereas full substitution significantly reduced silencing.⁹² Some cytotoxicity has also been reported with phosphorothioate (PS) linkages.⁹³

Figure 1.8: Four 2'-Deoxy Modifications



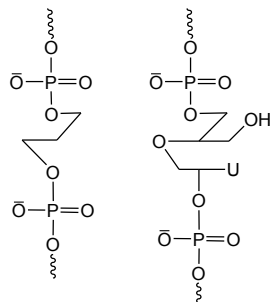
1.11 Flexibility and Enzymatic Recognition

Correct strand pre-organisation is desirable because it leads to more stable and faithful duplex hybridization, of which LNA's striking affinity towards RNA targets is an excellent example. The rigid LNA backbone impedes RNase H enzymatic cleavage, whereas LNA/DNA oligonucleotides are poor substrates at best.⁹³ Chimeric oligonucleotides containing both 2'-FANA and DNA units were found to be more potent antisense molecules than a fully modified 2'-FANA oligomer.⁹⁴ This suggests that the more flexible DNA units promote RNase H activity. In fact, introduction of a single deoxynucleotide unit within a 2'-FANA strand is sufficient to impart flexibility and enhance RNase H activity.^{59,95}

Dr. Maria Mangos from our laboratory expanded on this theme by inserting acyclic moieties such as 2',3'-secouridine or butanediol, **Figure 1.9**, and found that both significantly enhanced the target RNA cleavage by RNase H.⁹⁵ Unfortunately, a significant drop in thermal stability was observed with these sequences as compared to DNA and was believed to be a consequence of the high flexibility of the linker. This underlines the importance of maintaining a balance between flexibility and rigidity in synthetic therapeutic oligonucleotides. Flexibility may be essential to accommodate that unnatural shape of modified nucleotides in tight enzymatic

pockets and a combination of pre-organization and flexibility appears to be the key to high enzymatic efficiency.⁹⁶⁻¹⁰¹

Figure 1.9: Butanediol and 2',3'-Secouridine



1.12 Thesis Objectives

Our research group has been interested in the design^{95, 100, 102-105} and characterization of the structural and biological properties⁹⁵ of synthetic nucleic acids, particularly for use in antisense and more recently the RNAi strategies. Previous work in our laboratory have demonstrated that a combination of pre-organization and flexibility has a beneficial effect on RNase H efficiency and the current work attempts to extends this to the RNAi pathway. In doing so, this thesis reports improvements to the synthesis of 3'-deoxy-3'-thiothymidine and the first incorporation of this modified nucleoside into RNA oligonucleotides. Because this modification mimics the structure of ribonucleosides (*north* pucker), we thought it would be compatible with the RNAi cellular pathway. As such, we hoped it would provide solutions to some of the challenges facing siRNA therapeutics (e.g., enhanced cellular activity). By synthesizing a small library of modified siRNAs, the impact of the 3'-S modification in the thermal stability and gene silencing activity of siRNA were examined for the first time. Particular substitutions at the scissile position of the passenger strand of siRNA duplexes enabled a closer examination of the mechanism of RISC cleavage.

1.13 References

- 1 Darwin, C., *On The Origin of Species by Means of Natural Selection, or The Preservation of Favoured Races in the Struggle for Life*. First Edition ed.; John Murray: London, 1859; 'Vol.' p.
- 2 Mendel, G., Experiments on Plant Hybridization (German: Versuche über Pflanzen-Hybriden). *Verh. Naturforsch. Ver. Brünn* **1866**, 4, 3–47.
- 3 Miescher, F., Die Spermatozoen einiger Wirbelthiere, Ein Beitrag zur Histochemie., *Verh. Nat.forsch. Ges. Basel* **1874**, 6, 138–208.
- 4 Mirksy, A. E., The discovery of DNA. *Scientific American* **1968**, June, 78.
- 5 Miescher, F., Ueber die chemische Zusammensetzung der Eiterzellen. *Die Histochemischen und physiologischen Arbeiten*. **1871**, 2, 3-23.

- 6 Avery, T.; Macleod, C. M.; McCarty, M., Studies on the chemical nature of the substance inducing transformation of pneumococcal types. I. induction of transformation by a deoxyribonucleic acid fraction isolated from pneumococcus type III. *J. Exp. Med.* **1944**, 79, (I), 37.
- 7 Vischer, E.; Zamenhof, S.; Chargaff, E., Microbial nucleic acids: the deoxypentose nucleic acids of avian tubercle bacilli and yeast. *J. Biol. Chem.* **1949**, 177, 429.
- 8 Franklin, R. E.; Gosling, R. G., Molecular Configuration in Sodium Thymonucleate. *Nature (London)* **1953**, 171, (April 25), 740-741.
- 9 Watson, J. D.; Crick, F. H. C., Molecular Structure of Nucleic Acids: A Structure for Deoxyribose Nucleic Acid. *Nature (London)* **1953**, April 25, (171), 737-738.
- 10 Watson, J. D.; Crick, F. H. C., Genetic implications of the structure of deoxyribonucleic acid. *Nature (London)* **1953**, 171, 964.
- 11 Pollock, M. R., The Discovery of DNA : An Ironic Tale of Chance, Prejudice and Insight. *J. Gen. Microbiol.* **1970**, 63, 1-20.
- 12 Ströck, M., overview of the structure of DNA. In <http://en.wikipedia.org/wiki/User:Mstroeck>, ed.; DNA_helix.png, 'Ed.' 'Eds.' Wikipedia: Vienna, 2006; 'Vol.' p^pp Permission is granted to copy, distribute and/or modify this document under the terms of the GNU Free Documentation License, Version 1.2 or any later version published by the Free Software Foundation; with no Invariant Sections, no Front-Cover Texts, and no Back-Cover Texts.
- 13 Blackburn, G. M.; Gait, M. J., *Nucleic Acids in Chemistry and Biology*. Second ed.; Oxford University Press: New York, 1996; 'Vol.' p.
- 14 Chantrenne, H., The polyribosomes, agents of protein synthesis. *Arch Biol* **1965**, 76, (2), 307-16.
- 15 Nirenberg, M. W.; Matthaei, J. H., The Dependence of Cell-Free Protein Synthesis in E. coli upon Naturally Occurring or Synthetic Polyribonucleotides. *Proc. Natl. Acad. Sci. U. S. A.* **1961**, 47, (10), 1588-1602.
- 16 Crouch, R. J.; Toulmé, J. J. e., *Ribonucleases H*. ed.; John Libbey: Paris, 1998; 'Vol.' p 265.
- 17 Croke, S. T., Progress in antisense technology. *Ann. Rev. Med.* **2004**, 55, 61-95.
- 18 Stein, C. A.; Cheng, Y.-C., Antisense Oligonucleotides as Therapeutic Agents-Is the Bullet Really Magical? *Science* **1993**, 261, 1004-1012.
- 19 Croke, S. T., Review: Molecular mechanisms of action of antisense drugs. *Biochim. Biophys. Acta* **1999**, 1489, 31-44.
- 20 Koziolkiewicz, M.; Gendaszewska, E.; Maszewska, M.; Stein, C. A.; Stec, W. J., The mononucleotide-dependent, nonantisense mechanism of action of phosphodiester and phosphorothioate oligonucleotides depends upon the activity of an ecto-5'-nucleotidase. *Blood* **2001**, 98, 995-1002.
- 21 Vaerman, J. L.; Moureau, P.; Deldime, F.; Lewalle, P.; Lamineur, C.; Morschhauser, F.; Martiat, P., Antisense Oligodeoxyribonucleotides Suppress Hematologic Cell Growth Through Stepwise Release of Deoxyribonucleotides. *Blood* **1997**, 90, 331-9.
- 22 Kool, E. T., Preorganization of DNA: Design Principles for Improving Nucleic Acid Recognition by Synthetic Oligonucleotides. *Chem. Rev.* **1997**, 97, 1473-1487.
- 23 Mesmaeker, A. d.; Haner, R.; Martin, P.; Moser, H. E., Antisense Oligonucleotides. *Acc. Chem. Res.* **1995**, 28, 366-374.
- 24 Fire, A.; Xu, S.; Montgomery, M. K.; Kostas, S. A.; Driver, S. E.; Mello, C. C., Potent and specific genetic interference by double-stranded RNA in *Caenorhabditis elegans*. *Nature (London)* **1998**, 391, 806-811.
- 25 Hamilton, A. J.; Baulcombe, D. C., A species of small antisense RNA in posttranscriptional gene silencing in plants. *Science* **1999**, 286, (950-952).
- 26 Elbashir, S. M.; Harborth, J.; Lendeckel, W.; Yalcin, A.; Weber, K.; Tuschl, T., Duplexes of 21-nucleotide RNAs mediate RNA interference in cultured mammalian cells. *Nature (London)* **2001**, 411, 494-498.
- 27 Dykxhoorn, D. M.; Lieberman, J., Running Interference: Prospects and Obstacles to Using Small Interfering RNAs as Small Molecule Drugs. *Annual Review of Biomedical Engineering* **2006**, 8, 377-402.

- 28 Martin, S. E. N. J. C., Applications of RNA Interference in Mammalian Systems. *Annual Review of Genomics and Human Genetics* **2007**, 8, 82-108.
- 29 Elbashir, S. M.; Lendeckel, W.; Tuschl, T., RNA interference is mediated by 21-and 22-nucleotide RNAs. *Genes Dev.* **2001**, 15, 188-200.
- 30 Zamore, P. D.; Tuschl, T.; Sharp, P. A.; Bartel, D. P., RNAi: Double-stranded RNA directs the ATP-dependent cleavage of mRNA at 21 to 23 nucleotide intervals. *Cell (Cambridge, Mass.)* **2000**, 101, 25-33.
- 31 Ketting, R. F.; Fischer, S. E. J.; Bernstein, E.; Sijen, T.; Hannon, G. J.; Plasterk, R. H. A., Dicer functions in RNA interference and in synthesis of small RNA involved in developmental timing in *C. elegans*. *Genes Dev.* **2001**, 15, 2654-2659.
- 32 Stark, G. R.; Kerr, I. M.; Williams, B. R.; Silverman, R. H.; Schreiber, R. D., How cells respond to interferons. *Annu. Rev. Biochem.* **1998**, 67, 22-264.
- 33 Elbashir, S.; Martinez, J.; Patkaniowska, A.; Lendeckel, W.; Tuschl, T., Functional anatomy of siRNAs for mediating efficient RNAi in *Drosophila melanogaster* embryo lysate. *EMBO J.* **2001**, 20, 6877-88.
- 34 Parker, J.; Barford, D., Argonaute: a scaffold for the function of short regulatory RNAs. *Trends Biochem. Sci.* **2006**, 31, 622-30.
- 35 Rand, T.; Petersen, S.; Du, F.; Wang, X., Argonaute2 cleaves the antiguided strand of siRNA during RISC activation. *Cell (Cambridge, Mass.)* **2005**, 123, 621-29.
- 36 Schwarz, D. S.; Hutvagner, G.; Haley, B.; Zamore, P. D., Evidence that siRNAs function as guides, not primers, in the *Drosophila* and human RNAi pathways. *Mol. Cell* **2002**, 10, 537-548.
- 37 Matranga, C.; Tomari, Y.; Shin, C.; Bartel, D.; Zamore, P., Passenger-strand cleavage facilitates assembly of siRNA into Ago2-containing RNAi enzyme complexes. *Cell (Cambridge, Mass.)* **2005**, 123, 607-20.
- 38 Mello, C. C.; Conte, D., Revealing the world of RNA interference. *Nature (London)* **2004**, 431, 338-342.
- 39 Song, J.-J.; Smith, S. K.; Hannon, G. J.; Joshua-Tor, L., Crystal Structure of Argonaute and Its Implications for RISC Slicer Activity. *Science (Washington, DC, United States)* **2004**, 305, (5689), 1434-1437.
- 40 Carstea, E. D.; Hough, S.; Wiederholt, K.; Welch, P. J., State-of-the-art modified RNAi compounds for therapeutics. *Idrugs* **2005**, 8, 642-647.
- 41 Far, R. K. K.; Sczakiel, G., The activity of siRNA in mammalian cells is related to structural target accessibility: a comparison with antisense oligonucleotides. *Nucleic Acids Res.* **2003**, 31, 4417-4424.
- 42 Hough, S. R.; Wiederholt, K. A.; Burrier, A. C.; Woolf, T. M.; Taylor, M. F., Why RNAi makes sense. *Nat. Biotechnol.* **2003**, 21, 731-732.
- 43 Czauderna, F.; Fechtner, M.; Dames, S.; Ayguen, H.; Klippel, A.; Pronk, G. J.; Giese, K.; Kaufmann, J., Structural variations and stabilizing modifications of synthetic siRNAs in mammalian cells. *Nucleic Acids Res.* **2003**, 31, (11), 2705-2716.
- 44 Morrissey, D.; Blanchard, K.; Shaw, L.; Jensen, K.; Lockridge, J.; al., e., Activity of stabilized short interfering RNA in a mouse model of hepatitis B virus replication. *Hepatology* **2005**, 41, 1349-56.
- 45 Reynolds, A.; Leake, D.; Boese, Q.; Scaringe, S.; Marshall, W.; Khvorova, A., Rational siRNA design for RNA interference. *Nat. Biotechnol.* **2004**, 22, 326-30.
- 46 Khvorova, A.; Reynolds, A.; Jayasena, S., Functional siRNAs and miRNAs exhibit strand bias. *Cell (Cambridge, Mass.)* **2003**, 115, 209-16.
- 47 Schwarz, D.; Hutvagner, G.; Du, T.; Xu, Z.; Aronin, N.; Zamore, P., Asymmetry in the assembly of the RNAi enzyme complex. *Cell (Cambridge, Mass.)* **2003**, 115, 199-208.
- 48 Bertrand, J.; Pottier, M.; Vekris, A.; Opolon, P.; Maksimenko, A.; Malvy, C., Comparison of antisense oligonucleotides and siRNAs in cell culture and in vivo. *Biochem. Biophys. Res. Commun.* **2002**, 296, 1000-1004.
- 49 Chiu, Y. L.; Rana, T. M., siRNA function in RNAi: A chemical modification analysis. *RNA* **2003**, 9, 1034-1048.

- 50 Freier, S. M.; Altmann, K.-H., The ups and downs of nucleic acid duplex stability: structure-stability studies on chemically-modified DNA:RNA duplexes. *Nucleic Acids Res.* **1997**, *25*, 4429-4443.
- 51 Kurreck, J., Antisense technologies. Improvement through novel chemical modifications. *Eur. J. Biochem.* **2003**, *270*, (8), 1628-1644.
- 52 Manoharan, M., 2'-Carbohydrate modifications in antisense oligonucleotide therapy: importance of conformation, configuration and conjugation. *Bba-Gene Struct Expr.* **1999**, 1489, 117-130.
- 53 Fattal, E.; Bochet, A., Ocular delivery of nucleic acids: Antisense oligonucleotides, aptamers and siRNA. *Advanced Drug Delivery Reviews* **2006**, *58*, 1203-1223.
- 54 Manoharan, M., RNA interference and chemically modified small interfering RNAs. *Curr. Opin. Chem. Biol.* **2004**, *8*, 570-579.
- 55 Agrawal, S.; Zhao, Q., Antisense therapeutics in neuropharmacology. *Curr. Opin. Chem. Biol.* **1998**, *2*, 519-528.
- 56 Agrawal, S.; Kandimalla, E. R., Antisense therapeutics: is it as simple as complementary base recognition? *Mol. Med. Today* **2000**, *6*, 72-81.
- 57 Weidner, D. A.; Valdez, B. C.; Henning, D.; Greenberg, S.; Busch, H., Phosphorothioate oligonucleotides bind in a non sequence-specific manner to the nucleolar protein C23/nucleolin. *FEBS Lett.* **1995**, *366*, 146-150.
- 58 Srinivasan, S. K.; Teway, H. K.; Iversen, P. L., Characterization of binding sites, extent of binding, and drug interactions of oligonucleotides with albumin. *Antisense Res Dev.* **1995**, *5*, (2), 131-9.
- 59 Mangos, M. M. Factors Governing The Design, Selection and Cleavage of Sugar-Modified Duplexes by Ribonuclease H. Ph.D. Thesis, McGill University, Montreal, 2005.
- 60 De Fabritiis, P.; Calabretta, B., Antisense oligodeoxynucleotides for the treatment of chronic myelogenous leukaemia: Are they still a promise? *Haematologica* **1995**, *80*, 295-9.
- 61 Webb, A.; Cunningham, D.; Cotter, F.; Clarke, P. A.; Di Stephano, F.; Ross, P.; Corbo, M.; Dziewanowska, Z., BCL-2 antisense therapy in patients with non-Hodgkin lymphoma. *Lancet* **1997**, *349*, 1137-41.
- 62 Crooke, S. T., Vitravene (TM) - another piece in the mosaic. *Antisense Nucleic Acid Drug Dev.* **1998**, *8*, Vii-Viii.
- 63 Rajagopal, J.; Doudna, J. A.; Szostak, J. W., Stereochemical course of catalysis by the Tetrahymena ribozyme. *Science* **1989**, *244*, 692-694.
- 64 Milligan, J. F.; Uhlenbeck, O. C., Determination of RNA-protein contacts using thiophosphate substitutions. *Biochemistry* **1989**, *28*, 2849-2855.
- 65 Eckstein, F., Nucleoside Phosphorothioates. *Ann. Rev. Biochem.* **1985**, *54*, 367-402.
- 66 Dahm, S. C.; Uhlenbeck, O. C., Role of divalent metal ions in the hammerhead RNA cleavage reaction. *Biochemistry* **1991**, *30*, 9464.
- 67 Wallace, J. C.; Edmonds, M., Polyadenylated nuclear RNA contains branches. *Proc. Natl. Acad. Sci. USA* **1983**, *80*, (950-954).
- 68 LaPlanche, L. A.; James, T. L.; Powell, C.; Wilson, W. D.; Uznanski, B.; Stec, W. J.; Summers, M. F.; Zon, G., Phosphorothioate-modified oligodeoxyribonucleotides. III. NMR and UV spectroscopic studies of the Rp-Rp, Sp-Sp, and Rp-Sp duplexes, [d(GGSAATTCC)]₂, derived from diastereomeric O-ethyl phosphorothioates. *Nucleic Acids Res.* **1986**, *14*, (22), 9081-9093.
- 69 Giannaris, P. A.; Damha, M. J., Oligoribonucleotides containing 2',5'-phosphodiester linkages exhibit binding selectivity for 3',5'-RNA over 3',5'-ssDNA. *Nucleic Acids Res.* **1993**, *21*, 4742-4749.
- 70 Bhan, P.; Bhan, A.; Hong, M.; Hartwell, J. G.; Saunders, J. M.; Hoke, G. D., 2',5'-Linked oligo-3'-deoxyribonucleoside phosphorothioate chimeras: thermal stability and antisense inhibition of gene expression. *Nucleic Acids Res.* **1997**, *25*, 3310-3317.
- 71 Kandimalla, E. R.; Manning, A.; Zhao, Q. Y.; Shaw, D. R.; Byrn, R. A.; Sasisekharan, V.; Agrawal, S., Mixed backbone antisense oligonucleotides: Design, biochemical and biological properties of oligonucleotides containing 2'-5'-ribo- and 3'-5'-deoxyribonucleotide segments. *Nucleic Acids Res.* **1997**, *25*, 370-378.

- 72 Wasner, M.; Arion, D.; Borkow, G.; Noronha, A.; Uddin, A. H.; Parniak, M. A.; Damha, M. J., Physicochemical and Biochemical Properties of 2',5'-Linked RNA and 2',5'-RNA:3',5'-RNA "Hybrid" Duplexes. *Biochemistry* **1998**, *37*, 7478-7486.
- 73 Egli, M., Conformational preorganization, hydration, and nucleic acid duplex stability. *Antisense Nucleic Acid Drug Dev.* **1998**, *8*, 123-129.
- 74 Koshkin, A. A.; Singh, S. K.; Nielsen, P.; Rajwanshi, V. K.; Kumar, R.; Meldgaard, M.; Olsen, C. E.; Wengel, J., LNA (locked nucleic acids): synthesis of the adenine, cytosine, guanine, 5-methylcytosine, thymine and uracil bicyclonucleoside monomers, oligomerization, and unprecedented nucleic acid recognition. *Tetrahedron* **1998**, *54*, (14), 3607-3630.
- 75 Singh, S. K.; Nielsen, P.; Koshkin, A. A.; Wengel, J., LNA (locked nucleic acids): Synthesis and high-affinity nucleic acid recognition. *Chemical Communications* **1998**, 455-456.
- 76 Obika, S.; Nanbu, D.; Hari, Y.; Andoh, J.-i.; Morio, K.-i.; Doi, T.; Imanishi, T., Stability and structural features of the duplexes containing nucleoside analogues with a fixed N-type conformation, 2'-O,4'-C-methyleneribonucleosides. *Tetrahedron Lett.* **1998**, *39*, 5401-5404.
- 77 Koshkin, A. A.; Nielsen, P.; Meldgaard, M.; Rajwanshi, V. K.; Singh, S. K.; Wengel, J., An RNA mimic forming exceedingly stable LNA : LNA duplexes. *J. Am. Chem. Soc.* **1998**, *120*, 13252-13253.
- 78 Chastain, M.; Tinoco, I., Structural Elements in RNA. *Prog. Nucleic Acid Res. Mol. Biol.* **1991**, *41*, 131-177.
- 79 Gray, D. M.; Ratliff, R. L.; Vaughan, M. R., Circular-Dichroism Spectroscopy of DNA. *Methods Enzymol.* **1992**, *211*, 389-406.
- 80 Gryaznov, S.; Chen, J.-K., Oligodeoxyribonucleotide N3'->P5' Phosphoramidates: Synthesis and Hybridization Properties. *J. Am. Chem. Soc.* **1994**, *116*, (7), 3143-3144.
- 81 Kissman, H. M.; Weiss, M. J., The Synthesis of 1-(Aminodeoxy-β-D-ribofuranosyl)-2-pyrimidinones. New 3'- and 5'-Aminonucleosides. *JACS* **1958**, *80*, 2575 - 2583.
- 82 Ding, D.; Gryaznov, S. M.; Lloyd, D. H.; Chandrasekaran, S.; Yao, S.; Ratmeyer, L.; Pan, Y.; Wilson, W. D., An oligodeoxyribonucleotide N3'->P5' phosphoramidate duplex forms an A-type helix in solution. *Nucleic Acids Res.* **1996**, *24*, (2), 354-360.
- 83 Reist, E. J.; Benitez, A.; Goodman, L., The Synthesis of Some S'Thiopentofuranosylpyrimidines. *J. Org. Chem.* **1964**, *29*, (3), 554-558.
- 84 Chladek, S.; Nagyvary, J., Nucleophilic Reactions of Some Nucleoside Phosphorothioates. *J. Am. Chem. Soc.* **1972**, *94*, 2079-2085.
- 85 Jahn-Hofmann, K.; Engels, J. W., Efficient solid phase synthesis of cleavable oligodeoxynucleotides based on a novel strategy for the synthesis of 5'-S-(4,4'-dimethoxytrityl)-2'-deoxy-5'-thionucleoside phosphoramidites. *Helv. Chim. Acta* **2004**, *87*, (11), 2812-2828.
- 86 Rybakov, V. N.; Rivkin, M. I.; Kumarev, V. P., Some substrate properties of analogues of oligothymidylates with p-s-C-5' bonds. *Nucleic Acids Res.* **1981**, *9*, (1), 189-201.
- 87 Kuimelis, R. G.; McLaughlin, L. W., Ribozyme-Mediated Cleavage of a Substrate Analogue Containing an Internucleotide-Bridging 5'-Phosphorothioate: Evidence for the Single-Metal Model. *Biochemistry* **1996**, *35*, (16), 5308 -5317.
- 88 Tedeschi, A. L. Synthesis and Biological Evaluation of Oligonucleotides Containing 3'- and 5'-S-Phosphorothiolate Internucleotide Linkages. M.Sc. Thesis, McGill University, Montreal, 2004.
- 89 Cosstick, R.; S.Vyle, J., Synthesis and properties of dithymidine phosphate analogues containing 3'-thiothymidine. *Nucleic Acids Res.* **1990**, *18*, (4), 829-835.
- 90 Parrish, S.; Fleenor, J.; Xu, S.; Mello, C.; Fire, A., Functional anatomy of a dsRNA trigger: differential requirement for the two trigger strands in RNA interference. *Mol. Cell* **2000**, *6*, 1077-87.
- 91 Braasch, D. A.; Jensen, S.; Liu, Y.; Kaur, K.; Arar, K.; White, M. A.; Corey, D. R., RNA Interference in Mammalian Cells by Chemically-Modified RNA. *Biochemistry* **2003**, *42*, (26), 7967-7975.
- 92 Harborth, J.; Elbashir, S.; Vandeburgh, K.; Manninga, H.; Scaringe, S.; al., e., Sequence, chemical, and structural variation of small interfering RNAs and short hairpin RNAs and the effect on mammalian gene silencing. *Antisense Nucleic Acid Drug Dev.* **2003**, *13*, 83-105.
- 93 Kurreck, J.; Wyszko, E.; Gillen, C.; Erdman, V. A., Design of antisense oligonucleotides stabilized by locked nucleic acids. *Nucleic Acids Res.* **2002**, *30*, 1911-1918.

- 94 Lok, C.-N.; Viazovkina, E.; Min, K.-L.; Nagy, E.; Wilds, C. J.; Damha, M. J.; Parniak, M. A., Potent gene-specific inhibitory properties of mixed-backbone antisense oligonucleotides comprised of 2'-deoxy-2'-fluoro-D-arabinose and 2'-deoxyribose nucleotides. *Biochemistry* **2002**, 41, (10), 3457-67.
- 95 Mangos, M. M.; Min, K.-L.; Viazovkina, E.; Galarneau, A.; Elzagheid, M. I.; Parniak, M. A.; Damha, M. J., Efficient RNase H-Directed Cleavage of RNA Promoted by Antisense DNA or 2'F-ANA Constructs Containing Acyclic Nucleotide Inserts. *J. Am. Chem. Soc.* **2003**, 125, (3), 654-661.
- 96 Noronha, A.; Wilds, C. J.; Lok, C.-N.; Arion, K. V. D.; Parniak, M. A.; Damha, M. J., Synthesis and Biophysical Properties of Arabinonucleic Acids (ANA): Circular Dichroic Spectra, Melting Temperatures, and Ribonuclease H Susceptibility of ANA-RNA Hybrid Duplexes. *Biochemistry* **2000**, 39, (24), 7050 -7062.
- 97 Damha, M.; Usman, N.; Ogilvie, K., The rapid chemical synthesis of arabinonucleotides. *Tetrahedron Lett.* **1987**, 28, (1515), 1633-1636.
- 98 Damha, M. J.; Giannaris, P. A.; Marfeys, P., Antisense L/D-Oligodeoxynucleotide Chimeras: Nuclease Stability, Base-Pairing Properties and Activity at Directing Ribonuclease H. *Biochemistry* **1994**, 33, 7877-7885.
- 99 Watts, J. K.; Sadalpure, K.; Choubdar, N.; Pinto, B. M.; Damha, M. J., Synthesis and Conformational Analysis of 2'-Fluoro-5-methyl-4'-thioarabinouridine (4'S-FMAU). *J. Org. Chem.* **2006**, 71, (3), 921-925.
- 100 Wilds, C.; Damha, M., 2'-Deoxy-2'-fluoro-beta-D-arabinonucleosides and oligonucleotides (2'F-ANA): synthesis and physicochemical studies. *Nucleic Acids Res.* **2000**, 28, (18), 3625-35.
- 101 Sabatino, D.; Damha, M. J., Oxepane Nucleic Acids: Synthesis, Characterization, and Properties of Oligonucleotides Bearing a Seven-Membered Carbohydrate Ring. *J. Am. Chem. Soc.* **2007**, 129, (26), 8259-8270.
- 102 Damha, M. J.; Wilds, C. J.; Noronha, A.; Brukner, I.; Borkow, G.; Arion, D.; Parniak, M. A., Hybrids of RNA and Arabinonucleic Acids (ANA and 2'F-ANA) Are Substrates of Ribonuclease H. *J. Am. Chem. Soc.* **1998**, 120, (49), 12976-12977.
- 103 Denisov, A.; Noronha, A. M.; Wilds, C. J.; Trempe, J.-F.; Pon, R. T.; Gehring, K.; Damha, M. J., Solution structure of an arabinonucleic acid (ANA)/RNA duplex in a chimeric hairpin: comparison with 2'-fluoro-ANA/RNA and DNA/RNA hybrids. *Nucleic Acids Res.* **2001**, 29, (21), 4284-4293.
- 104 Trempe, J.; Wilds, C. J.; Denisov, A. Y.; Pon, R. T.; Damha, M. J.; Gehring, K., NMR Solution Structure of an Oligonucleotide Hairpin with a 2'F-ANA/RNA Stem: Implications for RNase H Specificity toward DNA/RNA Hybrid Duplexes. *J. Am. Chem. Soc.* **2001**, 123, (21), 4896 -4903.
- 105 Watts, J. K.; Choubdar, N.; Sadalpure, K.; Robert, F.; Wahba, A. S.; Pelletier, J.; Mario Pinto, B.; Damha, M. J., 2'-Fluoro-4'-thioarabino-modified oligonucleotides: conformational switches linked to siRNA activity. *Nucl. Acids Res.* **2007**, 35, (5), 1441-1451.

Chapter 2: Experimental Materials and Methods

2.1 General Methods

2.1.1 General Reagents

Required solvents were obtained by refluxing and subsequent distillation from drying agents under inert atmospheres: acetonitrile (CH₃CN, Fisher), methylene chloride (CH₂Cl₂, Fisher), and pyridine (C₅H₅N, Fisher) were dried over calcium hydride (CaH₂, Aldrich) and tetrahydrofuran (C₄H₄O, THF, Fisher) was dried over a sodium metal-benzophenone system (Aldrich). Anhydrous N,N-diisopropylethylamine (DIPEA, Aldrich) and anhydrous dioxane (Aldrich), as well as acetone, chloroform, diethyl ether, ethanol, glacial acetic acid, hydrochloric acid, methanol, triethylamine (TEA) and concentrated aqueous ammonia were used as received.

Reagents such as sodium bicarbonate (NaHCO₃), anhydrous sodium sulphate (Na₂SO₄), p-anisylchlorodiphenylmethane (MMTCl), benzoyl chloride (BzCl), 4-dimethylaminopyridine (DMAP), *O*-(benzotriazol-1-yl)-1,1,3,3-tetramethyluronium hexafluorophosphate (HBTU), and mesoyl chloride (MsCl) were purchased from Sigma-Aldrich and used as received.

Thymidine, cytidine, and N,N-diisopropylaminophosphonamidic chloride phosphitylating reagent were purchased from Chemgenes Corp. (Ashland, MA) and used as received.

2.1.2 Chromatography for Nucleosides and Intermediates

Analytical thin layer chromatography (TLC) was performed on Merck Kieselgel 60 F₂₅₄ aluminium sheets coated with fluorescent indicator doped silica gel (0.2 mm x 20 cm x 20 cm). Compounds were visualized by illumination with a handheld 254 nm UV lamp and by dipping the TLC plate in a dilute sulphuric acid solution (3% in MeOH) with subsequent heating. Preparatory scale flash column chromatography was performed using SilicycleTM ultra-pure silica gel (230-400 mesh) under constant nitrogen pressure (5-10psi). Chloroform with an increasing gradient of methanol (0-15%) was used as eluant.

2.1.3 Instruments

Circular Dichroism Spectra. CD spectra were generated using a JASCO J-810 spectropolarimeter, with software supplied by the manufacturer, between 210-350 nm at a scan rate 50 nm/min. The temperature-controlled sample chamber was used as required.

NMR Spectra. NMR spectra were recorded using 200 MHz, 400 MHz and 500 MHz Varian Mercury spectrophotometers. ¹H-NMR, ³²P-NMR and 2D-NMR (¹H-¹H COSY) were used to characterize compounds. Deuterated solvents, including acetonitrile-*d*₃, chloroform-*d*₃, and dichloromethane-*d*₂, were obtained from Cambridge Isotope Laboratories.

Mass Spectrometry.

Low-resolution electrospray ionization mass-spectrometry was performed on a ThermoQuest Finnigan LCQ Duo mass spectrometer in the positive ion mode. Samples were routinely dissolved in methanol.

UV-Visible Spectra. Absorbance spectra in the visible and UV ranges were obtained using a Varian Cary I or Cary 300 spectrophotometer with software supplied by the manufacturer. All spectra were obtained in water or aqueous buffers, and a Peltier temperature-controlled sample chamber was used as required.

2.2 Synthesis of 3'-Deoxy-3'-Thiothymidine Nucleoside and its 3'-S-Phosphorothioamidite Derivative

2.2.1 5'-O-p-Monomethoxytritylthymidine (3.2)

Thymidine (5.09 g, 21 mmol) was co-evaporated with three 20 mL aliquots of anhydrous pyridine before being dissolved in 200 mL of anhydrous pyridine. The flask was purged with dry nitrogen, p-anisylchlorodiphenylmethane (MMTCl, 7.78 g, 1.2 eq) was added and the mixture was allowed to stir overnight at room temperature. The mixture was then diluted with 100 mL of dichloromethane and extracted with 100 mL of saturated sodium chloride (brine). The organic layer was dried over Na₂SO₄, filtered and evaporated under reduced pressure. The crude product was purified by flash column chromatography, using silica neutralised with Et₃N and a chloroform : methanol gradient to afford the product (**3.2**) (10.78 g, 99%) as a white foam. R_f 0.48 (chloroform : methanol 9:1). ¹H-NMR (acetone-d₆): δ = 9.97(s, 1H, NH), 8.02(s, 1H, 6H), 7.48-6.90(m, 14H, trityl H), 6.39-6.34(m, 1H, 1'H), 4.61-4.57(m, 1H, 4'H), 4.06-4.02(m, 1H, 3'H), 3.79(s, 3H, OCH₃), 3.41-3.32(m, 2H, 5'H_{a+b}), 2.85(s, 1H, 3'OH), 2.44-2.26(m, 2H, 2'H_{a+b}), 1.46(s, 3H, 5CH₃). ESI-MS(+) *m/z* 537.1 [M+Na]⁺, expected 537.7 [M+Na]⁺.

2.2.2 3'-O-Methanesulphonyl-5'-(monomethoxytrityl)thymidine (3.3)

Methanesulfonyl chloride (2.25 mL, 3 eq) was added dropwise to a flask, cooled to 0 °C, containing 5'-O-p-mnomethoxytritylthymidine (**3.2**) (5.02 g, 9.7 mmol) in 70 mL anhydrous pyridine. The reaction was stirred at 0 °C for 3 h and subsequently stirred overnight at room temperature. The orange reaction mixture was diluted with 100 mL of saturated aqueous NaHCO₃ solution and extracted 3 times with 50 mL of dichloromethane. The organic layer was dried over Na₂SO₄, filtered and evaporated under reduced pressure to yield 3'-O-methanesulphonyl-5'-(monomethoxytrityl)thymidine (**3.3**) (5.214g, 91%) as a brown foam. R_f 0.48 (chloroform : methanol 9:1). ESI-MS(+) *m/z* 615.0 [M+Na]⁺, expected 615.7 [M+Na]⁺.

2.2.3 2,3'-Dideoxy-5'-(monomethoxytrityl)anhydrothymidine (3.4)

3'-O-methanesulphonyl-5'-(monomethoxytrityl)thymidine (**3.3**) (4.03g, 6.8 mmol) was dissolved in an alkaline ethanolic solution (165 mL EtOH, 65 mL Et₃N) and refluxed for 18 h. The crude reaction mixture was evaporated under reduced pressure to a viscous oil, diluted with 80 mL water and extracted twice with 60 mL dichloromethane. The organic layer was dried over Na₂SO₄, filtered and evaporated under reduced pressure to yield 2,3'-dideoxy-5'-(monomethoxytrityl)anhydrothymidine (**3.4**) (3.212g, 95%) as a beige foam. R_f 0.37 (chloroform : methanol 9:1). ESI-MS(+) *m/z* 497.1 [M+H]⁺, expected 497.5 [M+H]⁺.

2.2.4 3'-Acetylthio-3'-deoxy-5'-(monomethoxytrityl)thymidine (3.5)¹

Sodium thioacetate was prepared by adding thioacetic acid (1.2 mL, 1.1eq) drop wise to a stirred solution of sodium hydride (0.3g, 1eq) in 10 mL of dry dioxane at 0 °C. After stirring for one hour, the sodium thioacetate solution was added to 2,3'-dideoxy-5'-(monomethoxytrityl)anhydrothymidine (**3.4**, 1.5g, 3.0 mmol) in 10 mL of anhydrous dioxane. The reaction was refluxed at 100 °C for 3 h and then kept at 50 °C for 16h. The crude mixture was then diluted with 25 mL of saturated aqueous NaHCO₃ and extracted four times with 20 mL of dichloromethane. The organic layer was then washed with 50 mL of water, dried over Na₂SO₄, filtered and evaporated under reduced pressure. The crude product was purified by flash column chromatography, using silica neutralised with Et₃N and a chloroform : methanol gradient to afford the product (**3.5**) (1.54 g, 90%) as a brown foam. R_f 0.61 (chloroform : methanol 9:1). ¹H-NMR (CDCl₃, 500 MHz): δ = 8.48(s, 1H, NH), 7.68(s, 1H, 6H), 7.44-7.25(m, 12H, trityl H), 6.85(d, 2H, *O*-anisyl H), 6.28(t, 1H, 1'H), 4.65(m, 1H, 4'H), 4.19(m, 1H, 3'H), 3.79(s, 3H, OCH₃), 3.70(s, 3H, SCOCH₃), 3.50(m, 2H, 5'H_{a+b}), 2.78(m, 1H, 2'H_a), 2.45(m, 1H, 2'H_b), 1.49(s, 3H, 5CH₃). See Appendix 1 for full NMR spectrum. ESI-MS(+) *m/z* 595.1 [M+Na]⁺, expected 595.7 [M+Na]⁺.

2.2.5 3'-deoxy-3'-S-5'-(monomethoxytrityl)thymidine (3.6)

3'-Acetylthio-3'-deoxy-5'-(monomethoxytrityl)thymidine (**3.5**) (500 mg, 0.874 mmol) and dithiothreitol (266 mg, 1.5 eq) were dissolved in 35 mL EtOH and deoxygenated by bubbling with argon gas for 45 minutes. The ethanolic solution was then cooled to 5°C and 2 mL of 10 M NaOH was added. Complete deacetylation was achieved after ~2 hours of stirring, and the reaction was stopped by neutralization with a dilute aqueous HCl solution.

The solvent was removed in vacuo and the crude product was purified on a neutralised silica gel column using a gradient of chloroform and methanol. Appropriate fractions were

combined and concentrated to dryness, then dissolved in dry benzene and sublimated to afford **(3.6)** (427 mg, 92%) as a wonderfully fluffy pale yellow foam. R_f 0.43 (chloroform : methanol-20:1). $^1\text{H-NMR}$ (CDCl_3 , 500 MHz): δ = 10.1(s, 1H, NH), 7.98(s, 1H, 6H), 7.67-7.24(m, 14H, trityl H), 6.18(dd, 1H, 1'H), 3.96-3.90(m, 2H, 3'+4'H), 3.77(s, 3H, OCH_3), 3.52(dd, 1H, 5'H_a), 3.44 (dd, 1H, 5'H_b), 2.88(s, 1H, 3'SH), 2.73-2.64(m, 1H, 2'H_a), 2.46-2.34(m, 1H, 2'H_b), 1.55(s, 3H, 5CH₃). See Appendix 1 for full NMR spectrum. ESI-MS(+) m/z 553.1 $[\text{M}+\text{Na}]^+$, expected 553.6 $[\text{M}+\text{Na}]^+$.

2.2.6 3'-Deoxy-5'-Monomethoxytritylthymidine-3'-S-phosphorothioamidite (3.8)

3'-deoxy-3'-S-5'-(monomethoxytrityl)thymidine **(3.6)** (200 mg, 0.377 mmol) was placed in an oven dried amber amidite vial and anhydrous CH_2Cl_2 (2.1 mL), N,N -diisopropylethylamine (1.3 eq, 85 μL), and N,N -diisopropylaminophosphonamidic chloride (0.95 eq, 80 μL) were added. The reaction was shaken for 30 minutes and connected directly to the DNA synthesiser in order to reduce the exposure of the sensitive thio moiety to atmospheric oxygen. An aliquot taken for analysis and purified by a short hexane:EtOAc column had R_f 0.40 (chloroform : methanol-20:1). $^{31}\text{P-NMR}$ (CDCl_3): 165.2, 163.6 ppm. See Appendix 1 for full NMR spectrum. ESI-MS(+) m/z 753.3 $[\text{M}+\text{Na}]^+$, expected 753.8 $[\text{M}+\text{Na}]^+$.

2.3 Oligonucleotide Synthesis

2.3.1 General Reagents

Unilynker[®] CPG, the standard 2'-deoxy and ribo 5'-O-dimethoxytrityl-3'-O-(2-cyanoethyl) N,N -diisopropylphosphoramidites and 2' OMe amidites, as well as all reagents for the DNA synthesiser were purchased from Chemgenes Corp. (Ashland, MA). Rasayan Inc. (Encinitas, CA) supplied the 2'-deoxy-2'-fluoro-arabinothymidine 3'-O-(2-cyanoethyl) N,N -diisopropylphosphoramidite.

In the solid phase oligonucleotide synthesis cycle, 5'-dimethoxytrityl and 5'-monomethoxytrityl groups were removed with 3% (w/v) trichloroacetic acid in dichloromethane. Activation of phosphoramidite coupling step was achieved with 0.25 M 4-ethylthiotetrazole in ACN and any unreacted hydroxyl groups were capped with a combination of the Cap A solution (10% (v/v) acetic anhydride and 10% (v/v) dry 2, 4, 6-collidine in anhydrous THF) and the Cap B solution (16% (v/v) dry N -methyl imidazole in anhydrous THF). A 0.1 M solution of iodine in THF/pyridine/water (25/20/2, v/v/v) was employed to oxidise the phosphite triesters to the more stable phosphotriesters.

2.3.2 Derivatization of Solid Support²

In a glass vial, oven baked at 170 °C for 24h in order to reduce water absorbed on the surface, 1g of long chain alkylamine controlled pore glass (500 Å, LCAA-CPG, Dalton Chemical Laboratories) was shaken overnight with 10 mL of 3% trichloroacetic acid (TCA) in dichloromethane. After filtration, the LCAA-CPG was washed successively with 30 mL of dichloromethane, 80 mL of pyridine, and 50 mL of ether, and dried for several hours under vacuum (<0.5 mbar).

The dry LCAA-CPG was then shaken overnight with 200 mg of succinic anhydride, 20 mg of 4-dimethylaminopyridine (DMAP) and 8 mL of dry pyridine. The LCAA-CPG was then filtered for a second time, washed successively with the same solvents as above, and dried on the filter for 30 min. In second oven-dried vial, 1g of the freshly succinylated LCAA-CPG was combined with 0.1 mmol of the desired 5'-protected nucleotide, 0.1 mmol of HBTU, 0.1 mmol of DMAP and 10 mL dry acetonitrile and shaken overnight. The derivatized, functionalised LCAA-CPG was then filtered for a third time and washed successively as above. The loading of nucleoside per g of CPG was determined by the absorption of liberated trityl groups and varied between 80-110 µmol of nucleoside per gram of solid support. An amount of derivatized CPG, prepared as above or purchased Unilynker (ChemGenes), appropriate for a 1 µmol synthesis was loaded into an ABI-compatible synthesizer column with cellulose filters (ChemGenes) and crimped closed with aluminium seals (ChemGenes).

2.3.3 General Automated Solid-Phase Synthesis of Oligonucleotides

Oligonucleotide syntheses were performed on an Applied Biosystems 3400 DNA synthesizer using standard β-cyanoethyl phosphoramidite chemistry. CPG prepared as previously described was acetylated with the manufacturer's capping cycle to block free hydroxyl groups still remaining on the surface. Unilynker CPG was used as received.

The 2'-deoxyribonucleoside phosphoramidites were prepared as 0.1 M solutions in anhydrous acetonitrile and the ribonucleoside, 2'F-ANA, and 2'OMe as 0.15 M solutions in anhydrous acetonitrile. The 3'-deoxy-3'-thiothymidine phosphorothioamidites were prepared as 0.15 M solutions in anhydrous dichloromethane.

The polymeric oligonucleotides were assembled step-wise from the phosphoramidite monomers to create the desired sequence, shown in **Figure 2.1**. The 5' hydroxyl of the growing oligonucleotide is released and coupled to the P group of the incoming nucleoside, using the reagents outlined in **Table 2.1** below. Step 4a. is used for natural phosphate backbones, and 4b. to generate phosphorothioate backbones.

Figure 2.1: Schematic of DNA Synthesiser Solid-Phase Synthesis of Oligonucleotides

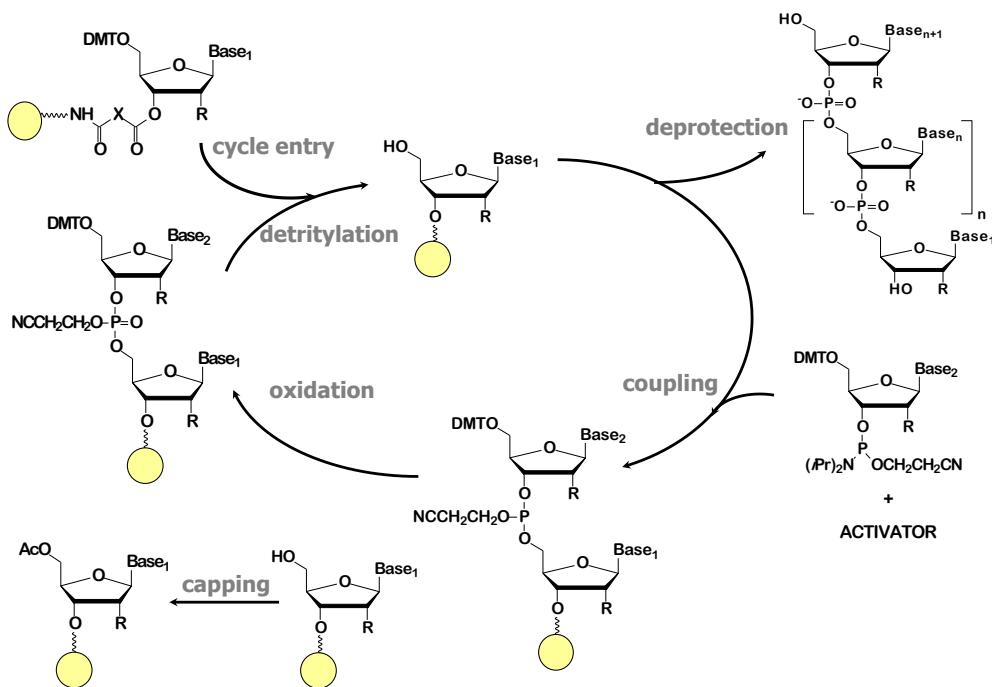


Table 2.1: Reagents for Solid-Phase Synthesis of Oligonucleotides

Function	Time for reaction
1. Detritylation	for DMT = 120 s, MMT = 240 s
2. Coupling	3'-deoxy-3'-thiothymidine = 150 s; A,G,C,U, 2'-F-ANA, 2'-OMe = 600 s; dT, dG = 300 s;
3. Capping	
4. a. Oxidation	15 s
b. Sulphurization	1390 s, assisted twice by the delivery of fresh reagent

The efficiency of each coupling step was monitored internally by the conductance of the trityl groups released during TCA treatment.

2.4 Deprotection and Purification of Oligonucleotides

2.4.1 General Reagents

Sterile water was prepared by autoclaving deionised water (MilliQ Direct-Q 3 UV system) with 0.1 % (v/v) diethyl pyrocarbonate (DEPC, Aldrich) for 1.5 h at 121° C (15 PSI) in an electric steam sterilizer³. Eppendorf vials and pipette tips were sterilized as described above, and latex gloves were worn to reduce exposure of the oligonucleotide to nucleases. Ammonium hydroxide (29%, Fisher), 95% ethanol (Commercial Alcohol Inc.) and triethylamine trihydrofluoride (TREAT-HF, Aldrich) were used as received.

Electrophoresis grade *N,N'*-methylene-bisacrylamide, ammonium persulphate (APS), *N,N,N',N'*-tetramethylethylenediamine (TEMED) and urea were obtained and used as received from Amersham Biosciences (Arlington Heights, IL). Bromophenol blue (BPB), xylene cyanol (XC), 2-Amino-2-(hydroxymethyl)-1,3-propanediol (Tris), boric acid, and ethylene-diamine tetraacetate dihydrate (EDTA) were purchased from Bio-Rad (Mississauga, ON). Biological grade formamide and Stains-All[®] were obtained from Sigma. All aqueous electrophoresis solutions were made with deionized water (MilliQ Direct-Q 3 UV system) and sterile water was used for any solution in direct contact with oligonucleotides.

Gel solutions of 20% and 24% acrylamide were prepared by mixing appropriate volumes of 40% (w/v H₂O) acrylamide stock solution (Amersham), 10 x TBE buffer (890 mM EDTA, 890 mM boric acid, 25 mM EDTA, pH 8.3) and water, with sufficient urea to produce a 7M concentration of urea. Aqueous samples of oligonucleotide were mixed with an equal volume of deionized formamide, prepared by stirring over a mixed bed ion-exchange resin (Bio-Rad AG 501-X8) for 30 min and filtration, prior to loading on the gels. Running dye markers contained 2% (w/v) of both XC and BPB, dissolved in a 2:1 (v/v) deionized formamide:10X TBE solution.

2.4.2 Cleavage from CPG and Deprotection of Oligomers

Freshly synthesised oligonucleotides were released from the CPG, and the phosphate backbone and exocyclic amines of the nucleobases were liberated from their respective protecting groups by treatment with a solution of aqueous ammonia (29%) in ethanol (3:1 v/v) for 24 h at 55 °C in a 1.5 mL screw-top microtube and then dried using a Speed-Vac[®] concentrator at room temperature. RNA-containing oligonucleotides were additionally shaken at room temperature for 48h with 100 µL/ µmole triethylamine trihydrofluoride (TREAT-HF, Aldrich) to remove the 2'-*O-tert*-butyldimethylsilyl protecting groups and purified by precipitation from 1 mL of cold butanol after the addition of 25 µL of 3M sodium acetate.

The dried oligonucleotides were then dissolved in sterile water, diluted as necessary to accommodate the spectrophotometer and quantified by absorption at 260 nm for the subsequent purification steps.

2.4.3 Analysis and Purification by Polyacrylamide Gel Electrophoresis (PAGE)

Fully deprotected oligonucleotides were analysed and purified by denaturing polyacrylamide gel electrophoresis (PAGE) and/or HPLC. Gel solutions were polymerised with 10% (w/v) aqueous ammonium persulfate (APS) and TEMED, and run on a vertical slab electrophoresis unit (Hoefer Scientific SE600, Fisher Scientific) with 0.75 mm spacers for

analytical gels and 1.5 mm spacers for preparatory runs. Oligonucleotide samples for analytical gels were dissolved in 15 μ L of deionized formamide:sterile water (2:1) and preparatory gels samples in 100-200 μ L.

Analytical gels were run at 500 V until the faster BPB dye was about 4 cm from the bottom of the gel plates and until it had almost run off the plate for preparatory runs. A dilute 0.5 x TBE running buffer (89 mM Tris/boric acid, 2.5 mM EDTA) was used for all runs. The gels were then UV shadowed by placing them on fluorescent TLC plates wrapped in plastic film and the results were captured by digital camera under the illumination of a handheld 254 nm UV lamp.

Analytical gels were then placed in a StainsAll[®] solution for at least 24h to dye the oligonucleotides and the images were recorded by digital camera. For preparative gels, the desired oligonucleotide band was excised from the gel, shaken in 5 mL of sterile water for 24h in a culture tube and the supernatant was dried down.

2.4.4 Reversed-Phase HPLC Analysis and Purification of Oligonucleotides

Analytical runs of reversed phase HPLC allowed for the investigation of the success of oligonucleotide synthesis and preparatory runs were used to isolate the desired full length material. A Waters 480/1525 HPLC chromatograph with a Phenomenex 3 μ m Oligo Reverse Phase Clarity Column (50 x 4.60 μ m) and a two solvent system consisting of 100mM triethylammonium acetate (A) in deionized water, and 100mM triethylammonium acetate in acetonitrile (B) was used. The solvent system was adjusted from 5% B in A to 20% B in A over a 22 minute period, with flow rate of 1 mL/min was. The elution profile was recorded by UV-Vis detection at 260 nm (the maximum absorbance of oligonucleotides) and 290 nm (to avoid saturating the detector) using the manufacturer's software. All solutions used for HPLC analysis and purification were filtered through a 0.22 μ m Nalgene filter to remove particulates.

2.4.5 Anion-Exchange HPLC Analysis of Oligonucleotides

Anion exchange HPLC was used to assess the success of oligonucleotide synthesis and to characterise oligonucleotides purified by PAGE. A Waters 480/1525 HPLC instrument with a Waters Protein-Pak[™] DEAE 5PW (7.5 mm x 75 mm) column and a two solvent system consisting of 1 M sodium perchlorate (NaClO₄, Aldrich) (A) and deionized water (B). A flow rate of 1 mL/min was maintained as the elution solvent was adjusted from 0% A to 30% A over 60 min, followed by 50% for 10 min and the elution profile was recorded by the manufacturer's

software by UV-Vis detection at 260 nm. The run finished with a 100% B washing step reduce anion carryover.

2.4.6 Desalting of Oligonucleotides

The crude oligonucleotides to be purified by either PAGE or HPLC were pre-purified (desalted) by size exclusion chromatography on Sephadex G-25[®] columns (Amersham Pharmacia Biotech) following the manufacturer's instructions and the resulting fractions were quantified at 260 nm. The absorbance data was converted into molar quantities by using the molar extinction coefficients (ϵ_{260}) calculated for each sequence as 90% of the sum of the molar extinction coefficients for the individual bases. The absorbance of the 3'-thio, 2'-F-ANA and 2'-OMe nucleosides were each assumed to be the same as those of their unmodified counterpart. Finally, the pure oligonucleotides were ready for characterization.

2.5 Characterization of Oligonucleotides

2.5.1 Characterization of Oligonucleotides by Mass Spectrometry

Dry oligonucleotide samples were dissolved in 25 μ L of 10mM ammonium acetate and a 3 μ L aliquot of this solution was injected on a small C18 trap and eluted with a gradient of ACN/H₂O in the mono-electrospray (Nano-ESI) inlet of a QTOF2 Mass Spectroscopy instrument (Micromass) located at Concordia University. The negative ion mode was selected for mass analysis, with the following parameters: Capillary Voltage: 3KV, Cone Voltage: 20V, Extraction Voltage: 2V, Inlet Temperature: 80C, Collision Cell Voltage: 5V, Collision Gas: Argon, MS resolution: 8000, MS accuracy: 50ppm.

2.5.2 UV-Thermal Denaturation of Oligonucleotides

Thermal denaturation profiles were obtained by monitoring the change in UV-absorbance at 260 nm with increasing temperature on a Varian CARY 1 or 300 UV-Vis spectrophotometer equipped with a Peltier temperature-controlled sample chamber, using software supplied by the manufacturer.

Oligonucleotide duplexes were prepared by combining equimolar amount of complementary strands, drying thoroughly and re-dissolving in 0.5-1 mL of a buffer consisting of 140 mM KCl, 1mM MgCl₂, and 5 mM Na₂HPO₄ at pH 7.2. The duplexes were denatured by heating to 90°C for 10-15 min, then allowed to hybridize as they slowly cooled at room temperature for 2-3 h and then overnight at 4°C overnight. The cold samples were transferred to

cold quartz cells (Hellma QS-1.000), and after being sealed with Teflon-wrapped stoppers, were allowed to equilibrate at 5°C in the cell holder of the spectrophotometer for 5 minutes.

The absorbance at 260 nm was measured at 0.5°C intervals as the temperature was increased at a rate of 0.5°C/min. The thermal melting temperature (T_m) values were calculated as the maximum of the first derivative plots of the absorbance *versus* temperature profiles, which coincides with the point at which the oligonucleotides population exists as an equal mixture of single-strands and duplexes.

2.5.3 Circular Dichroism Spectroscopy (CD)

Circular dichroic profiles were measured on a JASCO J-810 spectropolarimeter in quartz cells (Hellma QS-1.000) cooled to 5°C, using software supplied by the manufacturer, between 210-350 nm at a scan rate of 50nm/min.

The same oligonucleotide samples used for the thermal denaturation studies described above were used for CD measurements, after an identical heating and overnight cooling regime, and 10 minutes of equilibration time in the cold sample holder. The CD spectra were corrected by subtraction of a background scan of buffer, smoothed and were further corrected for concentration to enable determination of the molar ellipticity. Molar ellipticity was calculated from the equation $[\theta] = \theta/cl$, where θ is the relative intensity, c is the molar concentration of oligonucleotides and l is the path length of the cell in centimetres.

2.6 Biological Studies⁴

These experiments were conducted by Dr. Francis Robert of the Department of Biochemistry, McGill University.

2.6.1 RNAi Transfection

HeLa X1/5 cells, expressing the firefly luciferase gene, were maintained in Earle's Minimum Essential Medium (EMEM) cell culture medium supplemented with 10% fetal bovine serum (FBS), 2 mM L-glutamine, 1% non-essential amino acids, 1% MEM vitamins, 500 ml/ml G418, and 300 mg/ml Hygromycin. For transfection, 24-well plates were seeded with 1.0×10^5 cells per well. The following day, cells were incubated with increasing amounts of siRNAs premixed with lipofectamine- plus reagent (Invitrogen) using 1 ml of lipofectamine and 4 ml of the plus reagent per 20 pmol of siRNA (for the highest concentration tested). For the siRNA titrations, each siRNA was diluted in buffer (30mM HEPES-KOH, pH 7.4, 100mM KOAc, 2mM

MgOAc₂) and the amount of lipofectamine-plus reagent used relative to the siRNAs remained constant.

Cell viability was determined by measuring the cell metabolic activity, as an indicator of cellular toxicity resulting from siRNA transfection, using the Alamar Blue fluorimetric assay (Medicorp, Montreal, QC) as per the manufacturer's recommendations. The luciferase RLU values were normalized to their respective Alamar blue RFU values and any toxicity due to the experimental conditions was corrected.

2.6.2 Luciferase Activity Assay

Twenty-four hours after transfection, the cells were lysed in hypotonic lysis buffer (15mM K₃PO₄, 1mM EDTA, 1% Triton, 2mM NaF, 1 mg/ml BSA, 1mM DTT, 100mM NaCl, 4 mg/ml aprotinin, 2 mg/ml leupeptin and 2 mg/ml pepstatin).

Luminescence was measured, immediately following addition of the luciferin substrate solution, using a Fluostar Optima 96-well plate bioluminescence reader (BMG Labtech) and the values were normalized to the protein concentration of the cell lysate as determined by the DC protein assay (BioRad).

2.6.3 Luciferase mRNA Quantitation

Total cell RNA was extracted according to the RNeasy mini kit manufacturer's protocol (Qiagen, Mississauga, ON) and a 1 mg aliquot was used to prepare cDNA using random primers and SuperScript II Reverse Transcriptase (Invitrogen, Burlington, ON).

Quantitative real-time PCR was performed using the LightCycler (Roche, Laval, QC), SYBR green reagent, and gene-specific primers for luciferase (LUC5013 F1, 50-acgctgggcgtaatacagag-30; LUC5013 R1, 50-gtcgaagatgtggggttg-30; TIB MOLBIOL, Berlin, Germany) and the housekeeping gene GAPDH (huGAPD forward, 50-ggtgtctctctgacttc-30; huGAPD reverse, 50-ctcttctcttgtgctcttg- 30; TIB MOLBIOL).

2.7 References

- 1 Elzagheid, M. I.; Mattila, K.; Oivanen, M.; Jones, B. C. N. M.; Cosstick, R.; Lönnberg, H., Hydrolytic Reactions of the cis-Methyl Ester of 3'-Deoxy-3'-thiothymidine 3',5'-Cyclic(phosphorothiolate). *Eur. J. Org. Chem.* 2000, 1987-1991.
- 2 Damha, M. J.; Giannaris, P. A.; al., e., An improved procedure for derivatization of controlled-pore glass beads for solid-phase oligonucleotide synthesis. *Nucleic Acids Res.* 1990, 18, (13), 3813-3821.
- 3 Blackburn, P.; Moore, S., *The Enzymes*. ed.; Academic Press: New York, 1982; 'Vol.' p.
- 4 Watts, J. K.; Choubdar, N.; Sadalapure, K.; Robert, F.; Wahba, A. S.; Pelletier, J.; Mario Pinto, B.; Damha, M. J., 2'-Fluoro-4'-thioarabino-modified oligonucleotides: conformational switches linked to siRNA activity. *Nucl. Acids Res.* 2007, 35, (5), 1441-1451.

Chapter 3: Synthesis of 3'-Deoxy-3'-thiothymidine and Its Incorporation into Oligonucleotides

3.1 Relevance of 3',5'-Linked 3'-S-Phosphorothiolate Linkages

Nucleic acids maintain stable tertiary structures and catalyze chemical reactions without the diverse functional groups of proteins.^{1, 2} This economy prevents scientists from using site directed mutagenesis to replace a functional group, as is done with proteins, since this only affects hydrogen-bonding patterns. Thus, more elaborate methods involving the introduction of synthetic nucleosides containing non-native functional groups have been developed. There are four distinct positions in the phosphorus-sugar backbone where oxygen atoms are commonly substituted: 3', 5', and the two non-bridging phosphoryl oxygen atoms.

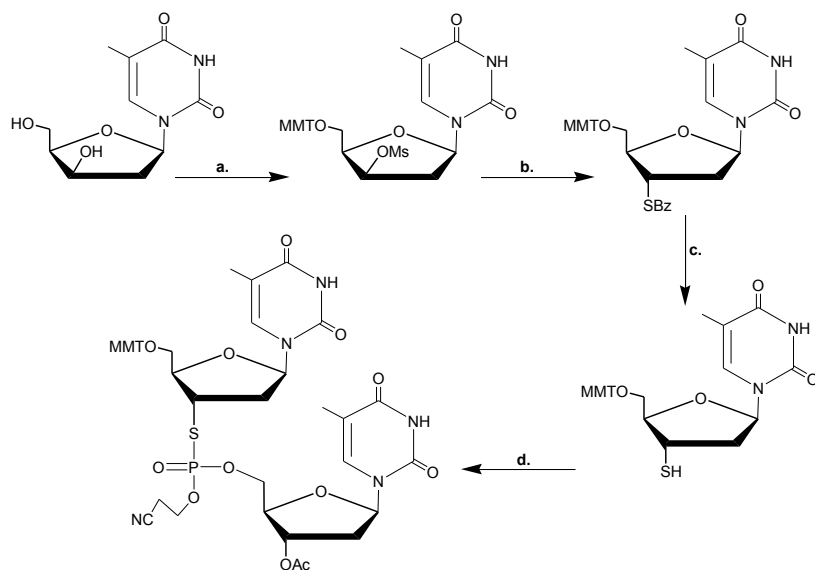
Sulphur is generally considered to be a conservative substitution for oxygen but there are important differences between the two; primarily the harder, more electronegative character of oxygen versus the softer, more polarisable character of sulphur. When the 3'-OH group of the furanose ring is replaced with a thiol function, these differences have a significant effect on the reactivity of the synthetic intermediates, the conformation of the sugar ring,³⁻⁶ the stability of the oligonucleotide⁷⁻¹¹ as well as biological implications, as will be explored in this chapter and the next. No studies directly examining the effect of bond length with 3'-S modification have appeared in the literature, however other studies involving the replacement of an oxygen atom with sulphur in nucleosides have found the difference in bond length to result in local changes but not to distort the overall structure beyond the normal range of oligonucleotides.¹²⁻¹⁵

3.2 Synthesis of 3'-Deoxy-3'-thiothymidine

The advent of 3'-thio modified nucleoside in the literature begins with Richard Cosstick *et al.*'s 1988 report of the synthesis of 5'-protected-3'-thiothymidine monomer and the solution coupling via *in situ* phosphorylation to yield the d(TspT) dimer,¹⁶⁻¹⁸ **Figure 3.1**. Other approaches to creating 3'-S-phosphorothiolate linkages include using phosphoramidites,¹⁹ phosphate triesters²⁰ and Michaelis-Arbusov type-reactions²¹ to create DNA-based dinucleotides and oligonucleotides.

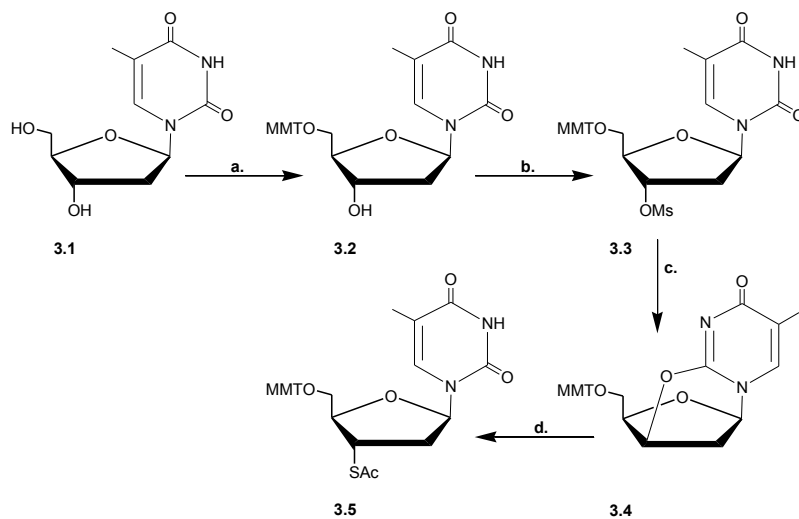
The synthetic pathway used to preparing the 3'-deoxy-3'-thiothymidine (3'S-dT) monomer, **Figure 3.2**, used in this work was mainly adapted by Anna Lisa Tedeschi for our lab²² from an earlier reported synthesis.²³ Improvements novel to this current work will be articulated in the following discussion.

Figure 3.1: Cosstick's Synthetic Scheme for 3'-Deoxy-3'-thiothymidine and its Incorporation into a Dinucleotide



- a. In 2 steps, per Horwitz et al.²⁴
 b. NaSBz, dimethylformamide, 100°C
 c. NH₃, MeOH, room temp., 1h
 d. (tetrazol-1-yl)₂-PO[CH₂]₂CN, 4:1 tetrahydrofuran-2,6-lutidine, -78°C, 15 min ; 3'-O-acetylthymidine, 20 min; then aqueous work-up.

Figure 3.2: 3'-Deoxy-3'-(thioacetyl)thymidine Synthetic Scheme



- a. MMTCl (1.5 eq), pyridine, rt, 10h, 99% yield.
 b. MsCl (3 eq), pyridine, rt, ON, 91% yield.
 c. Et₃N, EtOH, reflux, 16h, 95% yield.
 d. NaSAC, 1,4-dioxane, reflux 10h, 90% yield.

Starting with readily available thymidine (**3.1**), the 5'-hydroxyl group was regioselectively tritylated, due to steric constraints at the 3' position, to give 5'-O-(*p*-monomethoxytrityl)thymidine (**3.2**) in 99% yield. The 3'-hydroxyl was then mesylated to form 3'-O-methanesulfonyl-5'-O-(*p*-monomethoxytrityl)thymidine (**3.3**), 91% yield, and heated in ethanol to generate the 5'-O-(*p*-monomethoxytrityl)-2,3'-anhydronucleoside (**3.4**) in 95% yield with an inversion of stereochemistry at the C3' position. Sodium thioacetate was used to attack the C3' position, opening the newly formed ring and returning the nucleoside to the original stereochemistry, forming 3'-deoxy-5'-O-(*p*-monomethoxytrityl)-3'-(thioacetyl)thymidine (**3.5**) in 90% yield.

In the following deacetylation step, where a base is typically used to reveal the 3'-thiol group, experiments have been plagued with the formation of disulfide bonds, as is shown in **Figure 3.3**. This unwanted side reaction has led to lowered experimental yields,^{22, 25} where the disulfide (**3.7**) accounts for 10% or more of the isolated products. Following some experimentation, we found that this side product could be completely eliminated by the inclusion of dithiotreitol (DTT) in the reaction mixture, see **Table 3.1**. Thus, 3'-deoxy-5'-O-(*p*-monomethoxytrityl)-3'-thiothymidine (**3.6**) was isolated in a 92% yield by using a deoxygenated ethanolic solution of NaOH with 1.5 eq dithiothreitol.

Figure 3.3: Free Thiol and Disulfide Species Synthetic Scheme

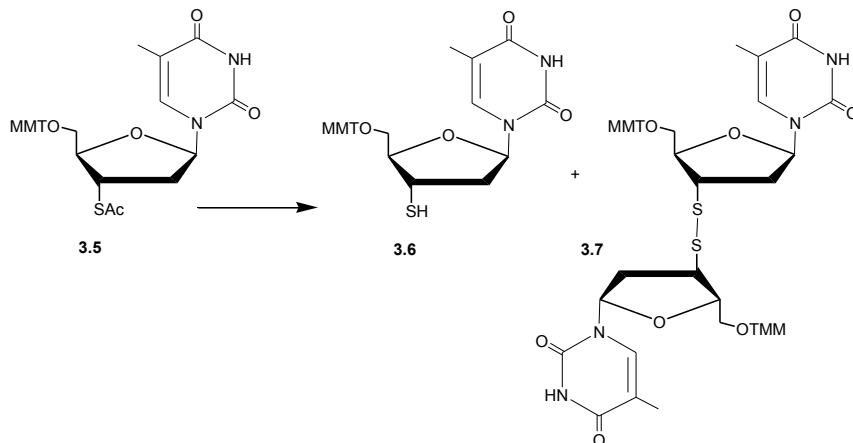
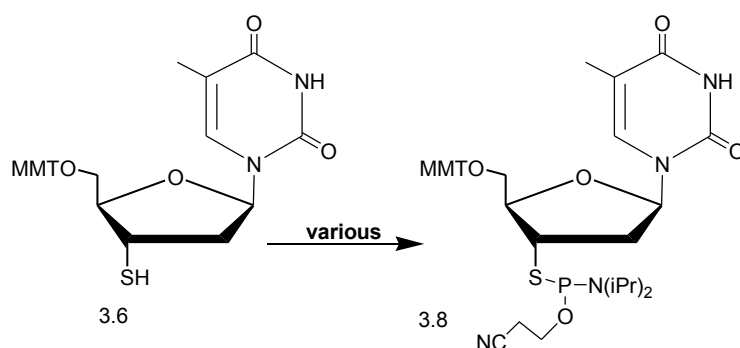


Table 3.1: Prevention of Disulfide Formation with DTT

Method	Product 3.6	Product 3.7
Dilute NaOH in EtOH, 2h neutralization with aq HCl	70%	10%
1.5 eq dithiothreitol, dilute NaOH in EtOH, 2h, neutralization with aq HCl	92%	n/a

In early experiments in our lab, 3'-deoxy-5'-(*p*-monomethoxytrityl)thymidine-3'-S-phosphorothioamidite (**3.8**), **Figure 3.4**, was synthesised using procedures typically employed for the native oxygen analog, namely 5 eq N,N-diisopropylethylamine, 1.5 eq dimethylaminopyridine and 1.5 eq N,N-diisopropylaminophosphonamidic chloride in dry THF with a longer reaction time to account for the less reactive character of sulphur.²² However, as the 3'-thio-phosphorothioamidite appears to be more sensitive than its 3'-oxygen counter part and attempts to purify it on neutralised silica columns did little to reduce the percentage of H-phosphonate side product present, alternative experimental procedures were explored. As these experiments fall into the category of oligonucleotide synthesis, they will be discussed in **Section 3.6** below.

Figure 3.4: 3'-S-Phosphorothioamidite Synthetic Scheme



3.3 Synthesis of Oligonucleotides Containing 3'-Deoxy-3'-thiothymidine Inserts

Coupling on automated solid support based DNA synthesizers has been optimized for native species and coupling efficiency can attain 99-99.5% for DNA and 95-98% for RNA.²⁶ These high rates are essential for creating long oligonucleotides but unfortunately 3'-thionucleosides are plagued with poor coupling yields.^{22, 25, 27} Most reports describe the synthesis of DNA oligomers containing one or very few 3'-S-phosphorothiolate linkages.^{1, 5, 6, 18-20, 27-34}

Cosstick reported the synthesis of the 5mer d(TTTspTT) on solid support with 80% coupling efficiency for the 3'-thionucleoside unit using 5-(*p*-nitrophenyl)tetrazole as an activator and tetrabutylammonium periodate as oxidant.³⁵ The mixed sequence 6mer d(GATspATC) was accomplished in slightly higher yields by delivering the reagents for the thioate coupling step by syringe.^{6, 29, 35} Cosstick *et al.* also explored a solution based disulfide approach to attempt to increase coupling yields^{5, 19, 31} but later abandoned it due to incompatibility with automated DNA synthesizers. Solubility issues with 5-(*p*-nitrophenyl)tetrazole in ACN led them back to the more common activators 4,5-dicyanoimidazole (DCI, 1M in ACN) and 4-ethylthiotetrazole (ETT, 0.25 M in ACN),²⁷ which were initially used in 15 minute coupling steps. This was later reduced to 2.5

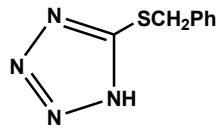
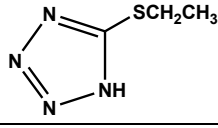
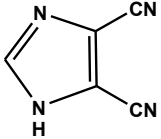
minutes for ETT^{34, 36} as no increase in yield was observed for extending the time beyond this point but later reports reverted to the 15 minute coupling time without explanation.^{34, 36} They also increased the 3'-thio-modified amidite concentration, to 0.15M in ACN, to enable the synthesis of oligomers containing up to five 3'-S-phosphorothiolate linkages.²⁵ In a recent oral presentation, R. Cosstick discussed the possibility of using dimer building blocks already containing an internal 3'-S-phosphorothiolate linkage presumably to get around poor coupling yields afforded by nucleoside 3'-S-phosphorothioamidite monomers.³⁷

An exploration of activators, oxidants and the preparation of the phosphorothioamidite was undertaken as part of this work to maximise the coupling of the 3'-S-dT nucleoside on the automated DNA synthesiser. In these experiments, and for all the oligonucleotides synthesised in this work, 2'-deoxyribonucleoside 3'-O-phosphoramidites were prepared as 0.1 M solutions in anhydrous acetonitrile and the ribonucleoside (RNA), 2'-F-ANA, and 2'-OMe RNA monomers as 0.15 M solutions in anhydrous acetonitrile. The 3'-deoxythymidine-3'-S-phosphorothioamidites were prepared as 0.15 M solutions in anhydrous dichloromethane. Commercially available, Cap A, Cap B and 3% trichloroacetic acid in dichloromethane solutions were used.

3.4 Activators for 3'-Thio Coupling

A comparison of the efficacy of 3'-thio coupling of three activators, 4-ethylthiotetrazole (ETT), 4,5-dicyanoimidazole (DCI) and 5-benzylthio-1-H-tetrazole (BTT) was performed by creating a dT-12mer with a single 3'-thio insert in position 5. The lower pK_a of ETT and BTT, **Table 3.2**, results in faster rates of reaction, as does, conversely, the greater nucleophilicity of DCI.³⁷

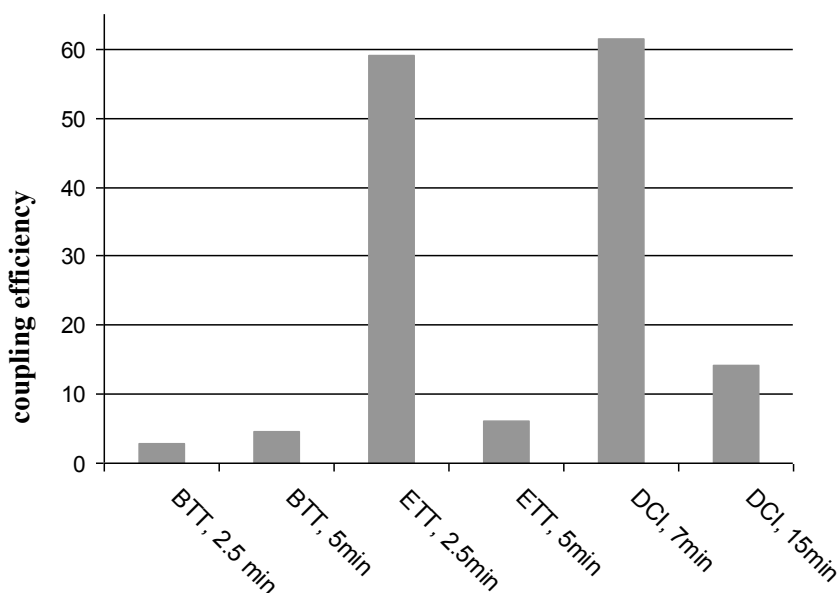
Table 3.2: A Comparison of the pK_a and Structure of Relevant Activators

Activator	pK _a ²⁷	Preparation	Structure
5-Benzylthio-1H-Tetrazole	4.1	0.5 M in ACN	
5-Ethylthio-1H-Tetrazole	4.3	0.25 M in ACN	
4,5-Dicyanoimidazole	5.2	1 M in ACN	

Oxidation was accomplished with a standard 0.1 M solution of iodine in THF/pyridine/water (25/20/2, v/v/v) and an extended detritylation time, 220s, was used to ensure complete removal of the *p*-monomethoxytrityl group (MMT). The coupling efficiency was characterised by reversed-phase HPLC analysis, where areas of the elution peaks for failure and full length oligonucleotides were compared. All values were normalised to a pure dT-12mer sample run.

As seen in **Figure 3.5**, ETT with a coupling time of 2.5 minutes or DCI with a coupling time of 7 minutes were equally effective in our hands, reflecting the findings of Cosstick.³⁸ The disappointing performance of BTT may be due to steric bulk and/or excessive acidity. Based on these results, ETT at 2.5 minutes was selected as the standard for all further syntheses.

Figure 3.5: Comparison of Activators for 3'-Thio Oligonucleotide Synthesis



3.5 Oxidants for the Preparation of dT₁₂ Containing a Single 3'-S-dT Unit

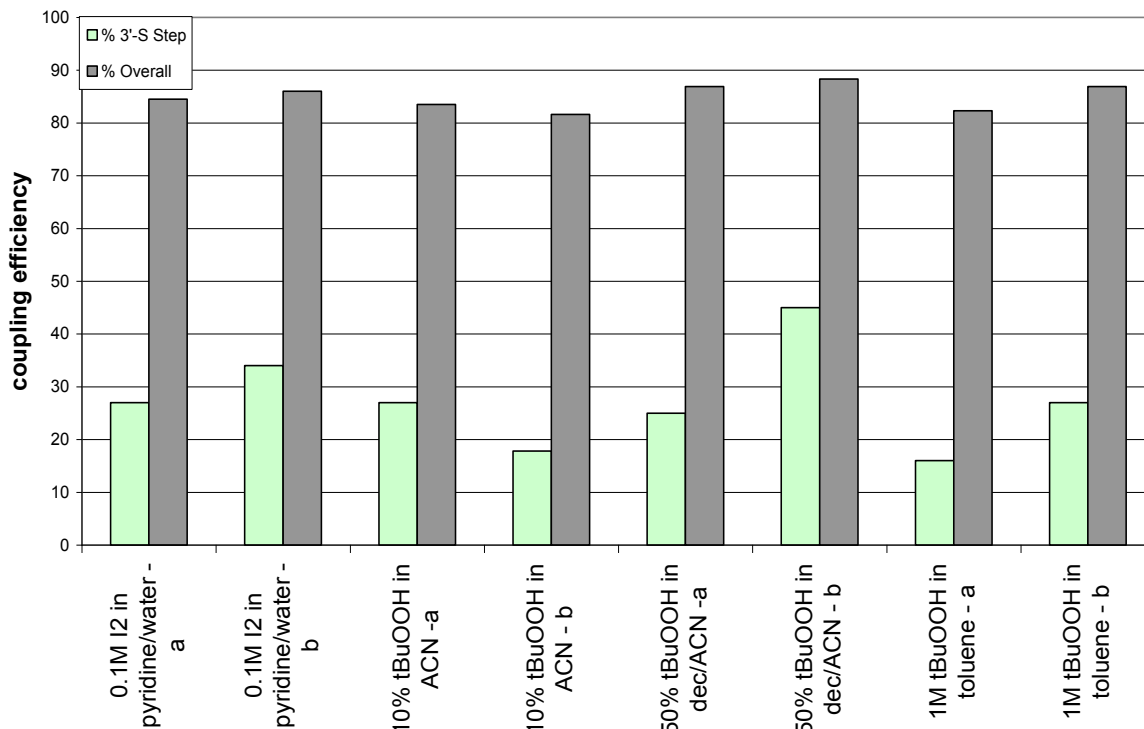
An exploration of milder oxidation conditions was undertaken in an attempt to improve the yield for the 3'-S modified oligonucleotide. Thus, a comparison of the efficacy of 3'-thio coupling with four oxidation systems, 0.1 M solution of iodine in THF/pyridine/water (25/20/2, v/v/v), 10% *tert*-butyl hydrogen peroxide (tBuOOH) in ACN, 50% tBuOOH in decane/ACN, and 1M tBuOOH in toluene, was performed by creating a dT-12mer with a single 3'-S-dT insert at position 5. The synthesis was carried out with 0.25M ETT in ACN, 2.5 minutes, as activator and an extended detritylation time, 220s, to ensure complete removal of the MMT group. The syntheses were monitored by coupling efficacy, measured internally by trityl conductance by the

DNA synthesiser. A summary of the conditions is presented below in **Table 3.3** and a comparison of efficacy in **Figure 3.6**.

Table 3.3: Oxidants for the Preparation of Thymidylic Acid (12 mer) Containing a Single 3'-S-dT Residue

Oxidant System	Delivery time (s)	Wait time (s)
0.1M I ₂ in THF/pyridine/water		
a.	20	25
b.	20	18
10% tBuOOH in ACN		
a. repeat delivery and wait steps	20	100
b. single delivery and wait steps	20	300
50% tBuOOH in decane/ACN		
a.	20	25
b.	20	15
1M tBuOOH in toluene		
a.	20	40
b.	30	20

Figure 3.6: Comparison of Oxidants Systems in the Preparation of dT₁₂ Containing a Single 3'-S-Phosphorothiolate Linkage



The best coupling efficiencies for the 3'-S step were with the 0.1M I₂ (20s, then 25s) and 50% tBuOOH (20s, then 15s) system. Thus, a further comparison of these two oxidants was performed with an oligoribonucleotide 21mer, 3'-ggCGAACUXCAGAAAUUAUU-5', using 0.25M ETT at 2.5 minutes and 220s of detritylation. The syntheses were monitored by coupling efficacy, measured internally by trityl conductance by the DNA synthesiser, as shown in **Table 3.4**. The lack of differentiation in the results led us to continue using the I₂ system since it was easier for practical reasons. This finding is supported by Joseph A. Piccirilli's group²⁷.

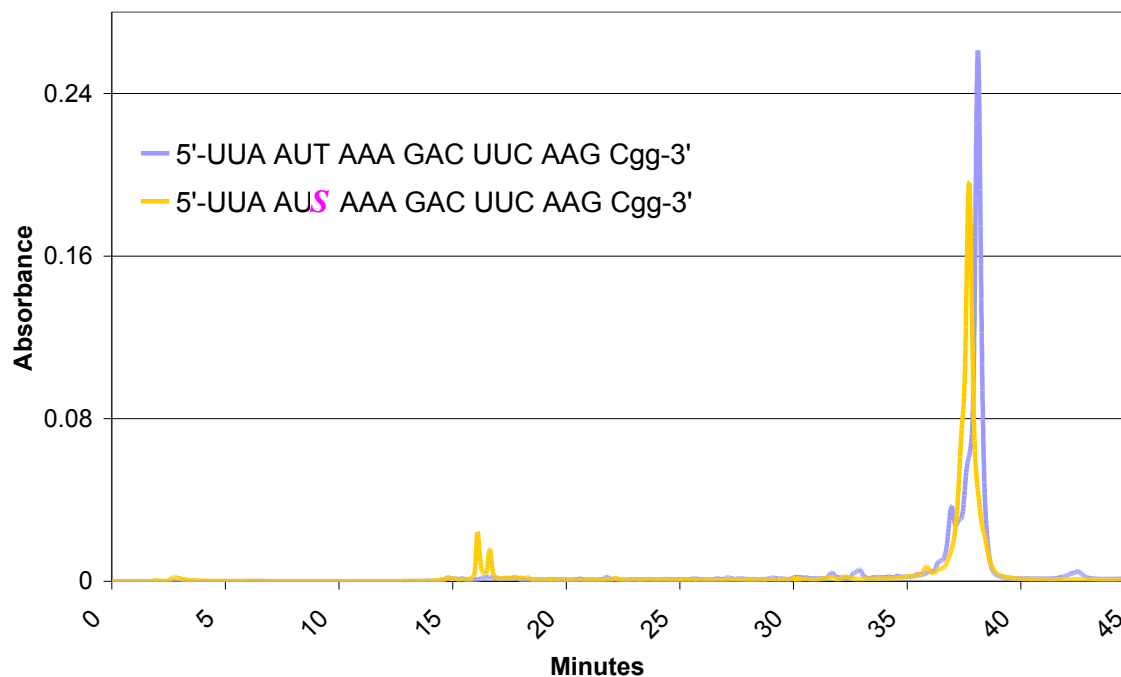
Table 3.4: Comparison of Overall Coupling Efficacy for Mixed Sequence 21mers with 2 Oxidants

Oxidant	Delivery	Wait	Comments	X=U	X=3'-S ^a
0.1M I ₂ in THF/pyr/water	20 s	25 s		97%	86%
50% tBuOOH in ACN	12 s	300 s	Repeat delivery and wait.	96%	86%

^aAverage of three runs.

A good synthesis with relatively efficient coupling of the 3'-S-dT insert will still result in considerable failure sequences where the insert does not couple, as seen around the 16-17 minute mark in the HPLC trace in **Figure 3.7**.

Figure 3.7: HPLC trace of Crude Oligoribonucleotides^a

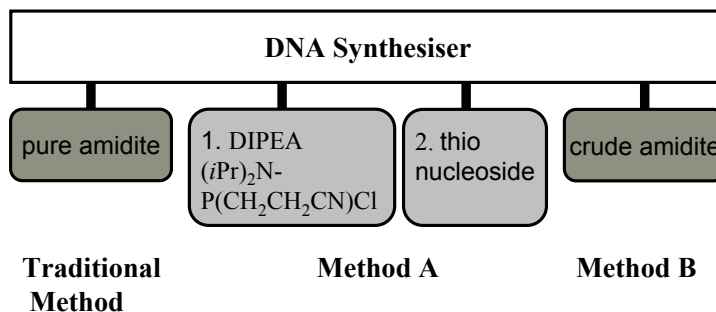


^aU,T,G,C = ribonucleosides, g = 2'-deoxyguanosine, S = 3'-deoxy-3'-thiothymidine.

3.6 Alternative Phosphitylation Conditions

As previously mentioned, standard methods for the synthesis of the 3'-S-phosphorothioamidite (**3.8**) resulted in a hard to purify product of low quality. Thus, two novel methods for avoiding exposure of the 3'-S-phosphorothioamidite to atmospheric conditions were explored, shown schematically in **Figure 3.8**.

Figure 3.8: Schematic Illustration of Three Phosphitylation Methods



In Method A, the oligonucleotide is propagated on the DNA synthesiser according to standard procedures (2.5 minutes of 0.25M ETT, I₂ oxidation and 220s of detritylation) until the point of 3'-thio insertion. Here, the growing oligonucleotide was detritylated under normal conditions and then the exposed 5'-hydroxyl is phosphitylated by addition of a DCM solution that is 0.1M in both N,N-diisopropylaminophosphonamidic chloride and N,N-diisopropylethylamine (DIPEA) delivered from an auxiliary amidite port. A solution of 0.15M solution of 3'-deoxy-5'-(*p*-monomethoxytrityl)-3'-thiothymidine nucleoside in DCM is then immediately delivered from another auxiliary amidite port. Normal automated synthesis is then resumed, so the 5'-MMT of the newly incorporated 3'-deoxy-3'-thiothymidine is removed and the oligonucleotide is extended.

In Method B, a 0.15M solution of meticulously dried 3'-deoxy-5'-(*p*-monomethoxytrityl)-3'-thiothymidine nucleoside in anhydrous CH₂Cl₂ is combined in situ with 0.95 eq of N,N-diisopropylaminophosphonamidic chloride and 1.5 eq of DIPEA in an amidite vial to react under a blanket of nitrogen for 30 minutes and then attached directly to an amidite port. The oligonucleotide synthesis is then run normally, and the in situ synthesized 3'-thio-phosphorothioamidite is delivered automatically, although crude, to the growing RNA chain.

The syntheses were monitored by coupling efficacy, measure internally by trityl conductance by the DNA synthesiser, as shown in **Table 3.5**. Method A was not judged a success but the incorporation of 3'-S-phosphorothioamidite with Method B was higher than had been previously achieved in our hands, despite the lower overall yield. However, as the characterisation

and biological activity of these 3'-thio modified oligoribonucleotides were the main objective of this work, we did not seek to further optimize the approach.

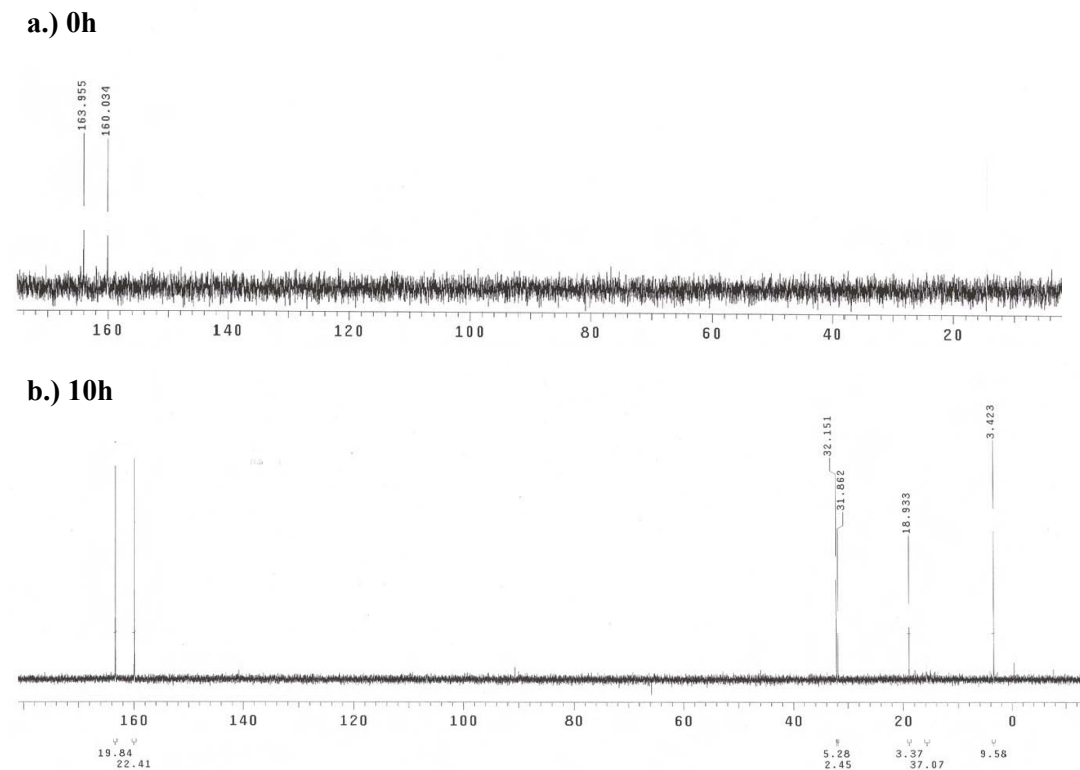
Table 3.5: Comparison of Coupling Efficacy for Alternative Phosphitylation Methods with dT-12mers

Method	3'-S Step Yield	Overall Yield
A	26%	25%
B	65%	56%

3.7 Phosphorothioamidite Stability

The stability of the 3'-S-phosphorothioamidite (**3.8**) was assessed by NMR to determine if the poor coupling yields during synthesis were due, in part, to deterioration of the reactive 3' group required for coupling. A quantitative ^{31}P NMR experiment, with an extended relaxation time (τ_2), was undertaken to record a spectrum each half hour for 24h of a sample of the 3'-S-phosphorothioamidite at room temperature in CDCl_3 . Two representative spectra are presented in **Figure 3.9**.

Figure 3.9: ^{31}P NMR of Phosphorothioamidite



For the first 8h of the experiment no changes were observed in the spectra, i.e. signals at 163 and 159 ppm remained in constant ratio, see **Figure 3.9**, but at 10h some additional signals of low intensity were observed between 80 and 20 ppm although these did not increase appreciably in intensity in the remaining 14h. Fresh samples of 3'-S-phosphorothioamidite were prepared in acetone-*d*₆, CDCl₃ and ACN-*d*₃ and quantitative ³¹P NMR spectra were recorded immediately. When a second spectrum of each was recorded 2 days later, the samples in acetone-*d*₆ and CDCl₃ were unchanged, but the ACN sample showed several new phosphorus species and a decline in the intensity of the phosphorothioamidite signals. Thymidine 3'-S-phosphorothioamidite (**3.8**) stored as a dry foam in the freezer for 2 months was unchanged. Thus, phosphorothioamidites stored in the freezer and freshly prepared in CH₂Cl₂ were taken to be stable on the DNA synthesiser for the ~8h run and no further concern about their stability was entertained.

3.8 Summary of Optimised Synthesis Conditions for Oligonucleotides Containing 3'-Deoxy-3'-thiothymidine

The optimal conditions for synthesis of oligoribonucleotides containing 3'-S-phosphorothiolate linkages, in our hands, is summarised in **Table 3.6**.

Table 3.6: Optimised Conditions for 3'-S-Phosphorothioamidite Coupling

Parameter	Recommendation
Activator	0.25 M ETT in ACN, 2.5 minutes
Oxidant	0.1M I ₂ in THF/pyr/water (25/20/2, v/v/v)
3'-S-Phosphorothioamidite Preparation	0.18 M 5'-MMT-3'-deoxy-3'-thiothymidine, 0.17 M N,N-diisopropylaminophosphonamidic chloride, and 0.23 M DIPEA in CH ₂ Cl ₂ reacted in amidite vial and delivered crude.

With these conditions, a small library of native and chimeric oligonucleotides was assembled on the DNA synthesiser and their characterization will be addressed in Chapter 4. Phosphorothioamidite coupling yields were adequate to produce sufficient samples for characterisation and biological assays but would prove a serious issue for wider application of these compounds.

3.9 References

- 1 Breaker, R. R.; Joyce, G. F., A DNA enzyme that cleaves RNA. *Chem. Biol.* **1994**, 1, 223-229.
- 2 Gold, L.; Polisky, B.; Uhlenbeck, O.; Yarus, M., *Annu. Rev. Biochem.* **1995**, 64, 763-797.

- 3 Watts, J. K.; Choubdar, N.; Sadalapure, K.; Robert, F.; Wahba, A. S.; Pelletier, J.; Mario Pinto, B.; Damha, M. J., 2'-Fluoro-4'-thioarabino-modified oligonucleotides: conformational switches linked to siRNA activity. *Nucl. Acids Res.* **2007**, *35*, (5), 1441-1451.
- 4 Inoue, N.; Minakawa, N.; Matsuda, A., Synthesis and properties of 4'-ThioDNA: unexpected RNA-like behavior of 4'-ThioDNA. *Nucleic Acids Res.* **2006**, *34*, 3476-3483.
- 5 Beever, A. P. G.; Fettes, K. J.; Sabbagh, G.; Murad, F. K.; Arnold, J. R. P.; Cosstick, R.; Fisher, J., NMR and UV studies of 3'-S-phosphorothiolate modified DNA in a DNA:RNA hybrid dodecamer duplex; implications for antisense drug design. *Organic & Biomolecular Chemistry* **2003**, *2*, (1), 114-119.
- 6 Beever, A. P. G.; Witch, E. M.; Jones, B. C. N. M.; Cosstick, R.; Arnold, J. R. P.; Fisher, J., Conformational analysis of 3'-S-PO₃-linked ribo- and deoxyribodinucleoside monophosphates. *Magn. Reson. Chem.* **1999**, *37*, (11), 814-820.
- 7 Eckstein, F., *Annu. Rev. Biochem.* **1985**, *54*, 367-402.
- 8 Cosstick, R.; Eckstein, F., Synthesis of d(GC) and d(CG) Octamers Containing Alternating Phosphorothioate Linkages: Effect of the Phosphorothioate Group on the B-Z Transition. *Biochemistry* **1985**, *24*, 3630-3638.
- 9 Burgers, P. M. J.; Eckstein, F., Diastereomers of 5'-O-adenosyl 3'-O-uridyl phosphorothioate: chemical synthesis and enzymic properties. *Biochemistry* **1978**, *18*, 592-96.
- 10 Bhan, P.; Bhan, A.; Hong, M.; Hartwell, J. G.; Saunders, J. M.; Hoke, G. D., 2',5'-Linked oligo-3'-deoxyribonucleoside phosphorothioate chimeras: thermal stability and antisense inhibition of gene expression. *Nucleic Acids Res.* **1997**, *25*, 3310-3317.
- 11 Woolf, T. M.; Jennings, C. G.; Rebagliati, M.; Melton, D. A., The stability, toxicity and effectiveness of unmodified and phosphorothioate antisense oligodeoxynucleotides in *Xenopus* oocytes and embryos. *Nucleic Acids Res.* **1990**, *18*, (7), 1763-1769.
- 12 Thewalt, U.; Bugg, C. E., Effects of Sulfur Substituents on Base Stacking and Hydrogen Bonding. The Crystal Structure of 6-Thioguanosine Monohydrate. *J. Am. Chem. Soc.* **1972**, *94*, (25), 8892-8898.
- 13 Xu, Y.; Kool, E. T., Chemical and enzymatic properties of bridging 5'-S-phosphorothioester linkages in DNA. *Nucleic Acids Res.* **1998**, *26*, (13), 3159-3164.
- 14 Minakawa, N.; Kaga, D.; Kato, Y.; Endo, K.; Tanaka, M.; Sasaki, T.; Matsuda, A., Synthesis and structural elucidation of 1-(3-C-ethynyl-4-thio-beta -D-ribofuranosyl)cytosine (4 -thioECyd). *J. Chem. Soc., Perkin Trans. I* **2002**, 2182 - 2189.
- 15 Boggon, T. J.; Hancox, E. L.; McAuley-Hecht, K. E.; Connolly, B. A.; Hunter, W. N.; Brown, T.; Walker, R. T.; Leonard, G. A., The crystal structure analysis of d(CGCGAASSCGCG)₂, a synthetic DNA dodecamer duplex containing four 4 -thio-2 -deoxythymidine nucleotides. *Nucleic Acids Res.* **1996**, *24*, (5), 951-961.
- 16 Denisov, A. Y.; Hannoush, R. N.; Gehring, K.; Damha, M. J., A Novel RNA Motif Based on the Structure of Unusually Stable 2',5'-Linked r(UUCG) Loops. *J. Am. Chem. Soc.* **2003**, *125*, (38), 11525-11531.
- 17 Cosstick, R.; Vyle, J. S., Synthesis and phosphorus-sulphur bond cleavage of 3-thiothymidylyl(3-5)thymidine. *J. Chem. Soc. Chem. Commun.* **1988**, 992-993.
- 18 Cosstick, R.; S.Vyle, J., Synthesis and properties of dithymidine phosphate analogues containing 3'-thiothymidine. *Nucleic Acids Res.* **1990**, *18*, (4), 829-835.
- 19 Fettes, K.; O'Neil, I.; Roberts, S. M.; Cosstick, R., Solid-phase synthesis of oligodeoxynucleotides containing 3'-S-phosphorothiolate linkages. *Nucleosides, Nucleotides & Nucleic Acids* **2001**, *20*, (4-7), 1351-1354.
- 20 Vyle, J.; Li, X.; Cosstick, R., New methods for the synthesis of 3'-S-phosphorothiolate internucleoside linkages. *Tetrahedron Lett.* **1992**, *33*, (21), 3017-3020.
- 21 Li, X.; Cosstick, R., Application of an intramolecular Michaelis-Arbusov reaction to the synthesis of nucleoside 3'-S,5'-O-cyclic phosphorothiolate triesters. *J. Chem. Soc., Perkin Trans. I* **1993**, 1091.
- 22 Tedeschi, A. L. Synthesis and Biological Evaluation of Oligonucleotides Containing 3'- and 5'-S-Phosphorothiolate Internucleotide Linkages. M.Sc. Thesis, McGill University, Montreal, 2004.
- 23 Eleuteri, A.; Reese, C. B.; Song, Q., Synthesis of 3,5-dithiothymidine and related compounds. *J. Chem. Soc., Perkin Trans. I* **1996**, *18*, 2237 - 2240.

- 24 Horwitz, J. R.; Chua, J.; Noel, M., Nucleosides V: The monomesylates of 1-(2'-deoxy-beta-D-lyxofuranosyl)thymidine. *J. Org. Chem.* **1964**, 29, 2076.
- 25 Cosstick, R. In *UK Stabilization of Multi-Stranded Nucleic Acid Structures Using 3'-S-Phosphorothiolate Linkages*, The XVII International Roundtable on Nucleosides, Nucleotides and Nucleic Acids (IRT XVII), Bern, Switzerland, 2006; Haenni, D. L., 'Ed.' 'Eds.' Bern, Switzerland, 2006; p[^]pp.
- 26 Davis, R. H., Large-scale oligoribonucleotide production. *Curr. Opin. Biotechnol.* **1995**, 6, (2), 213-217.
- 27 Sabbagh, G.; Fettes, K. J.; Gosain, R.; O'Neil, I. A.; Cosstick, R., Synthesis of phosphorothioamides derived from 3'-thio-3'-deoxythymidine and 3'-thio-2',3'-dideoxycytidine and the automated synthesis of oligodeoxynucleotides containing a 3'-S-phosphorothiolate linkage. *Nucleic Acids Res.* **2004**, 32, (2), 495-501.
- 28 Li, X.; Andrews, D.; Cosstick, R., Synthesis of a Dinucleoside 3'S-Phosphorothiolate Containing 2'-Deoxy-3'-Thioadenosine. *Tetrahedron* **1992**, 48, (13), 2729-2738.
- 29 Weinstein, L. B.; Earnshaw, D. J.; Cosstick, R.; Cech, T. R., Synthesis and Characterization of an RNA Dinucleotide Containing a 3'-S-Phosphorothiolate Linkage. *J. Am. Chem. Soc.* **1996**, 118, (43), 10341-10350.
- 30 Cosstick, R.; Vyle, J. S., Solid-phase synthesis of oligonucleotides containing 3'-thiothymidine. *Tetrahedron Lett.* **1989**, 30, 4693-4696.
- 31 Beevers, A. P. G.; Fettes, K. J.; O'Neil, I. A.; Roberts, S. M.; Arnold, J. R. P.; Cosstick, R.; Fisher, J., Probing the effect of a 3A-S-phosphorothiolate link on the conformation of a DNA:RNA hybrid; implications for antisense drug design. *Chemical Communications* **2002**, 14, 1458-1459.
- 32 Cosstick, R.; Buckingham, J.; Brazier, J.; Fisher, J., Stabilization Of Multi-Stranded Nucleic Acid Structures Using 3'-S-Phosphorothiolate Linkages. *Nucleosides, Nucleotides and Nucleic Acids Research* **2007**, 26, 555 - 558.
- 33 Jayakumar, H. K.; Buckingham, J. L.; Brazier, J. A.; Berry, N. G.; Cosstick, R.; Fisher, J., NMR studies of the conformational effect of single and double 3'-S-phosphorothiolate substitutions within deoxythymidine trinucleotides. *Magn. Reson. Chem.* **2007**, 45, (4), 340-345.
- 34 Bentley, J.; Brazier, J. A.; Fisher, J.; Cosstick, R., Duplex stability of DNA·DNA and DNA·RNA duplexes containing 3'-S-phosphorothiolate linkages. *Organic & Biomolecular Chemistry* **2007**, 5, 3698-3702.
- 35 Vyle, J. S.; Connolly, B. A.; Kemp, D.; Cosstick, R., Sequence- and Strand-Specific Cleavage in Oligodeoxyribonucleotides and DNA Containing 3'-Thiothymidine. *Biochemistry* **1992**, 31, 3012-3018.
- 36 Buckingham, J.; Sabbagh, G.; Brazier, J.; Fisher, J.; Cosstick, R., Control of DNA Conformation Using 3'-S-Phosphorothiolate-Modified Linkages. *Nucleosides, Nucleotides and Nucleic Acids* **2005**, 24, (5), 491-495.
- 37 Research, G. Technical Brief - ABOUT ACTIVATORS: Now and tomorrow. (May 5th),
- 38 Sun, S.; Yoshida, A.; Piccirilli, J. A., Synthesis of 3'-thioribonucleosides and their incorporation into oligoribonucleotides via phosphoramidite chemistry. *RNA* **1997**, 3, (11), 1352-1363.

Chapter 4: Physical and Biological Characterisation of Oligonucleotides Containing 3'-S-Phosphorothiolate Linkages

4.1 Introduction

Broad therapeutic use of RNAi depends on the development of synthetic oligonucleotides able to strongly induce RISC, and with good nuclease resistance, sufficient cell penetration and high affinity for the target mRNA.¹ Our laboratory has investigated the importance of pre-organization and flexibility in eliciting RNaseH in the antisense strategy,^{2, 3} and the rising importance of RNAi has prompted the present investigation into the use of 3'-deoxy-3'-thiothymidine (3'-S-dT) inserts in RNA. This project was initiated based on promising early experiments in our lab⁴ and other reports^{5, 6} of the 3'-thio modification in DNA. Because this modification mimics the structure of ribonucleosides (*north* pucker), we thought it would be compatible with the RNAi pathway while providing solutions to some of the challenges facing siRNA therapeutics, e.g., the development of siRNA chemistries that enhance or maintain cellular activity.

In the present chapter, the impact of this modification on the structure and activity of siRNA duplexes will be investigated by thermal denaturing experiments, circular dichroism and cell based assays, while drawing comparisons, when appropriate, to the known 3'-S-DNA oligonucleotides.

4.2 3'-Phosphorothiolate Linkages and Conformation

The conformation of nucleosides can be influenced by structural changes in the carbohydrate moiety. The absence of a 2' substituent in 2'-deoxynucleosides generally results in a dynamic equilibrium between the *north* and *south* conformers, although the *south* conformer is generally favoured.^{7,8} In this case, the electronegativity of its 3'-OH substituent leads to a strong *gauche* effect between the 3'-OH and the ring oxygen (O4'). As the *south* pucker is favored, this *gauche* effect must override the anomeric effect that stabilizes the *north* conformer. Substitution at the 3' position with the less electronegative sulphur atom lessens the *gauche* effect, allowing the anomeric effect to dominate and populate the *north* conformation.

Cosstick and co-workers investigated these effects with respect to 3'-thio modification by comparing the conformation of 3'-S-phosphorothiolate linked DNA (TspT) and RNA (IspU) dinucleotides to the conformations of native (phosphodiester-linked) dinucleotide TpT using ¹H NMR spectroscopy. They found that in both the DNA and RNA dimers the sugar ring conformations are affected by the 3'-S-phosphorothiolate modification, with a large increase in

the percentage of *north*-type puckering. This change was ascribed to the decrease in the influence of the *gauche* effect between the 3'-S substituent and the O4'-ring oxygen experienced when replacing an oxygen atom by the less electronegative 3'-sulphur atom. Further NMR studies by Cosstick's group on DNA trimers containing 3'-S-dT units confirmed that the 3'-S-phosphorothiolate linkage shifts the conformation of its own sugar ring to *north* along with that of its 3' neighbour.⁹ This phenomenon is possibly due to increased intramolecular base stacking. Surprisingly, two consecutive 3'-S-dT inserts do not affect the conformation of neighbouring nucleotides, indicating that the maximum effect of 3'-thio modifications can be achieved by non-consecutive incorporation,¹⁰ up to the saturation point of 3 inserts, either contiguous or alternating with native dT residues, in the 16mer sequence d(GCGTTTTTTTTTTGCG).¹¹ Cosstick and co-workers also reported that a single 3'-thio insert in a DNA dodecamer maintains its preferred *north* conformation and influences the conformation of its neighbour towards *north*, resulting in a reproducible increase in melting temperature of 2.5°C.¹² These observations are similar, although less dramatic, than those observed with LNA modified duplexes. LNA is able to shift the conformation of the neighbouring ribo and 2'-deoxyribonucleosides to 90% *north*¹³ and favours increased intrastrand base stacking.^{14, 15}

The above findings demonstrating the RNA-like (*north*) conformation of 3'-deoxy-3'-thionucleosides is of considerable interest in the search for suitable siRNA drugs, and suggest that this modification can be used to modify siRNA without compromising its potency.

4.3 A Library of Modified RNA Duplexes Containing 3'-Thio Linkages

A concise library of chemically modified RNA duplexes was synthesised. The duplexes were composed predominantly of native ribonucleotides, with inserts of 3'-deoxy-3'-thiothymidine (3'-S-dT), 2'-deoxy-2'-fluorouridine, 2'-OMe-uridine, and 2'-deoxynucleotides. For our RNAi investigation, we selected a mixed sequence short interfering RNA (siRNA) duplex shown to be effective in the down-regulation of the protein luciferase in modified HeLa cells. The annealed duplexes have a complementary region of 19 base pairs and 2-nt DNA overhangs on the 3' ends. Incorporating 2'-deoxynucleotide residues reduces synthesis costs and may possibly decrease the exonuclease degradation of siRNA in cells.⁵ Heavier DNA modification can reduce off-target effects.⁶

The small amounts of oligonucleotide produced by the low yielding syntheses in Chapter 3 were prioritized for thermal stability and RNAi analysis. When sufficient sample remained, the oligonucleotide was also characterized by MS, see **Table 4.1**.

Table 4.1: Mass Spectral Characterization of Selected Oligonucleotide Strands Used to Create the siRNA Duplex Library^a

sequence	exp mass	calc mass	Constituent of duplexes:
5'-GCUUGAAGUCUUUAAUUAAtt-3'	6616.7	6616.9	SiG1-16
5'-GCUUGAAGtCUUUAUUAAtt-3'	6670.5	6671.0	SiG23, 32
5'-GCUUGAAGUCUUUAAUSAAAtt-3'	6631.3	6631.1	SiG17, 26
5'-GCUUGAAGUCUUUAAUSUAAtt-3'	6630.3	6631.1	SiG18, 27
5'-GCU SGAAGUCUUUAAUUAAtt-3'	6697.4	6697.1 3H → 3Na	SiG20, 29
5'-GCUUGAAG SCUUUAUUAAtt-3'	6644.5	6644.9	SiG22, 31
5'-GCUUGAAG UCUUUAUUAAtt-3'	6685.8	6685.0 3H → 3Na	SiG24, 33
3'-ggCGAACUUCAGAAAUAAUU-5'	6673.8	6672.9	SiG1, 17-25
3'-ggCGAACUUCAGAAASUAAUU-5'	6841.3	6841.1 7H → 7Na	SiG5
3'-ggCGAACUSCAGAAAUAAUU-5'	6753.2	6753.1 3H → 3Na	SiG6, 26-34
3'-ggCGAAC SUCAGAAAUAAUU-5'	6708.6	6707.1 3H → 3Na	SiG7

^aA,C,G,U = standard ribonucleotides, S = 3'-deoxy-3'-thiothymidine, X = 2'-OMe nucleotides, U = 2'-deoxy-2'-fluorouridine, t = thymidine, g = 2'-deoxyguanosine

The library of duplexes can be divided into three broad categories by which strand(s) of the duplex are modified, as presented in the following three tables. The all-native RNA control duplex, and duplexes with a native RNA passenger strand and a modified RNA guide strand are shown in **Table 4.2**. Duplexes containing a native RNA guide strand and a modified RNA passenger strand are shown in **Table 4.3**. Duplexes containing a 3'-thio modified guide strand and a modified RNA passenger strand are shown in **Table 4.4**.

Table 4.2: An Inventory of Duplexes with a Native RNA Passenger Strand and a Modified RNA Guide Strand^{a,b}

Name	Sequence	T_m	ΔT_m	hysteresis ^c
SiG1	3'-ggCGAACUUCAGAAAUAAUU-5' 5'-GCUUGAAGUCUUUAAUUAAtt-3'	61.0 61.0 61.0		1.0 1.0 1.0
SiG2	3'-ggCGAACUUCAGAAAUAAU S -5' 5'-GCUUGAAGUCUUUAAUUAAtt-3'	61.1	+0.1	1.4
SiG3	3'-ggCGAACUUCAGAAAUAA SU -5' 5'-GCUUGAAGUCUUUAAUUAAtt-3'	57.9	-3.1	2.8
SiG4	3'-ggCGAACUUCAGAAAU S AAUU-5' 5'-GCUUGAAGUCUUUAAUUAAtt-3'	56.8	-4.2	-0.3
SiG5	3'-ggCGAACUUCAGAAA S UAAUU-5' 5'-GCUUGAAGUCUUUAAUUAAtt-3'	56.0	-5.0	2.1
SiG6	3'-ggCGAACU S CAGAAAUAAUU-5' 5'-GCUUGAAGUCUUUAAUUAAtt-3'	61.3*	+0.3	1.1
SiG7	3'-ggCGAAC S UCAGAAAUAAUU-5' 5'-GCUUGAAGUCUUUAAUUAAtt-3'	62.0	+1.0	1.0
SiG9	3'-ggCGAACUUCAGAAAU t AAUU-5' 5'-GCUUGAAGUCUUUAAUUAAtt-3'	61.1	+0.1	1.4
SiG10	3'-ggCGAACUUCAGAAAU t UAAUU-5' 5'-GCUUGAAGUCUUUAAUUAAtt-3'	60.1	-0.9	1.3
SiG11	3'-ggCGAACU t CAGAAAUAAUU-5' 5'-GCUUGAAGUCUUUAAUUAAtt-3'	61.9	+0.9	1.5
SiG12	3'-ggCGAAC t UCAGAAAUAAUU-5' 5'-GCUUGAAGUCUUUAAUUAAtt-3'	61.8	+0.8	1.5
SiG13	3'-ggCGAACUU t AGAAAUUCAUU-5' 5'-GCUUGAAGUCUUUAAUUAAtt-3'	52.5	-8.5	1.0
SiG14	3'-ggCGAACUU U AGAAAUAAUU-5' 5'-GCUUGAAGUCUUUAAUUAAtt-3'	55.5	-5.5	2.6
SiG15	3'-ggCGAACUU S AGAAAUAAUU-5' 5'-GCUUGAAGUCUUUAAUUAAtt-3'	59.9	-1.1	1.2
SiG16	3'-ggCGAACU S CAGAAAUAA UU -5' 5'-GCUUGAAGUCUUUAAUUAAtt-3'	59.6	-1.4	1.1*

^aA,C,G,U = standard ribonucleotides, **S** = 3'-deoxy-3'-thiothymidine, **S** = mismatch 3'-deoxy-3'-thiothymidine, **U** = 2'-OMe-uridine, **U** = mismatch uridine, **t** = mismatch thymidine, t = thymidine, g = 2'-deoxyguanosine

^b T_m experiments on aqueous solutions of $\sim 2 \times 10^{-6}$ M of each oligonucleotide strand, 140 mM KCl, 1 mM MgCl₂, 5 mM Na₂HPO₄ buffer (pH 7.2); uncertainty of ± 0.5 °C. ΔT_m calculated for heating curve, relative to control, by the baseline method. ^c Hysteresis between heating and cooling profiles was calculated from the derivative T_m values. *Data from second thermal run.

Table 4.3: An Inventory of Duplexes with a Native RNA Guide Strand and a Modified RNA Passenger Strand ^{a,b}

Name	Sequence	T_m	ΔT_m	hysteresis ^c
SiG17	3'-ggCGAACUUCAGAAAUAAUU-5' 5'-GCUUGAAGUCUUUAAU S AAtt-3'	62.5	+1.5	1.1
SiG18	3'-ggCGAACUUCAGAAAUAAUU-5' 5'-GCUUGAAGUCUUUAA S UAAtt-3'	61.3	+0.3	0.7
SiG19	3'-ggCGAACUUCAGAAAUAAUU-5' 5'-GCUUGAAG S CUUUAAUUAAtt-3'	59.6	-1.4	n.d.
SiG20	3'-ggCGAACUUCAGAAAUAAUU-5' 5'-GCU S GAAGUCUUUAAUUAAtt-3'	55.7	-5.3	0.9
SiG21	3'-ggCGAACUUCAGAAAUAAUU-5' 5'-GC S UGAAGUCUUUAAUUAAtt-3'	53.5	-7.5	1.1
SiG22	3'-ggCGAACUUCAGAAAUAAUU-5' 5'- G CUUGAAG S CUUUAAUUAAtt-3'	61.3	+0.3	0.7
SiG23	3'-ggCGAACUUCAGAAAUAAUU-5' 5'-GCUUGAAG t CUUUAAUUAAtt-3'	62.6	+1.6	0.8
SiG24	3'-ggCGAACUUCAGAAAUAAUU-5' 5'-GCUUGAAG U CUUUAAUUAAtt-3'	59.2	-1.8	1.4
SiG25	3'-ggCGAACUUCAGAAAUAAUU-5' 5'-GCUUGAAGU _{ps} CUUUAAUUAAtt-3'	59.7	-1.3	1.0

^aA,C,G,U = standard ribonucleotides, **S** = 3'-deoxy-3'-thiothymidine, **G,U** = 2'-OMe-ribouridine, **t** = thymidine, **U** = 2'-deoxy-2'-fluorouridine, **ps** = phosphorothioate (3'O-P(O)S-O5') linkage. n.d.= not determined

^b T_m experiments on aqueous solutions of $\sim 2 \times 10^{-6}$ M of each oligonucleotide strand, 140 mM KCl, 1 mM MgCl₂, 5 mM Na₂HPO₄ buffer (pH 7.2); uncertainty of ± 0.5 °C. ΔT_m calculated for heating curve, relative to control, by the baseline method.

^cHysteresis between heating and cooling profiles was calculated from the derivative T_m values.

Table 4.4: An Inventory of Duplexes with a 3'-Thio Modified RNA Guide Strand and a Modified RNA Passenger Strand^{a,b}

Name	Sequence	T_m	ΔT_m	hysteresis ^c
SiG26	3'-ggCGAACU S CAGAAAUUAUU-5' 5'-GCUUGAAGUCUUUAAU S AAtt-3'	62.1	+1.1	1.1
SiG27	3'-ggCGAACU S CAGAAAUUAUU-5' 5'-GCUUGAAGUCUUUAA S UAAtt-3'	62.6	+1.6	1.2
SiG28	3'-ggCGAACU S CAGAAAUUAUU-5' 5'-GCUUGAAG S CUUUAUUAAtt-3'	59.9	-1.1	0
SiG29	3'-ggCGAACU S CAGAAAUUAUU-5' 5'-GCU S GAAGUCUUUAAUUAAtt-3'	56.2	-4.8	2.4
SiG30	3'-ggCGAACU S CAGAAAUUAUU-5' 5'-GC S UGAAGUCUUUAAUUAAtt-3'	54.5	-6.5	1.5
SiG31	3'-ggCGAACU S CAGAAAUUAUU-5' 5'- G CUUGAAG S CUUUAUUUAAtt-3'	62.8	+1.8	2.2
SiG32	3'-ggCGAACU S CAGAAAUUAUU-5' 5'-GCUUGAAG t CUUUAUUUAAtt-3'	52.6	-8.4	1.3
SiG33	3'-ggCGAACU S CAGAAAUUAUU-5' 5'-GCUUGAAG U CUUUAUUUAAtt-3'	59.7	-1.3	1.4
SiG34	3'-ggCGAACU S CAGAAAUUAUU-5' 5'-GCUUGAAGU _{ps} CUUUAUUUAAtt-3'	61.2	+0.2	0.5

^aA,C,G,U = standard ribonucleotides, **S** = 3'-deoxy-3'-thiothymidine, **X** = 2'-OMe-uridine and guanosine, t = thymidine, **U** = 2'-deoxy-2'-fluorouridine, **ps** = phosphorothioate (3'O-P(O)S-O5') linkage

^b T_m experiments on aqueous solutions of $\sim 2 \times 10^{-6}$ M of each oligonucleotide strand, 140 mM KCl, 1 mM MgCl₂, 5 mM Na₂HPO₄ buffer (pH 7.2); uncertainty of ± 0.5 °C. ΔT_m calculated for heating curve, relative to control, by the baseline method.

^cHysteresis between heating and cooling profiles was calculated from the derivative T_m values.

4.4 Conformation and Thermal Stability of Duplexes

We incorporated 3'-deoxy-3'-thiothymidine (3'S-dT) residues in RNA:RNA 21mer duplexes in either the guide strand, the passenger strand or both strands, and examined their effects on thermal stability. The stability of a duplex is influenced by the type of bases present in both strands⁹ and is characterized by the melting temperature (T_m). The T_m value is determined by UV spectrophotometric methods and is defined as the temperature at which the oligonucleotide population is comprised of equimolar amounts of hybridized duplexes and completely dissociated single strands.

These measurements were carried out with 2 μM of each strand suspended in an aqueous buffer designed to mimic physiological conditions, adjusted to pH 7.2. The samples were first heated at 95°C to ensure total dissociation of the strands, cooled slowly and stored for at least 10 hours at 4°C to facilitate complete annealing of the strands. The cold samples were transferred to a pre-cooled UV spectrophotometer. The UV absorbance of the samples was measured at 260 nm as they were gradually heated (0.5°C/min) to 95°C and then re-cooled to 10°C.

At low temperatures, UV absorption is lower due to π -stacking interactions between neighbouring chromophores (purine and pyrimidine bases) in the intertwined strands, called a hypochromic effect.¹⁶ As the temperature increases, the duplexes dissociate and the absorbance increases, since there is much less π -stacking in single strands. The resulting sigmoidal ‘melting’ curve (A_{260} vs temperature) typically shows a sharp change in absorbance over a narrow temperature change (for example, see **Figure 4.1**). This reveals the cooperative nature of oligonucleotide association. The first derivative of the curve is usually a good approximation of the T_m , since the inflection point of the curve naturally occurs at the center of the transition. T_m values can also be determined from the mid-point of the hyperchromic change, as will be discussed below.

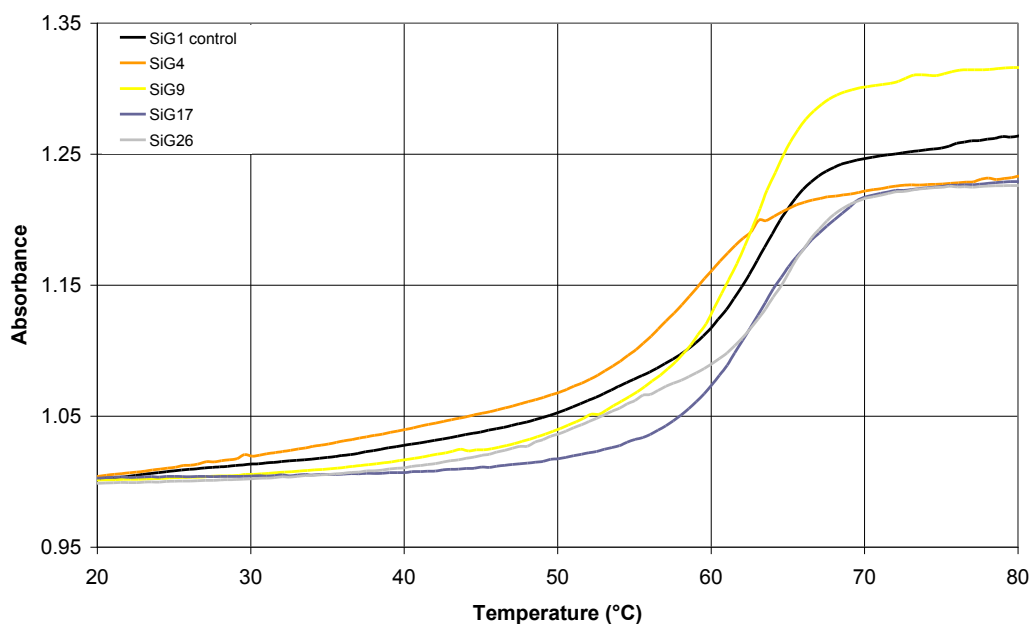
As seen in the representative samples in **Figure 4.1**, the sharp monophasic transitions indicate the presence of a single cooperative complex in each sample. The T_m profile of each duplex in the library is available in **Appendix 2**. The T_m values were calculated by the baseline method, **Tables 4.2-4.4**, where the T_m is taken as the midpoint between the upper and lower baselines defined by the low and high temperature regions of the T_m curve. The control RNA:RNA duplex has a T_m of 61°C, and the differently modified duplexes show both stabilising and destabilising effects.

The second ramp for both the heating and cooling stages found the T_m in each case to be slightly lower than the first cycle (average of 0.3°C for each), which fits expectations because the duplexes were not given enough time to reach their ideal lowest energy conformations. The hysteresis between heating and cooling stages was generally small (average 1.4°C) and no clear trends presented themselves among the groups. The runs were highly reproducible, as seen with the control samples, which were run on 3 consecutive days.

Another method for calculating T_m is the “derivative method”, where the first derivative of the curve is taken as the T_m value. T_m values calculated by the derivative method are available in **Appendix 2**. There is generally good agreement between the 2 methods of calculating T_m , with the hypochromic method typically calculating a value several degrees lower than the derivative method. The thermodynamic parameters ΔH , ΔS , ΔG , K_{eq} and KT_m were calculated using the

Varian Cary 300 spectrophotometer software from the individual T_m curves and also appear in **Appendix 2**.

Figure 4.1: Melting Temperature (T_m) Signatures of 5 Representative RNA:RNA Duplexes^a



^aAbsorbance data was normalised to the initial value for that sample. Greater hyperchromicity was observed in some samples due to loss of water and the subsequent increase in concentration.

Comparing the T_m values of the singly 3'-thio modified duplexes, SiG2-7 and SiG17-21, to the native RNA:RNA duplex, SiG1, in **Table 4.3**, we generally see smaller effects on stability when the modification is at the end of the guide or passenger strand. This is consistent with previous studies reporting that modifications are tolerated better at the end compared to the middle of a duplex due to end-fraying effects, which suppress the magnitude of destabilization.¹⁷ Interestingly, strong positional effects were observed. For example, significant destabilization was observed when the 3'-S-dT unit was placed within the 5'-region (positions 2-6) of either guide (e.g., SiG3-5) or passenger (e.g., SiG20 and 21) strand. The 3'-S-dT substitution is neutral (e.g., SiG6) or slightly destabilizing when centrally located (e.g., SiG15 and SiG19; $\Delta T_m = -1.1$ to -1.4 °C), whereas it is slightly stabilizing as the modification is moved within the 3'-region of either guide or passenger strand (e.g., SiG7, SiG17-18; $\Delta T_m = +0.3$ to $+1.5$ °C). This trend is also apparent in the doubly 3'-thio-substituted series, SiG26-30, where one observes an additive effect of the stabilizing/destabilizing units. However, that the disruption existed at all for some of the

duplexes was a surprising and disappointing finding for us, given earlier findings that 3'-thionucleoside residues stabilize DNA:RNA duplexes, in which the DNA strand is modified.^{4, 18, 19}

In **Table 4.5**, the comparison of the sets of samples where the same U residue has been substituted for 3'-S-dT or dT, SiG4-5 and SiG9-10 respectively, reveals that the dT substitutions are less thermally destabilising than the 3'-S-dT substitutions. On the other hand, very little difference between the dT and 3'-S-dT modified strands are observed when these units are moved away from the 5'-ends (compare SiG6-7 and SiG11-12).

Table 4.5: Melting Temperatures (T_m) of dT and 3'-S-dT Modified Duplexes

Sequence	X = 3'-S-dT	ΔT_m^*	X = dT	ΔT_m^*
3'-ggCGAACUUCAGAAAUXAAUU-5'	SiG4	-4.2	SiG9	+0.1
3'-ggCGAACUUCAGAAAXUAAUU-5'	SiG5	-5.0	SiG10	-0.9
3'-ggCGAACUXCAGAAAUUAAUU-5'	SiG6	+1.3	SiG11	+0.9
3'-ggCGAACXUCAGAAAUUAAUU-5'	SiG7	+1.0	SiG12	+0.8

ΔT_m relative to control

Adding two terminal 2'-OMe residues to SiG28, to give SiG31, provides an siRNA with the highest observed T_m in the library (1.8°C above the control), see **Table 4.6**. The 2'-OMe modification is thought to increase affinity for RNA targets by improving hybridization kinetics.²⁰ 2'-O-methylation of duplex SiG19, to give SiG22, is also stabilizing, but an opposite effect was observed when SiG6 was methylated to give SiG16.

Table 4.6: Melting Temperatures (T_m) of 3'-thio and 2'-OMe Modified Duplexes

Sequence	X = U	ΔT_m^*	X = 2'-OMe U	ΔT_m^*
3'-ggCGAACU ^S CAGAAAUUAA ^{XX} -5'	SiG6	+0.3	SiG16	-1.4
5'- ^{XX} UUGAAG ^S CUUUAUUAA ^{tt} -3'	SiG19	-1.4	SiG22	+0.3
5'- ^{XX} UUGAAG ^S CUUUAUUAA ^{tt} -3'	SiG28	-1.1	SiG31	+1.8

ΔT_m relative to control

Single mismatches on the guide strand where the C₁₀ residue was replaced with a dT, U or 3'-S-dT residue (SiG13-15 respectively), all led to decreases in T_m as summarized in **Table 4.7**. This effect was greatest for the dT, SiG13, and smallest for 3'-S-dT, SiG15; in other words, a 3'-S-dT mismatch is significantly less destabilizing. Perhaps here the 3'-S-dT base is engaging wobble base pairing with its “mismatch” G residue (G:3'S-dT).²¹ Comparing the T_m values of the

C → 3'-S-dT mismatch at position 10, SiG15, to the U → 3'-S-dT substitution at position 9, SiG6, we find the former to be slightly more destabilizing.

Table 4.7: Melting Temperatures (T_m) of Guide Strand Mismatches

Sample			Sequence	ΔT_m^*
SiG6	U ₉ → 3'-S-dT	substitution	3'-ggCGAACU S CAGAAAUUAUU-5'	+0.3
SiG13	C ₁₀ → dT	mismatch	3'-ggCGAACUU t AGAAAUUCAUU-5'	-8.5
SiG14	C ₁₀ → U	mismatch	3'-ggCGAACUU U AGAAAUUAUU-5'	-5.5
SiG15	C ₁₀ → 3'-S-dT	mismatch	3'-ggCGAACUU S AGAAAUUAUU-5'	-1.1

* ΔT_m relative to control

In the interest of exploring the dynamics of RISC at the passenger strand cleavage site,²² we made several substitutions at this position. Substitutions with dT and the 3'-S-dT were well tolerated, SiG23 and SiG24 respectively, in terms of thermal stability but substitution with 2'-F-rU, SiG25, had a destabilizing effect.

There are no reports of 3'-thio modified RNA duplexes in the literature. However, Cosstick's group has measured the T_m values of 3'-thio modified DNA (DNA*) hybridized to complementary DNA or RNA. For DNA*:DNA duplexes, Cosstick *et al.* reported that the 3'-thio modification caused a *decrease* in T_m of $\sim 1^\circ\text{C}/\text{modification}$ compared to a native DNA:DNA duplex. This finding was supported by experiments in our lab, although the observed effects were smaller with the homopolymeric thymidine stands examined by Anna Lisa Tedeschi of our laboratory.²³ Cosstick's group also reported that 3'-thio modifications in DNA*:RNA duplexes resulted in an *increase* of $\sim 1.4^\circ\text{C}/\text{modification}$ relative to its native counterpart.¹⁷ Our data show that 3'-S-dT may have a stabilizing or destabilizing effect depending on its location in the RNA:RNA duplex.

4.5 Analysis of Oligonucleotide Conformation by Circular Dichroism (CD) Spectroscopy

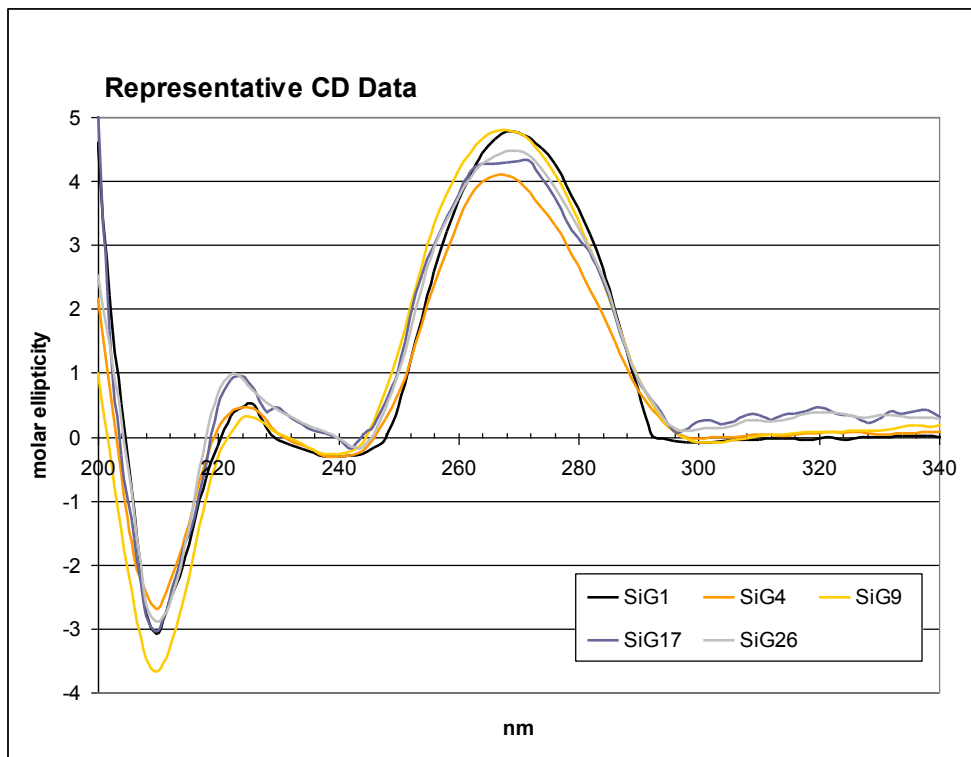
Circular dichroism (CD) spectroscopy provides useful information about the secondary structure of oligonucleotide duplexes: the ability of nucleic acids to absorb circularly polarized light, due to the chiral *N*-glycosidic bonds between the sugar and the nucleobases, increases when they adopt a global helical formation.²⁴

The CD instrument measures the molar ellipticity (differential absorbance of left and right circularly polarized light) across a range of wavelengths, resulting in a signature curve for each

type of helix. These spectra are usually characterised by reference to a sample of known helicity, making CD a qualitative method. It was employed in this instance to determine if the 3'-S-dT residues had an impact on the overall structure of the duplex. RNA:RNA duplexes are A-form helices, characterised by a strong absorbance around 260 nm and a fairly intense positive band at 210 nm, whereas DNA:DNA duplexes are B-form helices, with a positive band around 275 nm, a crossover around 260 nm and a negative band near 240 nm. "Hybrid" (DNA:RNA) duplexes can also be characterised by CD, and generally conform to the A-form (or A-like) structure.²⁵

The CD spectrum of each of the samples in the oligonucleotide duplex library was recorded to assess the impact of 3'-thio modification on the overall helical structure. A representative sample of each of the 5 types of duplexes is shown in **Figure 4.2** and the full data is available in **Appendix 3**. A comparison of the CD spectra of several duplexes modified on both strands, SiG26-31, is presented in **Figure 4.3**.

Figure 4.2: CD Spectra of Native and Modified RNA:RNA Duplexes



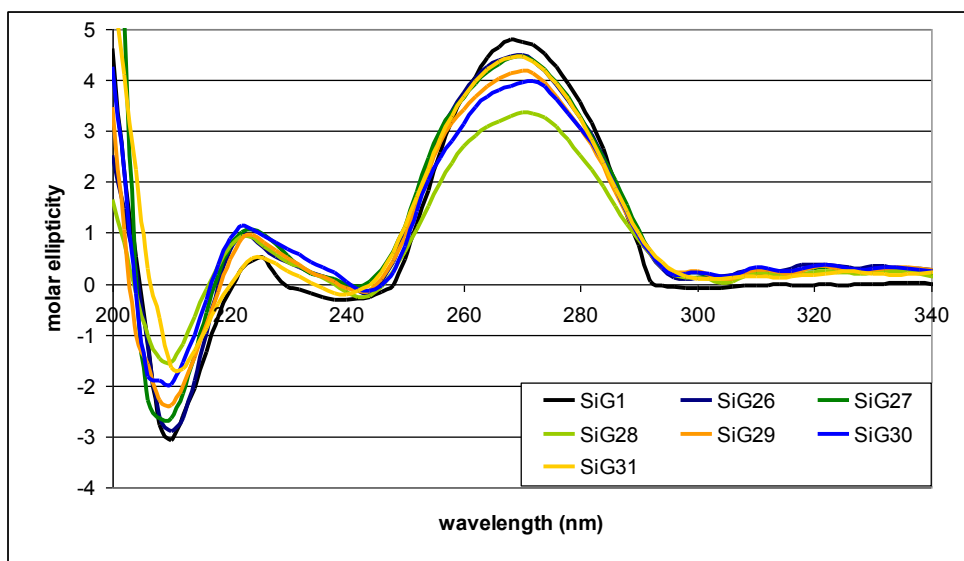
Buffer: 140mM KCl, 1 mM MgCl₂, 5mM Na₂HPO₄, pH 7.2

From a qualitative analysis of these spectra (**Figure 4.2**), and those of the rest of the library in **Appendix 3**, no significant change in the A-like global helix conformation resulting from 3'-thio modification is observed. For example, the clear A-form or RNA-like helical

formation of the control all-native RNA duplex, SiG1, is mirrored in several duplexes. These include duplexes containing a 3'-thio modification on the guide strand, SiG4, or on the passenger strand, SiG17, a dT insert on the guide strand, SiG9, and 3'-thio modifications on both the guide and passenger strands, SiG26.

For most cases, the CD traces are nearly superimposable reflecting the uniformity of their helical structures. The CD spectra of the doubly 3'-thio modified duplexes where destabilization was observed, SiG28-30, resemble that of the control, SiG1, except that their CD traces are less intense around the 265 nm band, see **Figure 4.3**. This region is often associated with base stacking. Likewise, duplexes containing mismatches were found to present a slight disruption of the CD signature (**Appendix 3**), likely reflecting steric interactions with the opposing RNA nucleotide strand.

Figure 4.3: CD Spectra of Guide and Passenger Strand Modified RNA:RNA Duplexes



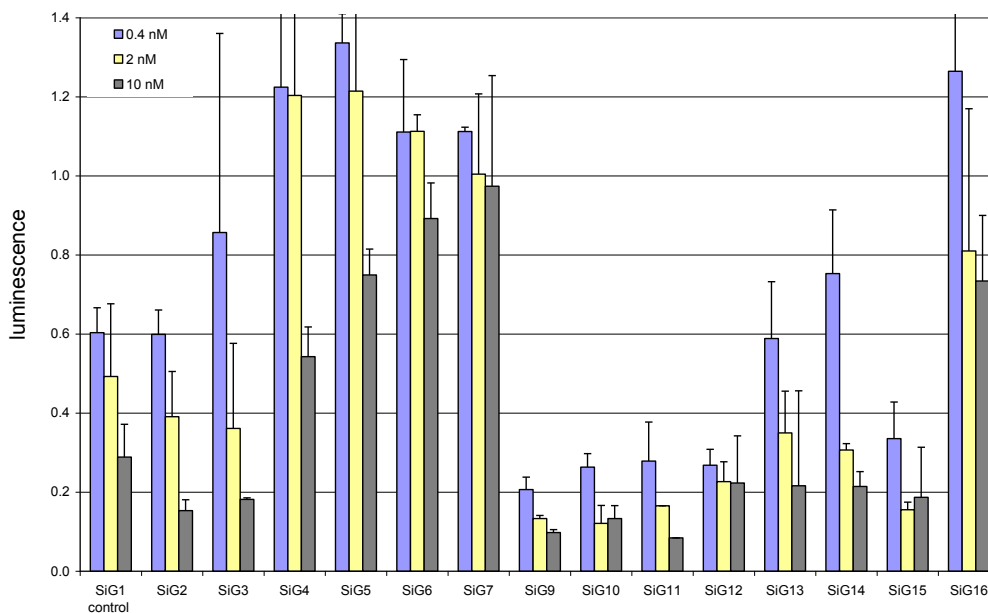
4.6 Evaluation the Gene Silencing Activity of 3'-Thio Modified siRNA

The entire library of siRNA duplexes, **Tables 4.1 to 4.3**, was evaluated for the ability to down-regulate the production of a target protein. A unique but practical method for doing this involves using HeLa cells that have been modified to express the luciferase enzyme, taken from the firefly genome, which emit light when exposed to the luciferin substrate.²⁴ As this is a property not found in the human genome, we are then able to directly measure the production of this single protein, the target of the siRNA, without false signals from other proteins. These assays were carried out in collaboration with Drs. Francis Robert and Jerry Pelletier (Biochemistry Department, McGill University).

HeLa X1/5 cells, expressing the firefly luciferase gene, were maintained in supplemented cell culture medium and seeded into 24-well plates. Cells were incubated with increasing amounts of siRNA premixed with lipofectamine for twenty-four hours, at which point the cells were lysed, exposed to a luciferin solution and the luminescence was measured.

As described above, earlier work with 3'-S-dT units in DNA duplexes, including the conformational work by Cosstick,²⁴ had led us to hope that this modification would prove useful in RNAi silencing assays. However, the 3'-S-dT modification gave mixed results in the luciferase knockdown assay, as seen in **Figures 4.4 to 4.6**. Luminescence, on the y-axis, represents the light produced by the sample relative to that produced by untreated cells. Effective siRNA duplexes result in lower luciferase production and thus have lower luminescence. That the luminescence observed in the series dilutions of each sample reflects greater effects for more siRNA (dose dependence) is a useful check that what we are observing is actually an RNAi effect.

Figure 4.4: RNAi Activity of Duplexes Modified Only on the Guide Strand



Comparing the RNAi efficacy of duplexes modified with 3'-S-dT on the guide strand, SiG2-7, and the dT modified guide strand series, SiG9-12, to the parent native siRNA duplex, SiG1, in **Figure 4.4**, we see that 3'-S-dT is poorly tolerated on the guide strand. The low RNAi activity of SiG3-5 may be exacerbated by the fact that the 3'-S-dT modifications in these duplexes are found in the 5'-proximal region shown to be associated with the surface of the Mid-PIWI lobe of RISC,²⁴ and the likely nucleation site for mRNA.²⁶ When 3'-S-dT on the guide strand is combined with terminal 2'-OMe residues, SiG16, the RNAi performance remained

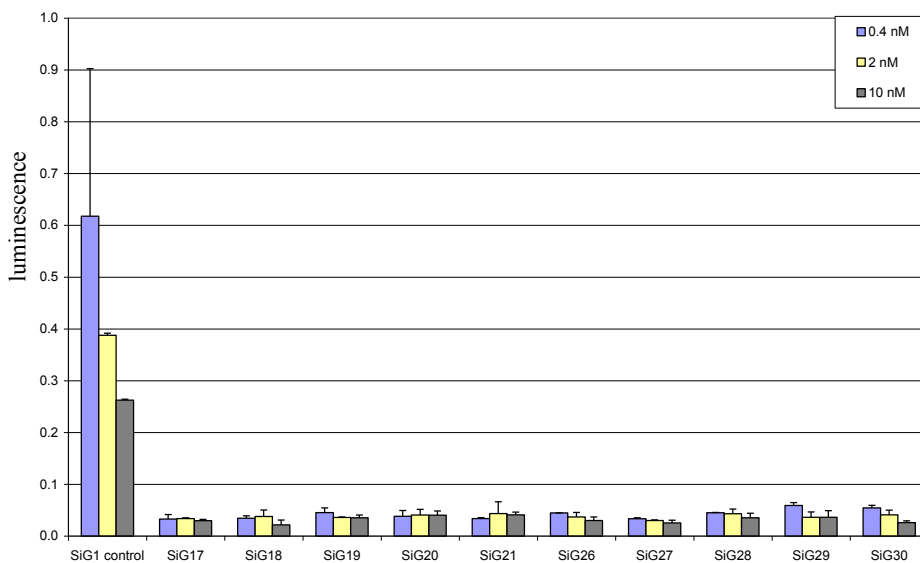
weak. Oddly, the wobble (G:3'-S-dT) paired duplex, SiG15, appears to be at least as active as the siRNA native control, SiG1.

In contrast, the dT substituted guide strand series SiG9-12 is more effective than the 3'-S-dT modified series, SiG2-7 (**Figure 4.4**). The tolerance of DNA (dT) substitutions is supported by other reports,⁶ although they are not generally associated with increased activity.

The strands containing a single mismatch, SiG13-14, were active despite their low T_m values. Leuschner *et al.* found non-central mismatch residues to be well tolerated.²⁴ In summary, with the exception of the wobble G:3'S-dT paired duplex, SiG15, the order of efficacy of modification on the guide strand was found to be dT > control > mismatch > 3'-S-dT.

More encouraging results were obtained with 3'-S-dT substitutions in the passenger strand, as shown in **Figure 4.5**. In fact, all passenger modified siRNA duplexes performed significantly better than the control, SiG1, but it is hard to distinguish different levels of efficacy and thus positional effects cannot be distinguished. The increased tolerance of modifications on the passenger strand is a recurrent phenomenon^{1, 27} due to the greater contact and thus discrimination imposed by RISC on the guide strand.

Figure 4.5: RNAi Activity of 3'-Thio Modified Passenger Strand with Native or Modified Guide Strands



Duplexes with 3'-S-dT present in both in the guide and passenger strands, SiG26-30, were as effective as duplexes modified on the passenger strand alone. Perhaps experiments at lower concentrations of siRNA would elucidate some advantages, but no benefits of modifying both strands are obvious from these results. However, it is interesting that modification on the

guide strand is tolerated at all. A modified passenger strand with terminal 2'-OMe residues, SiG31, or with a dT substitution, SiG32, hybridized with a 3'-thio modified guide strand had similar activity to those paired with native guide strands (SiG22 and SiG23, respectively).

Duplex SiG31, with 3'-thio modifications on both strands and terminal 2'-OMe in the passenger strand, is the most stable member of the library ($\Delta T_m +1.8^\circ\text{C}$) and among the most effective at inhibiting the production of luciferase.

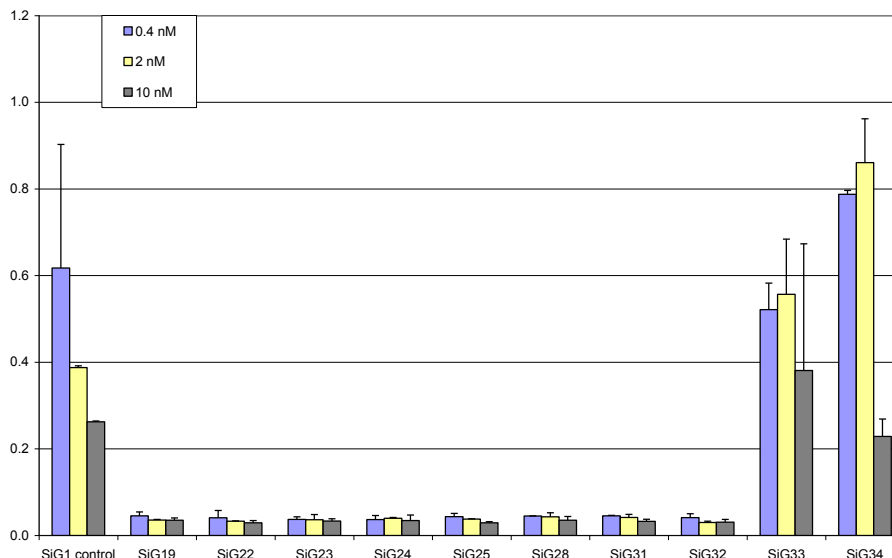
The phosphate bond located on the passenger across from the 10th residue on the guide strand of RNAi duplexes has been identified as the scissile bond for RISC cleavage of both the passenger strand and later, target RNA,^{17, 28} recall **Figure 1.5**. This position occurs between the passenger strand residues C₁₂ and U₁₃ in our duplexes. Cleavage at this position and the subsequent dissociation of the nicked passenger strand is essential to RNAi activity, making modification at this position an interesting way to probe the functioning of RISC. We found that substitution with dT, hybridized to native RNA SiG23 or to 3'-S-dT modified guide strand SiG32, resulted in a highly active RNAi duplex, see **Figure 4.6**. Thus a 2'-OH group vicinal to the scissile phosphate is not required for cleavage of the passenger strand. Leuschner *et al.* also found dT to be well tolerated on the passenger strand, as were neighbouring 2'-OMe residues but 2'-OMe at the key position blocked cleavage.²⁴ In our experiments 2'-OMe residues only occurred on strands with a 3'-thio modification, SiG16, SiG22 and SiG31.

The riboF modified passenger strand has good RNAi activity when paired with a native guide strand, SiG24, but poor activity when paired with a 3'-thio modified guide strand, SiG33. These results are the inverse of the T_m values and may reflect a local steric issue with RISC created by the combination of 3'-thio and 2'F-ribose modifications.

Schwartz *et al.* found that replacing a nonbridging oxygen of the scissile phosphate group, (3'O-P(O)O-O5') with a phosphorothioate (PS or 3'O-P(O)S-O5'), blocks cleavage, as this interferes with cation coordination required by RISC.²⁶ We were not able to reproduce these results for a duplex containing a PS-modified passenger strand and an unmodified guide strand, SiG25. However, our worst siRNA duplex contained the same PS-modified passenger strand bound to 3'-thio modified guide strand, SiG34, see **Figure 4.6**. On the other hand, the good RNAi activity of the 3'-thio modified passenger duplexes SiG19, 22, 28 and 31 indicates that the *bridging* oxygen atom at the 3' position on the nucleotide on both strands is not crucial for the coordination of the cation required for cleavage.

As sulphur is a good leaving group, the 3'-thio modification at the scissile position, SiG28, could result in higher potency compared to a 3'-oxygen group, SiG31. We were unable to assess such an effect due to the high potency of this series.

Figure 4.6: RNAi Activity of Modified Passenger Strand with Native or Modified Guide Strands



Flexibility can be very important in the confined space of enzymatic active sites. Therefore, the anticipated increased flexibility of 3'-deoxy-3'-thiothymidine compared to the native ribo U may be the only reason for the increased efficacy of 3'-S-dT residues on the passenger strand. However, the decreases in T_m are also due to this enhanced flexibility. Duplexes with terminal 2'-OMe residues, SiG22, or a dT substitution, SiG23, were equally effective.

In summary, 3'-thio modifications in the passenger strand were found to be the most effective in terms of RNAi activity (surpassing the native strand), whether paired with a native or 3'-thio modified guide strand.

4.7 Conclusion

The thermal stability of RNA:RNA duplexes containing a single 3'-deoxy-3'-thiothymidine (3'-S-dT) residue was observed to be highly dependent on the location of the modification. The RNAi activity of RNA*:RNA duplexes modified on the guide strand with 3'-deoxy-3'-thiothymidine was lower than that of the control duplex, but those modified on the passenger strand were more active. Duplexes containing a 3'-S-dT residue on both strands were as active as those modified only on the passenger strand. Individual dT substitutions, single mismatches or 2'-OMe terminal residues did not have detrimental effects on RNAi activity. Curiously, a guide strand modified siRNA duplex containing a G:3'-S-dT “mismatch” was as active as the unmodified duplex control. Comparison of the T_m data of this duplex to other

mismatch controls indicated that the 3'-S-dT residue likely engages in wobble base pairing with a G residue on the passenger strand.

Modification at the RISC cleavage position on the passenger strand resulted in an interesting addition to the work of Schwartz *et al.* on the mechanism of RISC cleavage.²⁶ As the 3'-S-dT residue at this position did not have a detrimental effect on RNAi activity, it suggests that the 3'-nonbridging oxygen is not involved in the coordination of the cation.

4.8 References

- 1 Dykxhoorn, D. M.; Lieberman, J., Running Interference: Prospects and Obstacles to Using Small Interfering RNAs as Small Molecule Drugs. *Annual Review of Biomedical Engineering* **2006**, 8, 377-402.
- 2 Patureau, B. Induction of RNase H Activity by Arabinose-Peptide Nucleic Acids. M.Sc. Thesis, McGill University, Montreal, 2005.
- 3 Mangos, M. Factors Governing the Design, Selection and Cleavage of Sugar-Modified Duplexes by Ribonuclease H. Ph.D. Thesis, McGill University, Montreal, 2005.
- 4 Tedeschi, A. L. Synthesis and Biological Evaluation of Oligonucleotides Containing 3'- and 5'-S-Phosphorothiolate Internucleotide Linkages. M.Sc. Thesis, McGill University, Montreal, 2004.
- 5 Buckingham, J.; Sabbagh, G.; Brazier, J.; Fisher, J.; Cosstick, R., Control of DNA Conformation Using 3'-S-Phosphorothiolate-Modified Linkages. *Nucleosides, Nucleotides and Nucleic Acids* **2005**, 24, (5), 491-495.
- 6 Beevers, A. P. G.; Fettes, K. J.; Sabbagh, G.; Murad, F. K.; Arnold, J. R. P.; Cosstick, R.; Fisher, J., NMR and UV studies of 3'-S-phosphorothiolate modified DNA in a DNA:RNA hybrid dodecamer duplex; implications for antisense drug design. *Organic & Biomolecular Chemistry* **2003**, 2, (1), 114-119.
- 7 Thibaudeau, C.; Plavec, J.; Carg, N.; Papchikhin, A.; Chattopadhyaya, J., How Does the Electronegativity of the Substituent Dictate the Strength of the Gauche Effect? *J. Am. Chem. Soc.* **1994**, 116, 4038-4043.
- 8 Hantz, E.; Laruea, V.; Ladama, P.; Moyeca, L. L.; Gouyetteb, C.; Dinhb, T. H., Solution conformation of an RNA-DNA hybrid duplex containing a pyrimidine RNA strand and a purine DNA strand. *International Journal of Biological Macromolecules* **2001**, 28, (4), 273-284.
- 9 Jayakumar, H. K.; Buckingham, J. L.; Brazier, J. A.; Berry, N. G.; Cosstick, R.; Fisher, J., NMR studies of the conformational effect of single and double 3'-S-phosphorothiolate substitutions within deoxythymidine trinucleotides. *Magn. Reson. Chem.* **2007**, 45, (4), 340-345.
- 10 Bentley, J.; Brazier, J. A.; Fisher, J.; Cosstick, R., Duplex stability of DNA-DNA and DNA-RNA duplexes containing 3'-S-phosphorothiolate linkages. *Organic & Biomolecular Chemistry* **2007**, 5, 3698-3702.
- 11 Beevers, A. P. G.; Fettes, K. J.; O'Neil, I. A.; Roberts, S. M.; Arnold, J. R. P.; Cosstick, R.; Fisher, J., Probing the effect of a 3A-S-phosphorothiolate link on the conformation of a DNA:RNA hybrid; implications for antisense drug design. *Chemical Communications* **2002**, 14, 1458-1459.
- 12 Lauritsena, A.; Wengel, J., Oligodeoxynucleotides containing amide-linked LNA-type dinucleotides: synthesis and high-affinity nucleic acid hybridization. *Chemical Communications* **2002**, (5), 530-531.
- 13 Nielsen, K. E.; Singh, S. K.; Wengel, J.; Jacobsen, J. P., Solution structure of an LNA hybridized to DNA: NMR study of the d(CTLGCTLTLCTLGC):d(GCAGAAGCAG) duplex containing four locked nucleotides. *Bioconjugate Chemistry* **2000**, 11, 228-238.
- 14 Obika, S.; Nanbu, D.; Hari, Y.; Andoh, J.-i.; Morio, K.-i.; Doi, T.; Imanishi, T., Stability and structural features of the duplexes containing nucleoside analogues with a fixed N-type conformation, 2'-O,4'- C-methylenribonucleosides. *Tetrahedron Lett.* **1998**, 39, 5401-5404.

- 15 Epple, C.; Leumann, C., Bicyclo(3.2.19-DNA, a new DNA analog with a rigid backbone and flexibly linked bases: pairing properties with complementary DNA. *Chemistry & Biology* **1998**, *5*, 209-216.
- 16 Majlessi, M.; Nelson, N. C.; Becker, M. M., Advantages of 2'-O-methyl oligoribonucleotide probes for detecting RNA targets. *Nucleic Acids Res.* **1998**, *26*, 2224–2229.
- 17 Elbashir, S.; Martinez, J.; Patkaniowska, A.; Lendeckel, W.; Tuschl, T., Functional anatomy of siRNAs for mediating efficient RNAi in *Drosophila melanogaster* embryo lysate. *EMBO J.* **2001**, *20*, 6877–88.
- 18 Brahms, J.; Brahms, S., Circular Dichroism of Nucleic Acids. In *Fine Structure of Proteins and Nucleic Acids*, ed.; Fasman, G. D., Timasheff, S. N., 'Ed.'^'Eds.' Dekker: 1970; 'Vol.' 4, p^pp 79.
- 19 Gray, D. M.; Hung, S. H.; Johnson, K. H., Absorption and circular dichroism spectroscopy of nucleic acid duplexes and triplexes. *Methods Enzymol.* **1995**, *246*, 19-34.
- 20 Elbashir, S. M.; Harborth, J.; Lendeckel, W.; Yalcin, A.; Weber, K.; Tuschl, T., Duplexes of 21-nucleotide RNAs mediate RNA interference in cultured mammalian cells. *Nature (London)* **2001**, *411*, 494-498.
- 21 Salazar, M.; al., e., The DNA strand in DNA.RNA hybrid duplexes is neither B-form nor A-form in solution. *Biochemistry* **1993**, *32*, (16), 4207-15.
- 22 Birmingham, A.; Anderson, E. M.; Reynolds, A.; Illey-Tyree, D.; Leake, D.; Fedorov, Y.; Baskerville, S.; Maksimova, E.; Robinson, K.; Karpilow, J.; al., e., 30 UTR seed matches, but not overall identity, are associated with RNAi off-targets. *Nat. Methods* **2006**, *3*, 199–204.
- 23 Yuan, Y.-R.; Pei, Y.; Ma, J.-B.; Kuryavyi, V.; Zhadina, M.; Meister, G.; Chen, H.-Y.; Dauter, Z.; Tuschl, T.; Patel, D. J., Crystal structure of *A. aeolicus* Argonaute, a site-specific DNA-guided endoribonuclease, provides insights into RISC-mediated mRNA cleavage. *Mol. Cell* **2005**, *19*, 405–419.
- 24 Leuschner, P. J. F.; Ameres, S. L.; Kueng, S.; Martinez, J., Cleavage of the siRNA passenger strand during RISC assembly in human cells. *EMBO reports* **2006**, *7*, (3), 314-320.
- 25 Hohjoh, H., RNA interference (RNAi) induction with various types of synthetic oligonucleotide duplexes in cultured human cells. *FEBS Lett.* **2002**, *521*, (1-3), 195-199.
- 26 Schwarz, D.; Tomari, Y.; Zamore, P., The RNA-induced silencing complex is a Mg²⁺-dependent endonuclease. *Current Biology* **2004**, *14*, (9), 787-91.
- 27 Chiu, Y. L.; Rana, T. M., siRNA function in RNAi: A chemical modification analysis. *RNA* **2003**, *9*, 1034-1048.
- 28 Elbashir, S. M.; Lendeckel, W.; Tuschl, T., RNA interference is mediated by 21- and 22-nucleotide RNAs. *Genes Dev.* **2001**, *15*, 188-200.

Contribution to Knowledge

This thesis reports the first incorporation of 3'-thionucleosides into RNA oligonucleotides, and examines their physicochemical and biological properties. Improvements to the synthesis of 3'-deoxy-3'-thiothymidine (3'-S-dT), particularly the use of dithiothreitol (DTT) to reduce the formation of disulfide bonds when revealing the 3'-thiol group, are described. In addition, an *in situ* method for the preparation of nucleosides 3'-S-phosphorothioamidite derivatives was developed to increase monomer coupling yields. The 3'-phosphorothioamidite was found to be stable when stored as a dry foam in the freezer for at least 2 months or 24h at room temperature in CH₂Cl₂.

Adjustments were made to the solid-phase synthesis cycle, particularly the coupling and oxidation steps, to obtain sufficient amounts of the 3'-S modified RNA strands for the characterisation and biological assays of a small library of native and modified RNA:RNA (siRNA) duplexes.

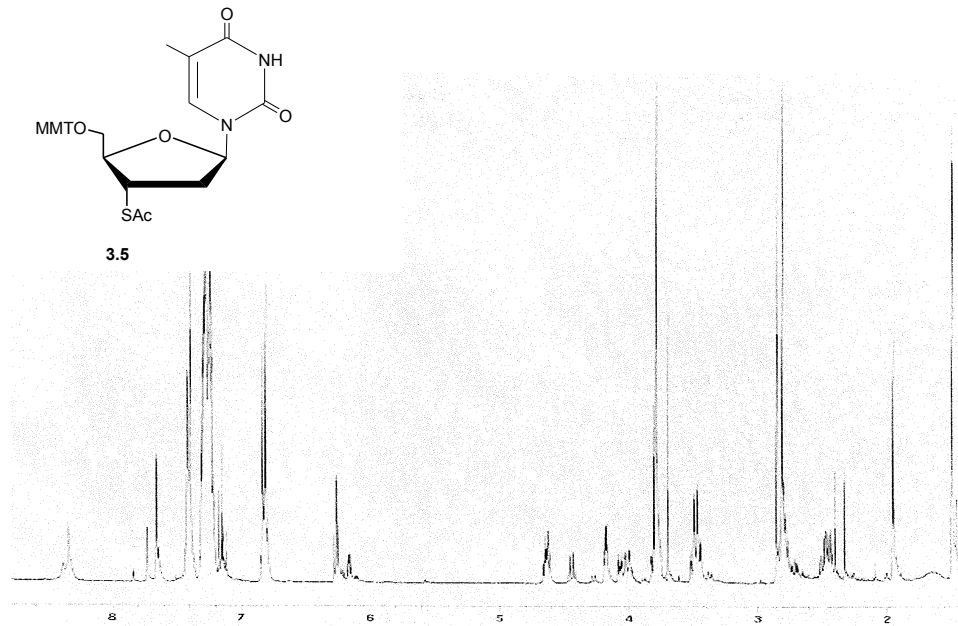
Thermal denaturation studies revealed that the incorporation of one 3'-S-dT insert in RNA:RNA duplexes can be either destabilizing or stabilizing depending on their location within the duplex. There were cases when one or two 3'-S-dT incorporations, or chimeric modifications (e.g., both 3'-S-dT and 2'-OMe rN) provided duplexes with greater thermal stability relative to the control native siRNA duplex. CD signatures of the modified duplexes were indicative of an A-like helix, as expected, although some perturbation in base stacking interactions was detected in certain duplexes.

Duplexes modified with 3'-S-dT residues on the guide strand generally led to a significant reduction in siRNA gene silencing activity, although a guide strand modified duplex containing a G:3'S-dT mismatch exhibited similar activity to the control (unmodified) siRNA duplex. The T_m data of this mismatch duplex suggests that the G and 3'S-dT bases are engaged in wobble base pairing interactions. Duplexes containing the 3'S-dT modification on the passenger strand or on both strands perform rather well, many surpassing the activity of the native siRNA control. Other substitutions such as dT, or terminal 2'-OMe ribonucleotide residues did not have detrimental effects on RNAi activity.

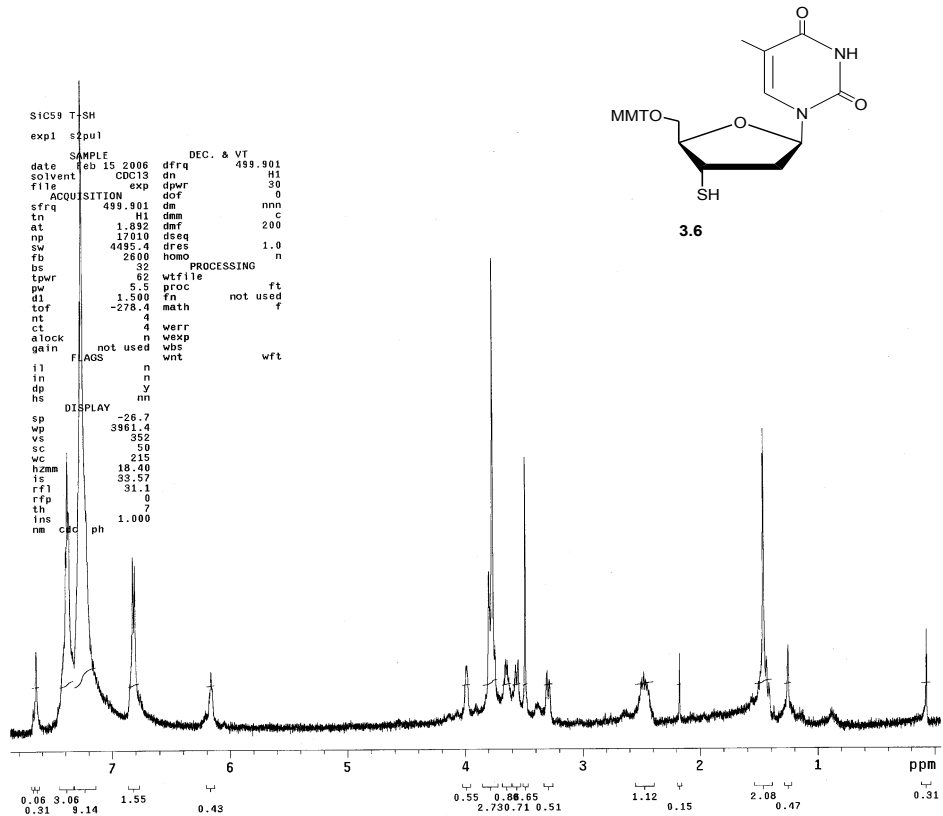
Specific substitutions at the scissile position of the passenger strand of siRNA duplexes indicate that the non-bridging 3'-oxygen is not involved in the coordination of the metal cation for RISC-induced cleavage.

Appendix 1: NMR Spectra of Selected Nucleosides

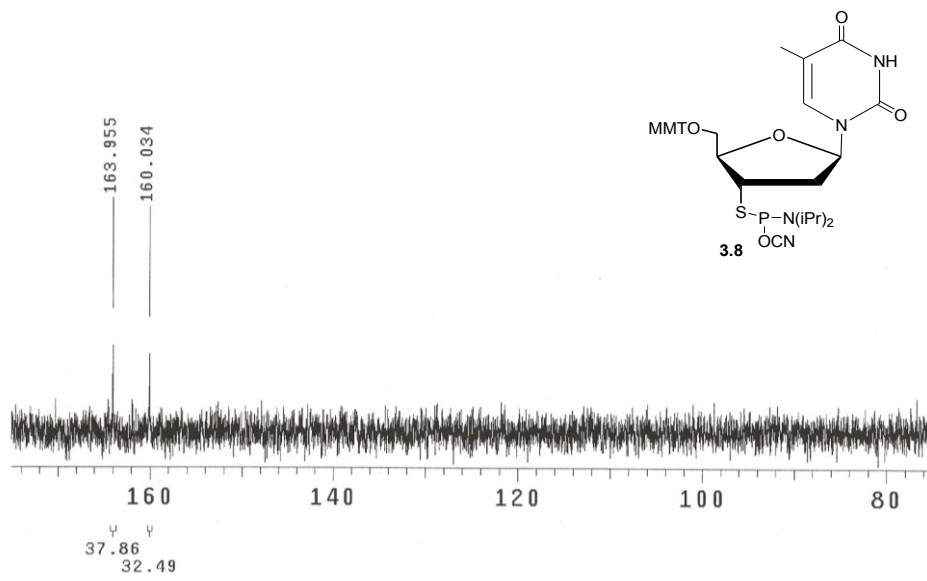
3'-acetyl-2',3'-dideoxy-5'-monomethoxytrityl-Thymidine



2',3'-dideoxy-3'-thio-5'-monomethoxytrityl-Thymidine

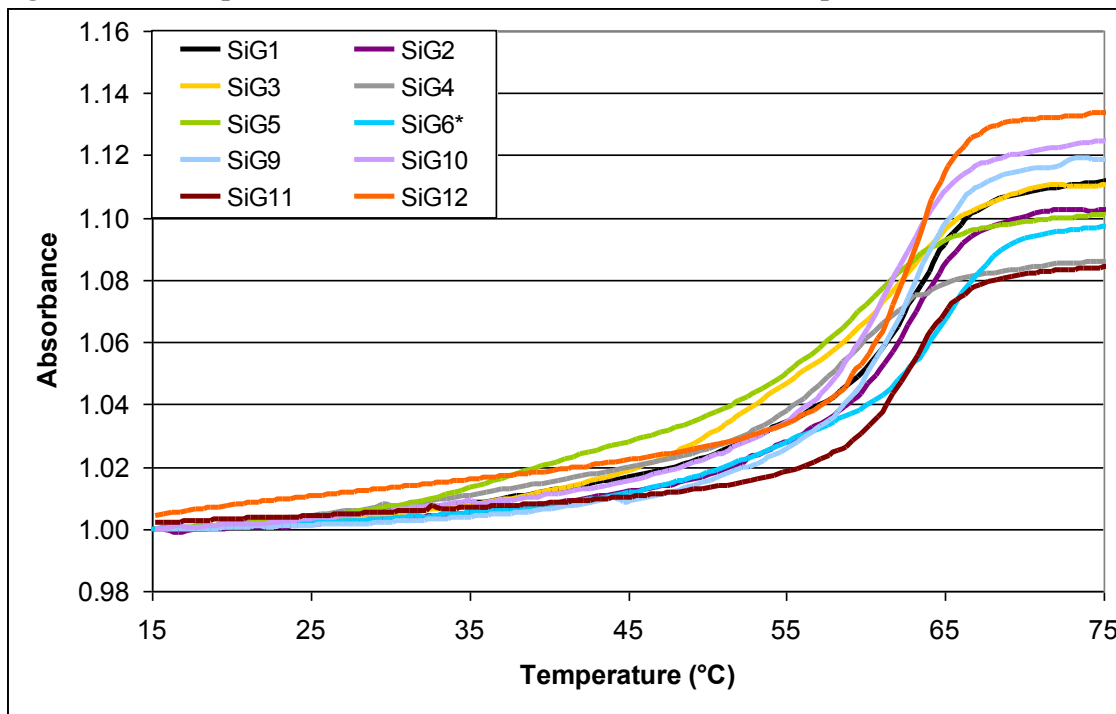


2',3'-dideoxy-3'-thiophosphoramidite-5'-monomethoxytrityl-Thymidine



Appendix 2: UV/Thermal Dissociation Profiles of RNA:RNA Duplexes

Figure A2.1: T_m Spectra of Guide Strand Modified RNA:RNA Duplexes



**Data for SiG6 from the second heating ramp.*

Figure A2.2: T_m Spectra of Guide Strand Mismatch RNA:RNA Duplexes

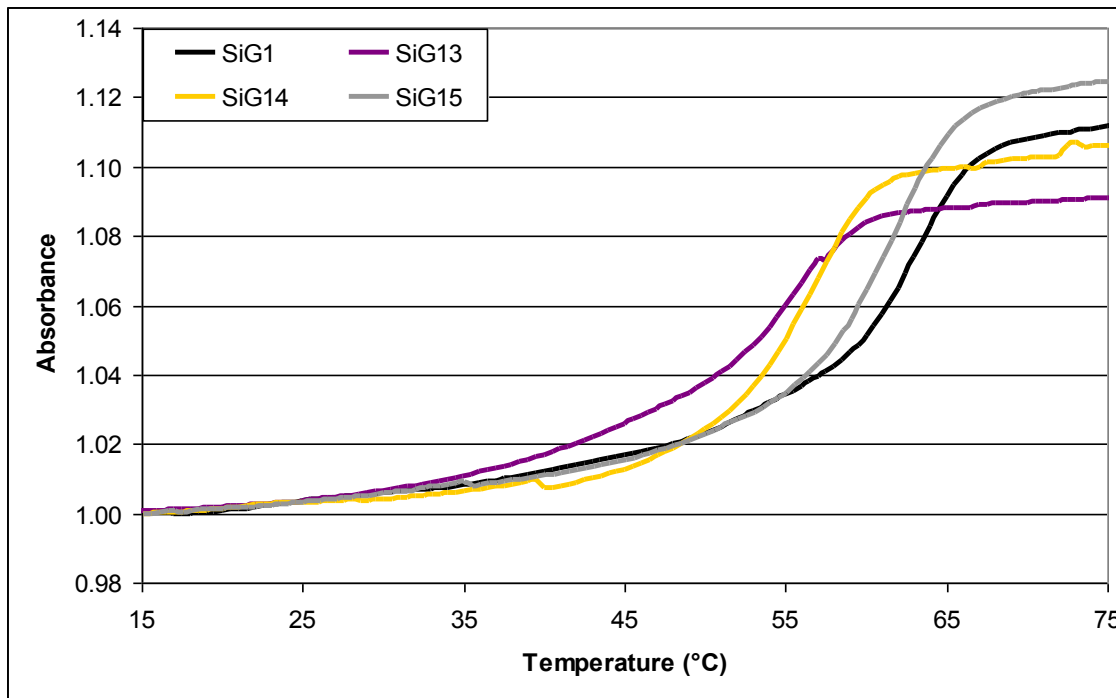
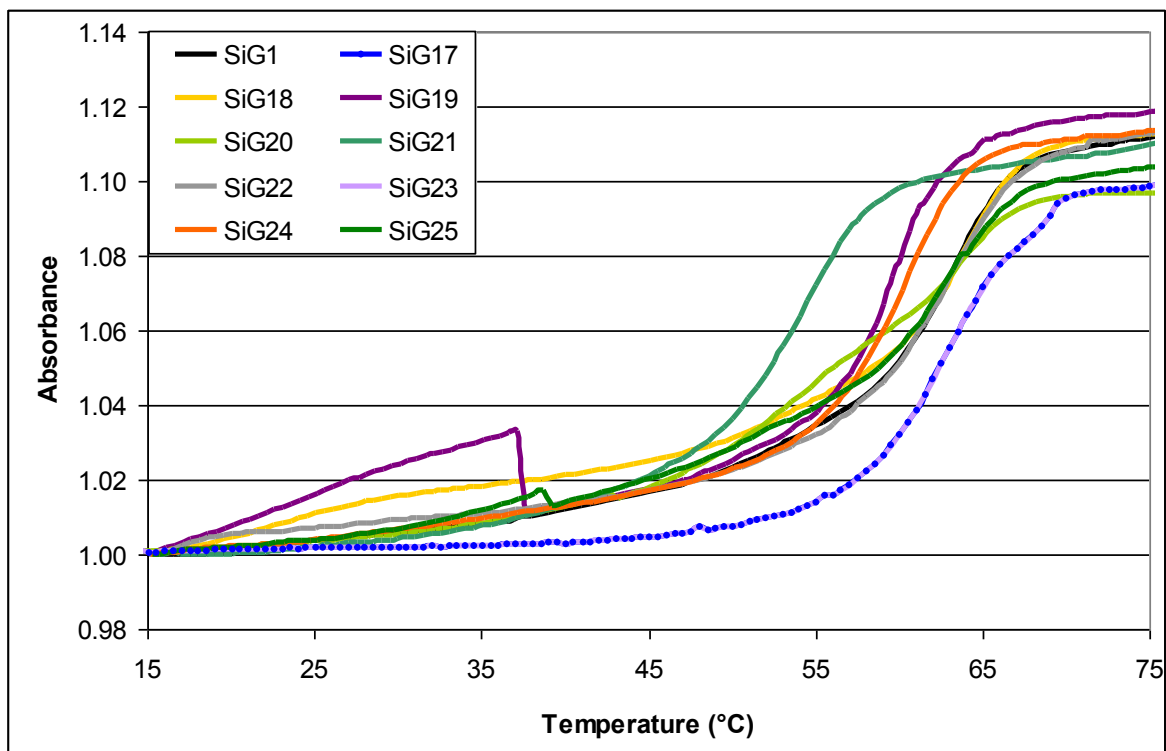


Figure A2.3: T_m Spectra of Passenger Strand Modified RNA:RNA Duplexes



Note: The data for SiG17 and SiG23 are so similar that they appear as a single line.

Figure A2.4: T_m Spectra of Guide and Passenger Strand Modified RNA:RNA Duplexes

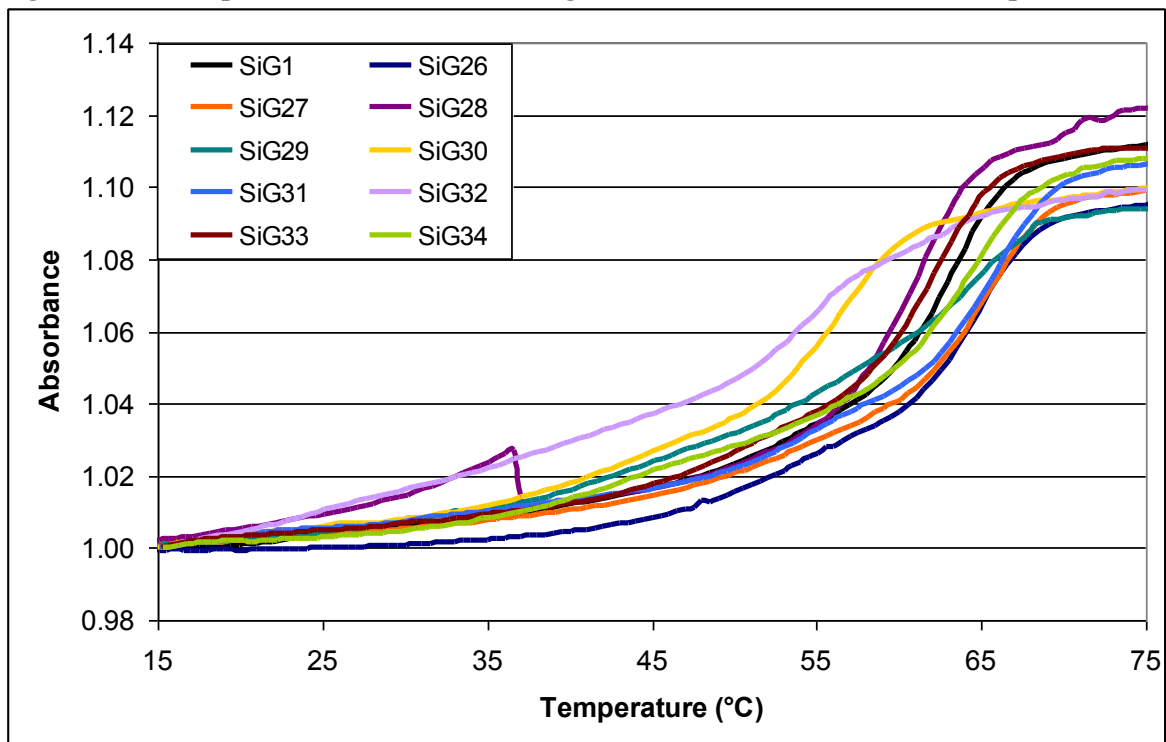


Table A2.1: T_m by First Derivative & Thermodynamic Parameters of RNA:RNA Duplexes

sample	T_m (°C) heating	T_m (°C) cooling	ΔT_m (°C) deriv – hypo	ΔH (J)	ΔS (J·K ⁻¹)	ΔG (J)	Keq	KT_m
SiG1-a	63.00	62.00	2.0	-304	-791	-67.75	7.39E+11	1.07E+06
SiG1-b	63.01	62.02	2.1	-110	-300	-84.22	5.69E+14	1.14E+06
SiG1-c	63.00	62.01	4.3	-620	-1736	-102.67	9.69E+17	1.06E+06
SiG2	63.24	61.80	2.3	-480	-1323	-85.56	9.76E+14	1.06E+06
SiG3	62.18	59.35	4.5	-303	-800	-64.15	1.73E+11	9.93E+05
SiG4	59.12	59.40	2.8	-465	-1289	-81.04	1.58E+14	1.08E+06
SiG5	60.56	58.45	2.3	-530	-1485	-87.54	2.17E+15	1.08E+06
SiG6*	65.07	63.94	2.8	-107	-201	-47.50	2.09E+08	1.01E+06
SiG7	64.30	63.29	2.1	-925	-2620	-143.38	1.32E+25	1.04E+06
SiG9	63.24	61.80	1.4	-626	-1756	-102.50	-9.06E+17	1.04E+06
SiG10	62.18	60.85	1.5	-584	-1636	-96.33	7.51E+16	1.13E+06
SiG11	63.27	61.77	3.5	-719	-2029	-113.82	8.73E+19	1.14E+06
SiG12	63.24	61.73	2.5	-443	-1197	-85.79	1.07E+15	1.14E+06
SiG13	56.01	55.00	-0.3	-241	-626	-54.79	3.98E+09	9.75E+05
SiG14	58.06	55.45	1.4	-479	-1345	-78.16	4.94E+13	1.14E+06
SiG15	59.62	58.40	0.5	-645	-1831	-90.78	2.02E+17	1.05E+06
SiG16	61.03	56.47	2.8	-362	-972	-72.85	5.78E+12	9.24E+05
SiG17	63.03	61.96	0.0	-441	-1199	-83.23	3.82E+14	1.06E+06
SiG18	64.12	63.42	7.5	-676	-1897	-110.68	2.46E+19	1.12E+06
SiG19	59.67	n.d.	0.5	-159	-379	-46.31	1.30E+08	9.71E+05
SiG20	63.23	62.32	1.8	-270	-703	-60.35	3.75E+10	9.67E+05
SiG21	54.06	52.97	0.6	-511	-1450	-78.15	4.91E+13	1.04E+06
SiG22	63.12	62.42	1.1	-532	-1473	-92.41	1.55E+16	1.04E+06
SiG23	63.18	62.36	3.1	-429	-1169	-80.48	1.26E+14	1.05E+06
SiG24	60.24	58.82	3.0	-629	-1776	-99.21	2.40E+17	1.10E+06
SiG25	62.79	61.76	2.5	-601	-1680	-100.15	3.51E+17	1.05E+06
SiG26	65.03	63.96	0.2	-576	-1601	-99.66	2.26E+17	1.01E+06
SiG27	65.11	63.92	8.5	-230	-593	-61.45	5.84E+10	1.00E+06
SiG28	60.13	n.d.	2.0	-271	-739	-50.24	6.34E+08	8.73E+05
SiG29	64.73	62.29	3.3	-180	-425	-52.80	1.78E+09	9.78E+05
SiG30	56.50	55.02	2.1	-438	-1222	-73.99	9.18E+12	1.08E+06
SiG31	66.12	63.92	2.6	-625	-1738	-107.11	5.83E+18	1.08E+06
SiG32	54.68	53.36	3.0	-366	-993	-69.58	1.55E+12	9.71E+05
SiG33	62.24	60.81	2.0	-600	-1677	-98.13	1.55E+17	1.02E+06
SiG34	64.29	63.76	2.1	-503	-1385	-89.67	5.12E+15	1.04E+06

*Data for SiG6 from second heating curve.

Appendix 3: Circular Dichroism Signatures of RNA:RNA Duplexes

Figure A3.1: CD Spectra of Guide Strand Modified RNA:RNA Duplexes

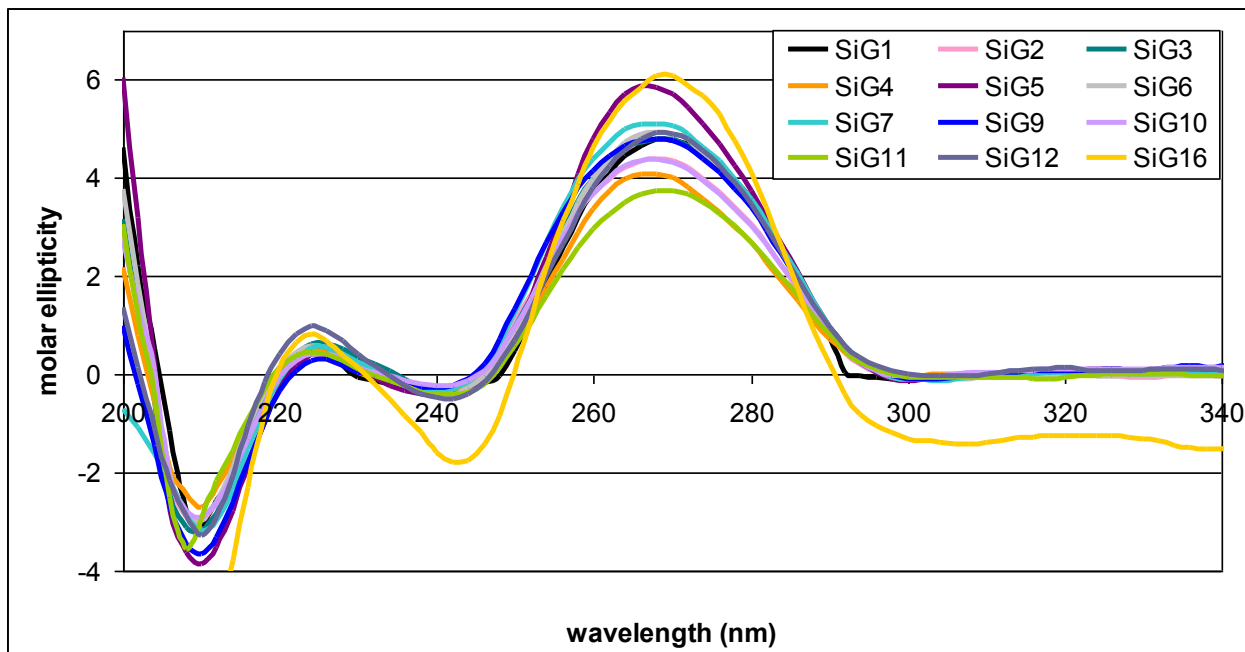


Figure A3.2: CD Spectra of Guide Strand Mismatch RNA:RNA duplexes

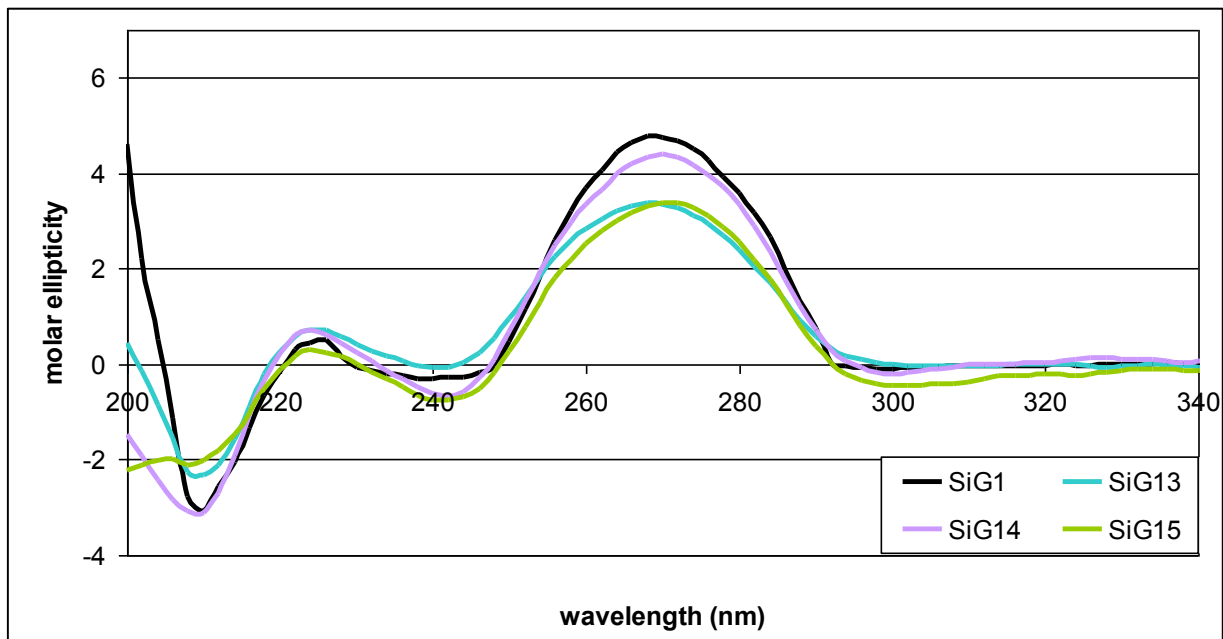


Figure A3.3: CD Spectra of Passenger Strand Modified RNA:RNA DCuplexes

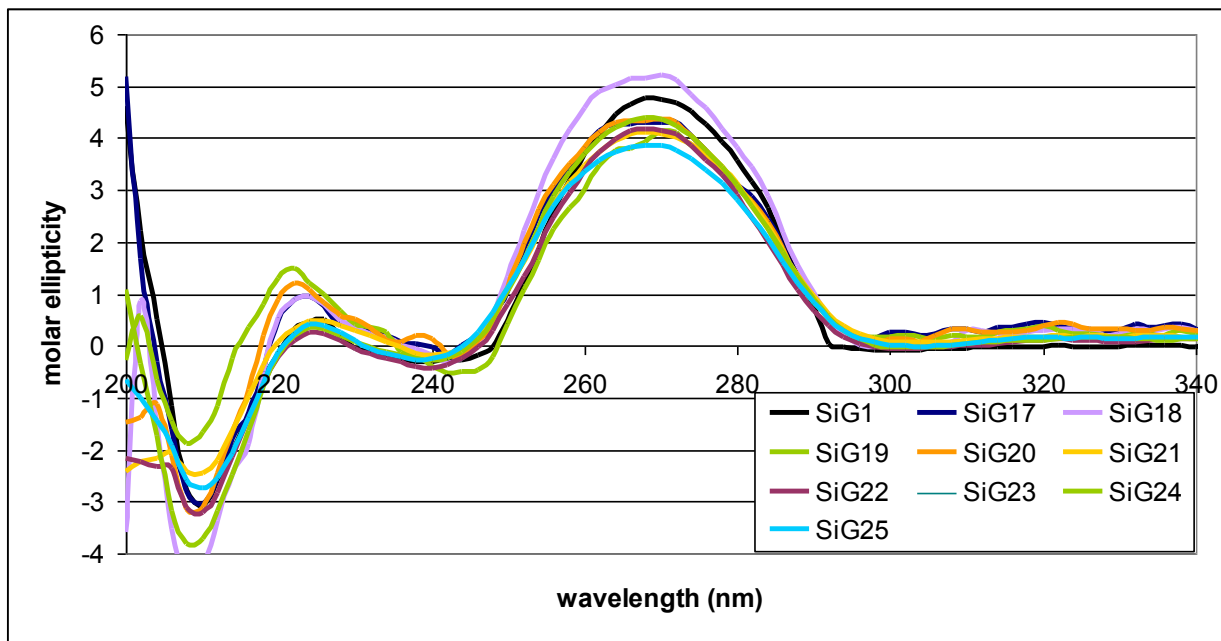


Figure A3.4: CD Spectra of Guide and Passenger Strand Modified RNA:RNA Duplexes

